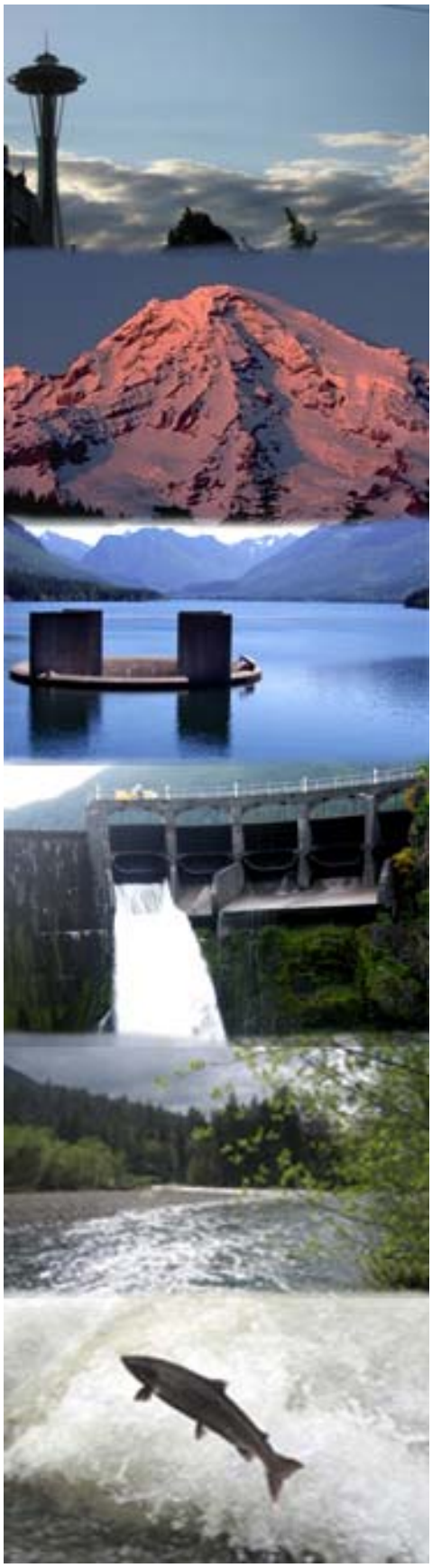

Technical Memorandum #5: Approach for Developing Climate Impacted Streamflow Data and its Quality Assurance/Quality Control

Prepared for:

Climate Change Technical Committee

Acknowledgments

Funding for the research conducted by the University of Washington for the Climate Change Technical Committee (CCTC) came from Washington State's Department of Ecology, Seattle Public Utilities, Cascade Water Alliance, and King County Department of Natural Resources and Parks. In addition, the members of the committee acknowledge all of the agencies that generously provided staff members and their time to participate in the committee's activities. Funding for the CCTC's facilitator was provided by King County Department of Natural Resources and Parks.

The report benefited from the committee members, including:

Member	**Affiliation**
Jane Lamensdorf-Bucher	King County Department of Natural Resources and Parks – Committee Chair
James Battin	NOAA
Geoff Clayton	Woodinville Water District Commissioner, Position 4
Holly Coccoli	Muckleshoot Tribe
Jefferson Davis	City of Kent
Paul Fleming	Seattle Public Utilities
Paul Hickey	Tacoma Water
Joan Kersnar	Seattle Public Utilities
Erin Leonhart	City of Kirkland
Maher Maher	Steward and Associates
Bruce Meaker	Snohomish PUD
Jim Miller	City of Everett
Phil Mote	University of Washington, Speaker
Steve Nelson	RH2 Engineering
Kelly Peterson	City of Kent
Jim Simmonds	King County Department of Natural Resources and Parks
Amy Snover	University of Washington, Principal, Climate Impacts Group
Chris Thorn	City of Auburn
Kurt Unger	Washington State Department of Ecology
Seshu Vaddey	US Army Corps of Engineers
Lara Whitely Binder	University of Washington, Climate Impacts Group
Facilitator and Technical Support Staff	
Tamie Kellogg	Committee Facilitator – Kellogg Consulting
Richard Palmer	Technical Lead, University of Washington, Principal Climate Impacts Group
Eset Alemu	Technical Support Staff, University of Washington
Donee Alexander	Technical Support Staff, University of Washington
Ben Enfield	Technical Support Staff, University of Washington
Kathleen King	Technical Support Staff, University of Washington
Courtney O'Neill	Technical Support Staff, University of Washington
Austin Polebitski	Technical Support Staff, University of Washington
Lee Traynham	Technical Support Staff, University of Washington
Matthew Wiley	Technical Support Staff, University of Washington

We would particularly like to acknowledge the efforts of Joan Kersnar of Seattle Public Utilities for her help with editing all of the products of the CCTC.

This document should be cited as: *Polebitski, A., L. Traynham, and R.N. Palmer. 2007. "Technical Memorandum #5: Approach for Developing Climate Impacted Streamflow Data and its Quality Assurance/Quality Control" A report prepared by the Climate Change Technical Subcommittee of the Regional Water Supply Planning Process, Seattle, WA.*

Table of Contents

List of Figures

List of Tables

Technical Memorandum #5
Approach for Developing Climate Impacted Streamflow Data and its Quality Assurance/Quality Control

Introduction

The potential impacts of climate change on Puget Sound regional hydrology are examined by generating and evaluating climate impacted streamflow data. These data consist of streamflow values at various locations along the rivers that serve as supply sources for the region (e.g. Green River, Sultan River, Cedar River, etc.). Generation of these data is a complex, multi-step process that requires the application of general circulation models (GCMs) to simulate future global climate conditions, a downscaling technique to disaggregate GCM output to a regional scale, and a hydrology model to simulate future regional instream flows. Previous Technical Memos have detailed the first two steps. This document summarizes the generation, calibration, and validation of climate impacted streamflow values for the Puget Sound region.

Process Overview

The Distributed Hydrology Soil Vegetation Model (DHSVM) was developed by researchers at the University of Washington and Princeton University. DHSVM 2.0, a physically based rainfall runoff model, is utilized to generate typical streamflow patterns given future climate change scenarios. The model combines meteorological data with GIS derived representations of elevation, soil type, soil thickness, and vegetation to simulate water and energy fluxes at and below land surfaces. Relative to the GCMs, DHSVM is a fine-scale model with resolution from 30 to 150 meters. The model is run at a 3-hour time step to simulate the daily energy fluxes that drive snowmelt processes. The equations used to represent energy fluxes are detailed elsewhere in the literature (Wigmosta et al., 1994).

Forcing data for seven variables are required in a DHSVM simulation. These variables are: air temp (°C), wind speed (m/s), relative humidity (%), incoming short wave radiation (W/m^2), outgoing long-wave radiation (W/m^2), precipitation (m/time step) and temperature lapse rate (°C/m). Because these values are not typically available at the spatial resolution needed, they are derived from available data including: minimum daily temperature, maximum daily temperature, total daily precipitation, station elevation, geographic position, and nearby wind records. Other variables, including soil porosity, vegetation type, leaf area are specified in geospatial files that are used to construct the model.

Calibration

For the basins studied, a typical configuration file for DHSVM contains hundred of parameters that can be modified in the calibration process. However, most of these input variables are derived from mapped, geospatial information such as soil type, vegetation type, and local geology. Because of this, many of the physical parameters associated with each type of soil type, vegetation type or geological formation do not vary significantly temporally. Land-cover and vegetation definitions and spatial characteristics are derived from 2001 LandSat images.

In the calibration procedure, macro-scale parameters, such as temperature lapse rate and precipitation lapse rates are calibrated first. A lapse rate is the change in a variable with elevation, for instance a temperature lapse rate. For precipitation this value is typically positive (increasing elevation results in increasing precipitation) and for temperature this value is usually negative (increasing elevation results in decreasing temperature). In the calibration of DHSVM, PRISM maps (Parameter-elevation Regressions on Independent Slopes Model maps, http://prism.oregonstate.edu/) establish the distribution of precipitation according to elevation, aspect, and slope. (PRISM Maps were developed by the Oregon Climate Service with support from the USDA Natural Resources Conservation Service, USDA Forest Service, NOAA Office of Global Programs, and others.) A monthly lapse rate is used for temperature. Through calibration of the lapse rate parameters, the general shape of the annual hydrograph for a location can be replicated. Through calibration of other parameters, such as soil porosity, soil depth and geologic conductivity, peaks in the shorter period hydrographs, such as daily or weekly peaks, can be replicated.

Cedar River Simulation Results

The Cedar River Watershed is calibrated using streamflows that contribute to the inflow of Chester Morse Reservoir and at locations below the reservoir (Figure 1). The red lines in the figure are mapped water courses while the blue lines are computer generated representations of the actual network. With the exception of Chester Morse Lake, the modeled stream network agrees well with the observed network. To evaluate the DHSVM model's ability to replicate the observed natural flows within the Cedar River, unaltered gaged points upstream of the reservoir are used for comparison. Once the natural flows are adequately modeled, a comparison of Seattle Public Utilities (SPU) recreated unaltered flows is performed. Table 1 presents calibration points in the Cedar River Basin, the length of record, and the data source.

Table 1: Data Sources for Calibration (Cedar River)

Gage	Gage Name	Maintainer	Period of Record
12115000	Cedar River near Cedar Falls	USGS	10/1/1945 - Present
12115500	Rex River near Cedar Falls	USGS	10/1/1945 - Present
12117000	Taylor Creek near Selleck	USGS	8/1/1956 - Present
Cedar 18	Flows entering between Chester Morse and Masonry Pool	SPU	10/1/1928 - Present

Gage 12115000 is the primary point of calibration as it represents the majority of inflows into Chester Morse. SPU's CUE Model Inflow Point, Cedar 1, is highly correlated with flow at USGS Gage 12115000 as the gage is just upstream. A USGS gage is located on the other major tributary feeding Chester Morse Reservoir, just above Gage 12115700 (modeled point CRY 02). The USGS Gage 12117000 measures flows just above the confluence of Taylor Creek with the Cedar River. Since Taylor Creek is below Masonry Dam but above Landsburg Diversion, this gage provides observed flow characteristic of lower basin tributaries. Table 2 describes the relationship between gaged data and the DHSVM output points for the watershed. Cedar 18 provides a measurement of how all flows entering below Gage 12115000 but above the dam at Masonry pool are being modeled.

Table 2: Mapping of DHSVM to SPU Flows

Gage	SPU Inflow Point	Translation
CRY05	Cedar 1	Chester Morse Inflow
CRY05 - CRY01	Cedar 18	Flow entering between Chester Morse Inflow and Masonry Pool Dam
CRY09 - CRY01	Cedar 2	Flow Below Masonry Pool Dam and Above Landsburg Diversion
CRY07-CRY09	Cedar 3	Inflow between 12117500 and Spawning Channel (below Diversion)
CRY06 - CRY07	Cedar 5	Inflow between Spawning Channel and Renton (12119000)

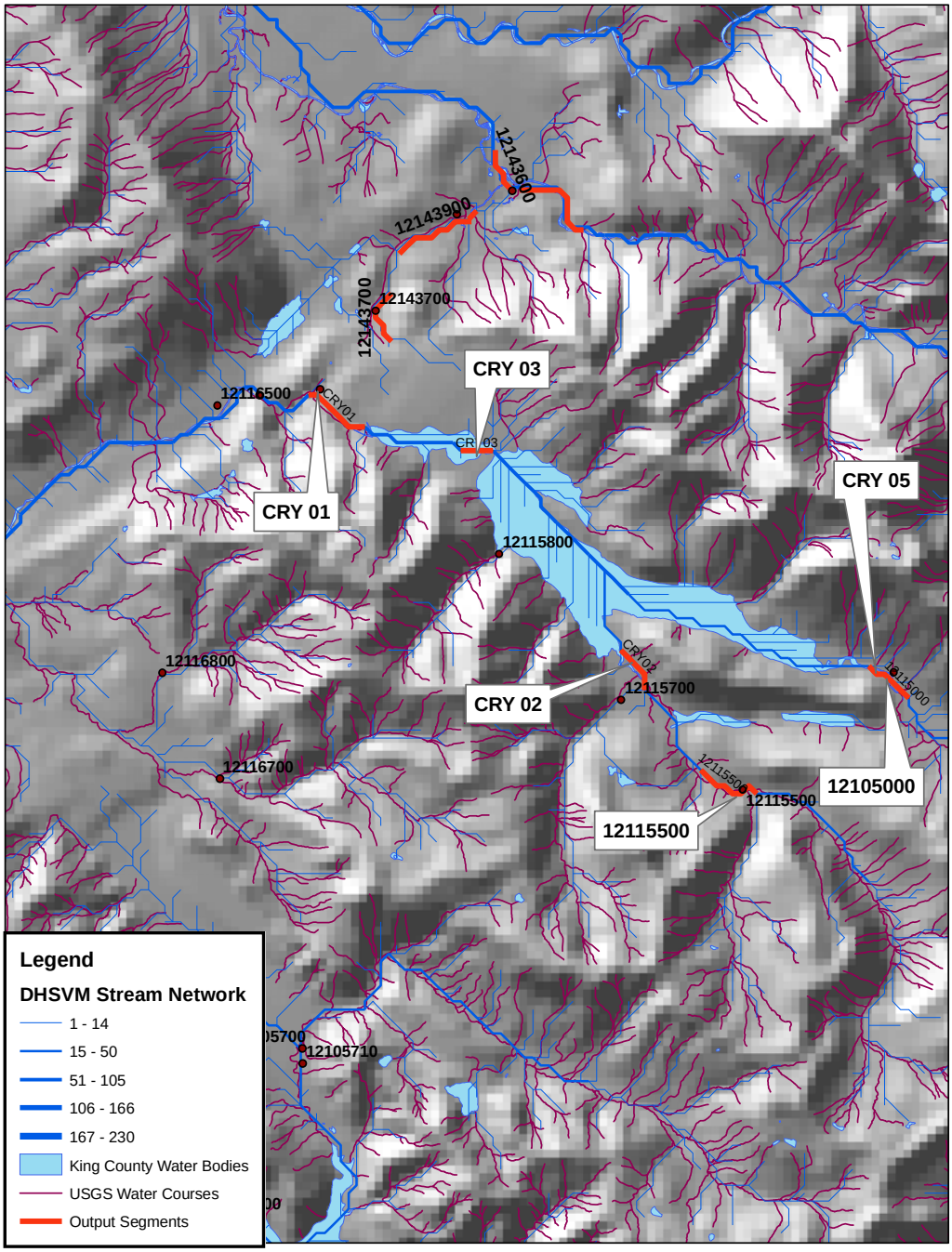

Figure 1: Chester Morse Inflow Points and USGS gaging stations

Figure 2 is a comparison of the daily simulated and observed streamflows at gage 12115000 for the period of available record (10/1/1945-9/30/2004). The simulated flow is slightly higher in the winter months and slightly under simulated in the early summer months. Overall, the median, seventy-fifth, and twenty-fifth percentile simulated flows agree with the observed record.

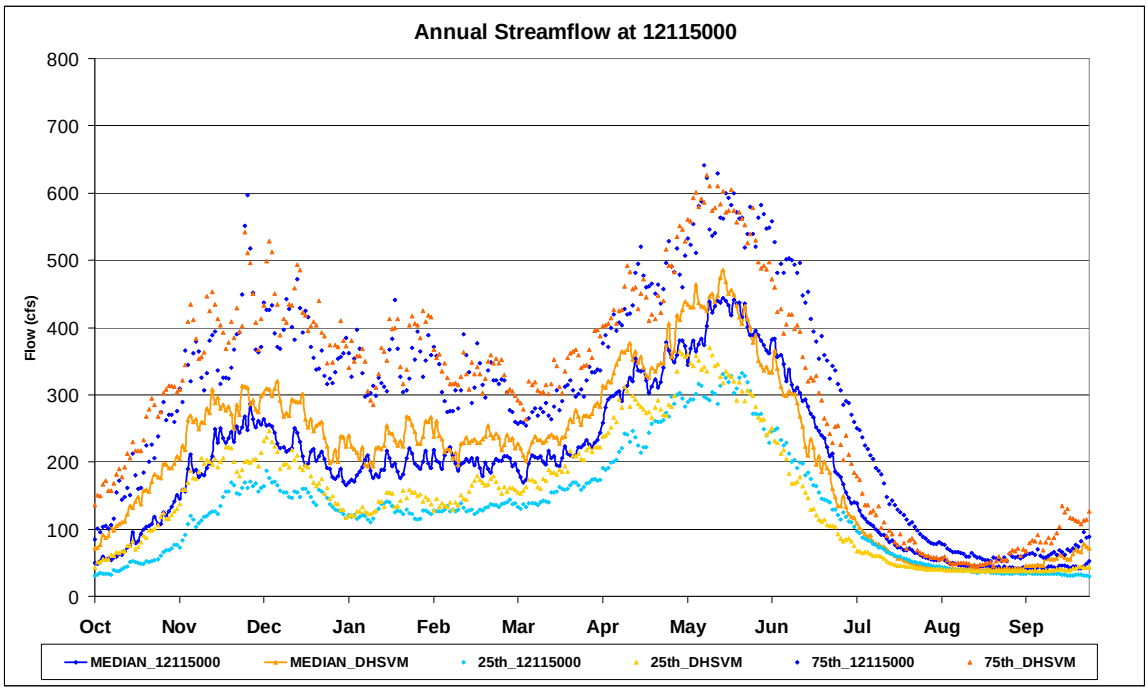

Figure 2: Annual hydrograph of Simulated vs. Observed Streamflow at 12115000

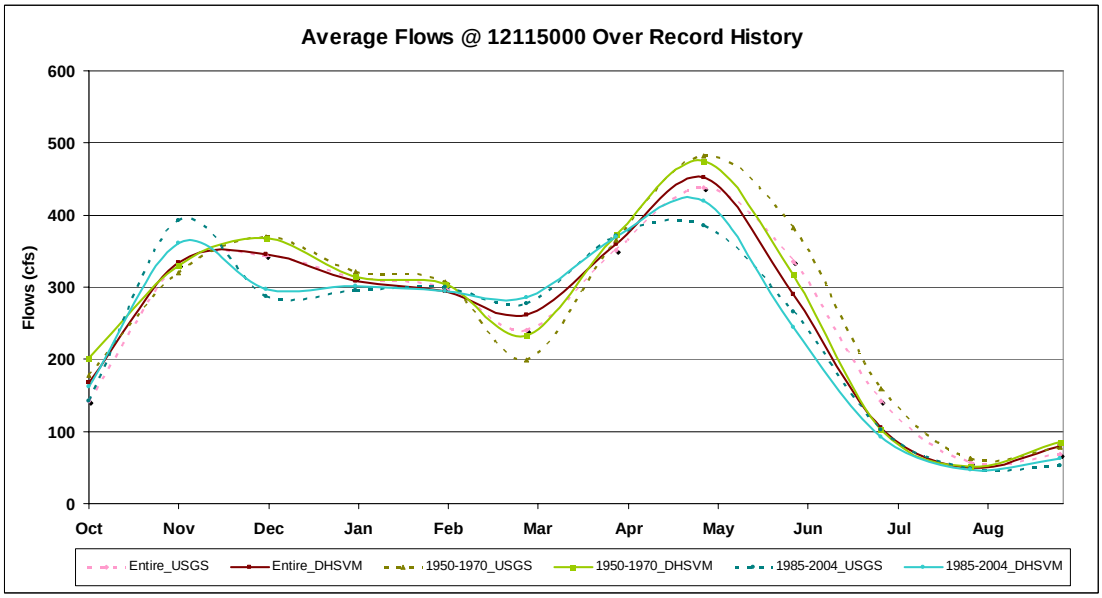

Figure 3 : Comparison of Annual Average Flows over Historic Record at 12115000

Figure 3 presents observed and simulated average monthly flows at Gage 12115000 for different intervals of record. The same pattern described above, slightly lower flows in early summer and

slightly higher flows in winter and early spring are evident and persistent through time. Each period of record is well simulated, with only modest biases present. An interesting feature of this plot is the higher fall and winter flows and lower spring flows between the 1950-1970 period and the 1985-2004 period. These differences may indicate a timing shift that will become more pronounced in a warmer climate. Figure 4 plots cumulative observed and simulated flow at Cedar 1. The model adequately represents the total mass entering the Chester Morse, with only a very slight positive bias over the seventy seven years simulated.

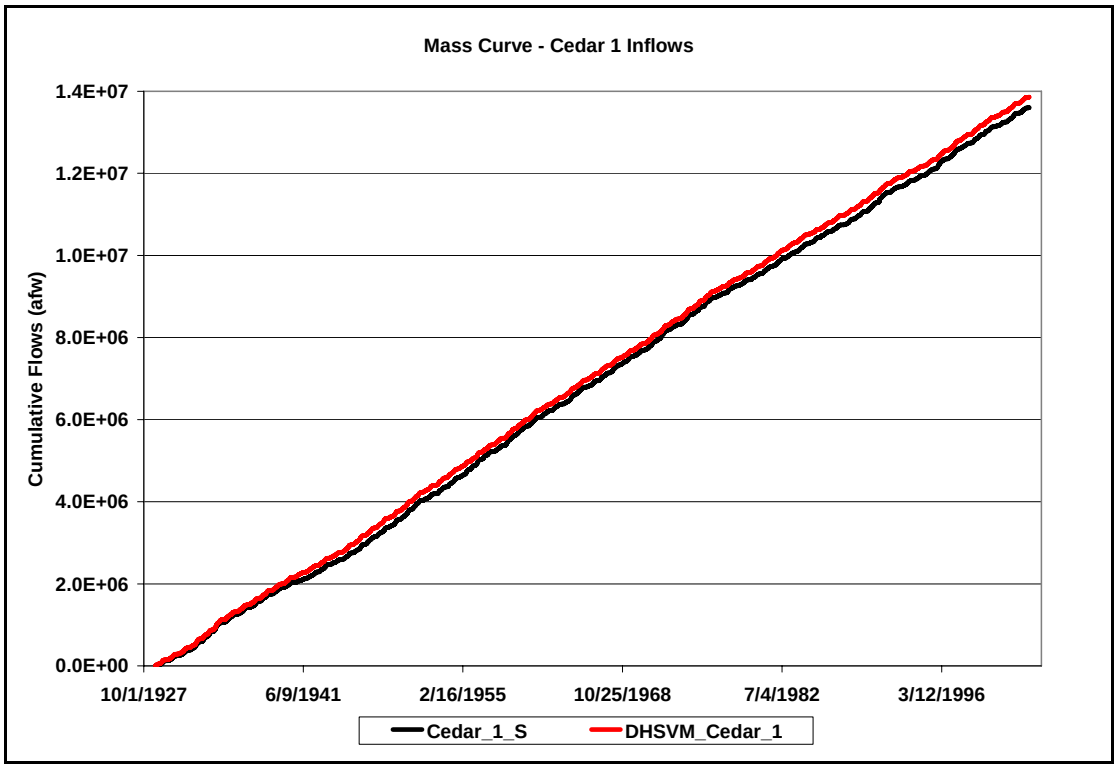

Figure 4: Mass Curve at Cedar 1

The cumulative mass curve for Cedar 18 inflows, which are the inflows below Cedar 1 and above the Masonry Pool Dam (CRY01) are slightly over estimated by the model in the first half of record and slightly under simulated in the second half. These differences are not easily attributable to a specific model response. It is also possible the differences are attributable to how the reconstructed flows were generated for Cedar 18. Regardless, the bias is small relative to the total flow entering the reservoir and is an excellent representation of the observed inflows. Cedar 1 has a 1.9% positive total mass balance and Cedar 18 has a -2.7% total mass balance when compared to the observed flows (Figure 5).

A time-series depiction of flows at Taylor Creek is shown in Figure 6. The model consistently under-predicts flows in the summer months but is a good representation of winter flows. The lower summer flows appear to represent baseflow amounts that are slightly under observed values. Although the modeled flows are low, in the 10-15 cfs range, the amount of flow observed in the stream is also very low, in the 20 cfs range for July and August.

An important metric for evaluating modeled streamflow is the representation of total mass in a given year. Figure 7 displays the percent error for total annual mass at two USGS gages in the Cedar Basin.

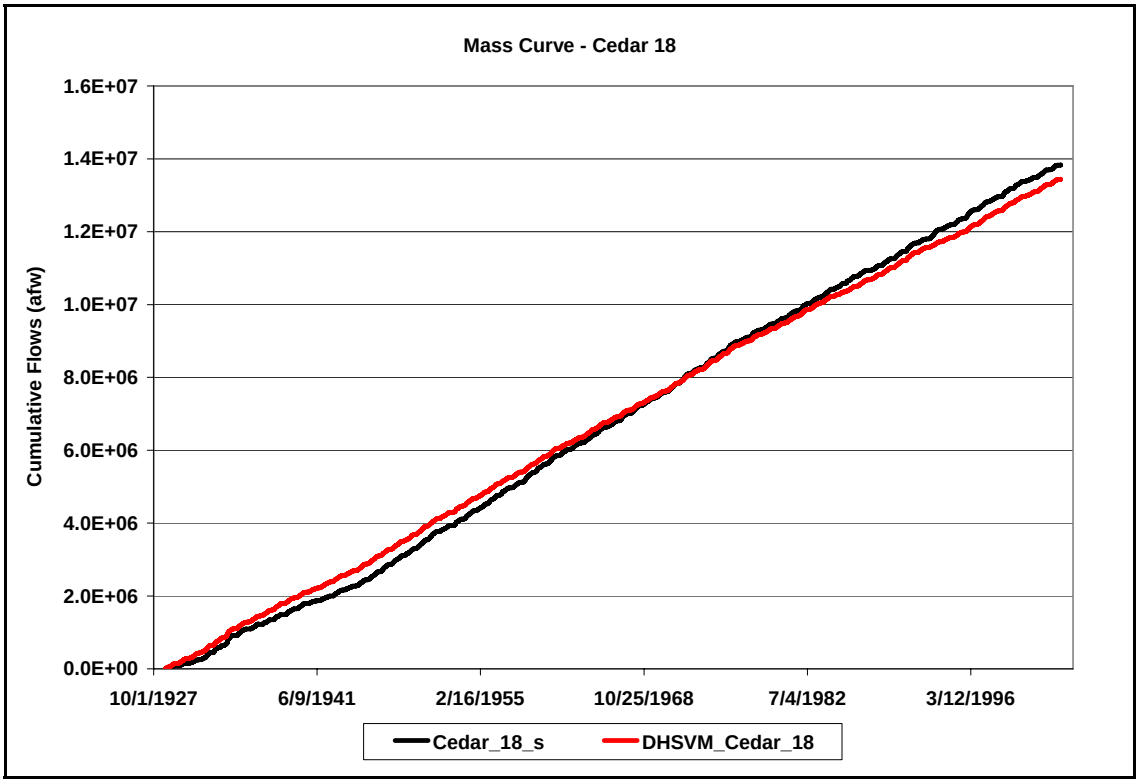

Figure 5: Mass Curve at Cedar 18

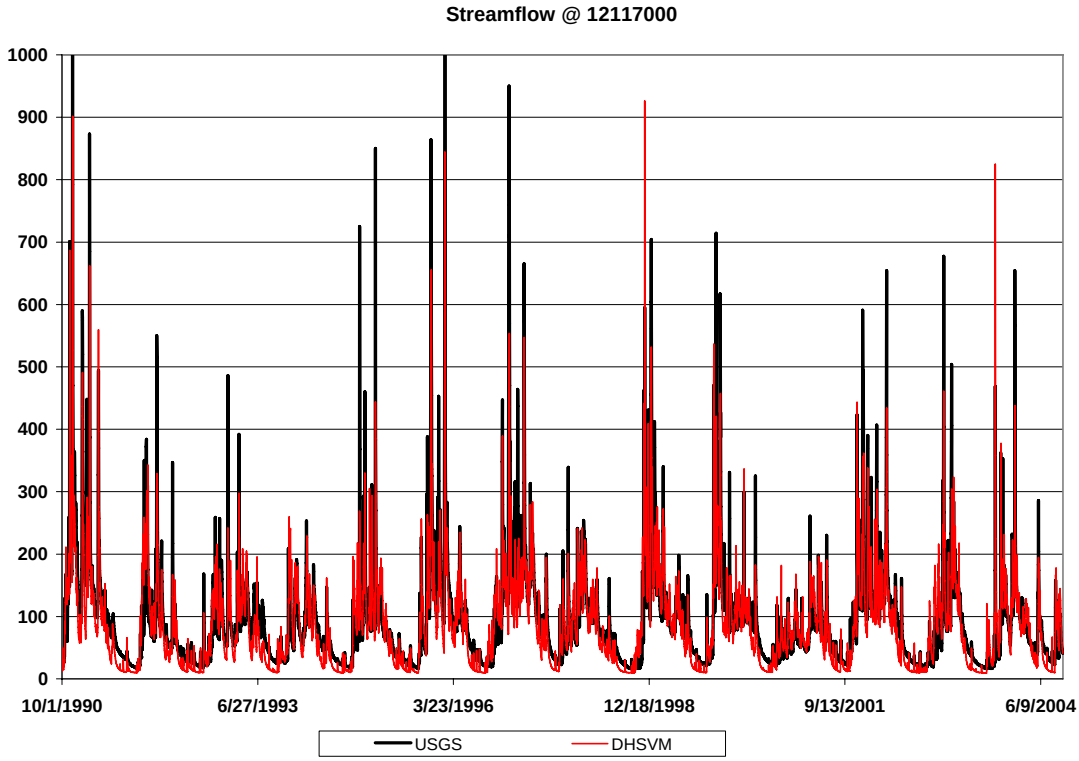

Figure 6: Time Series of Flows at Taylor Creek

Gage 12115000 shows little bias, with the error being evenly distributed, and consistently less than a 10% deviation from the observed mass. Gage 12117000 appears to have slightly more negative bias. This is partially due to the summer flows being lower in the model than the observed. There appears to be a temporal pattern present, with years 1960-1975 being consistently low, whereas in following years, 1975-1990, the mass error is closer to zero. The consistency of lower flow in the 1960 – 1975 period may be due to land use changes within the region. DHSVM represents land cover and land use statically and is represented by the most recent satellite images available (LandSat 2001 images).

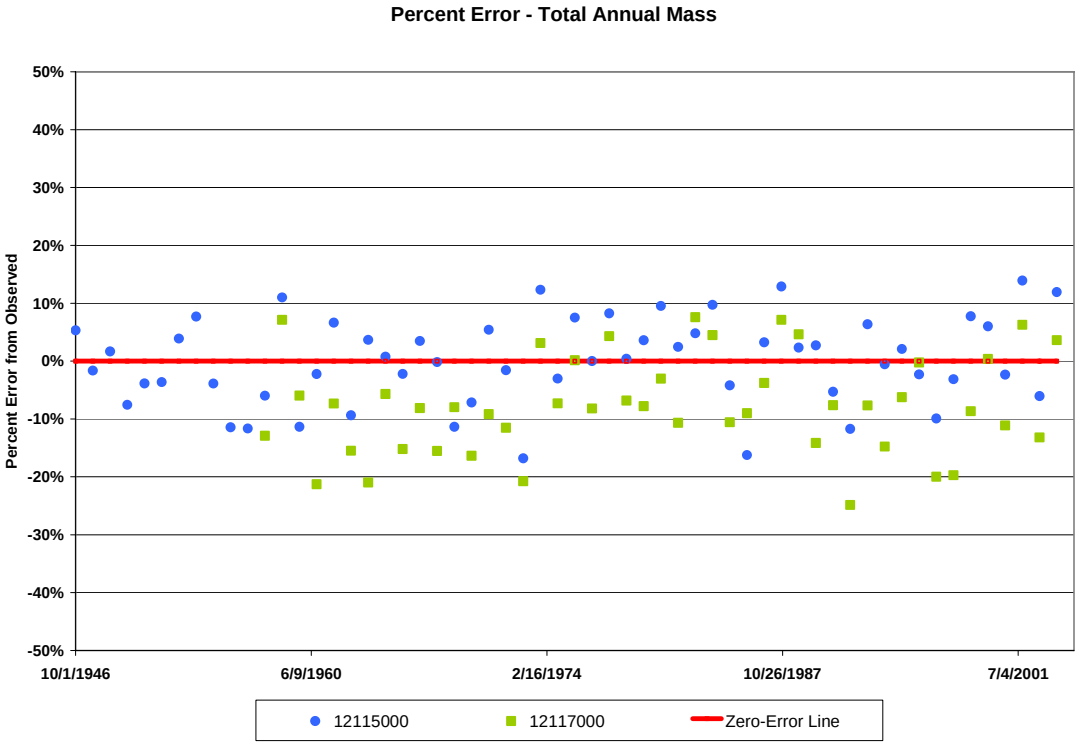

Figure 7: Percent Error in Total Annual Mass for 12115000 and 12117000

Overall, the model provides a good representation of flows above and below the reservoir at the USGS gages, and simulates the flows of Cedar 1 and Cedar 18 provided by SPU. Summer flows appear to be less than observed at gaging stations in the lower watershed. It is possible to bias-correct these summer flows, however, this is not recommended. Such statistical bias corrections detract from the physical representation of the hydrologic processes. Observed streamflow at gaging stations exhibit very slight biases, these are typically on the order of ten percent. These biases could be caused by shifts in the stream channels, changes in land cover or land use, and gage errors. To alleviate some of the bias, a correction routine is applied to flows entering below the Chester Morse Reservoir dam face and above the Landsburg diversion. The method used to bias correct streamflows is fully described in the appendices of this document.

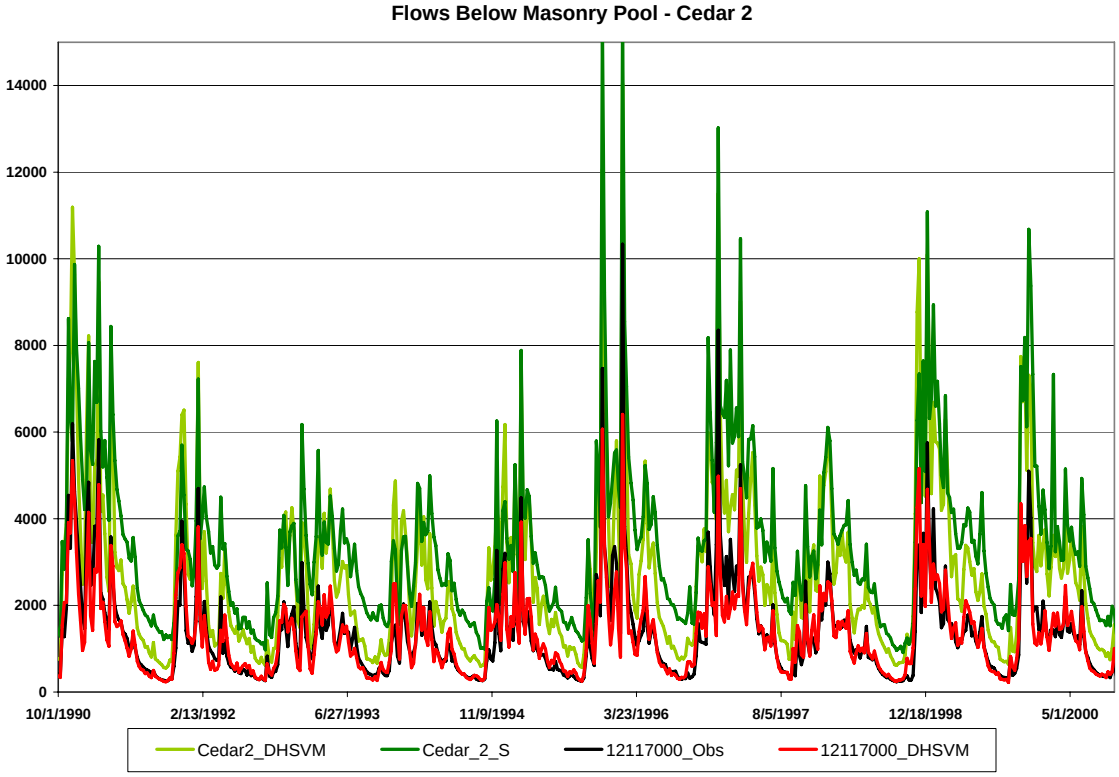

Figure 8: Bias-Corrected Flows at Taylor Creek and Cedar 2

Figure 8 presents the bias-corrected summer flows at Taylor Creek and Cedar 2 and the observed flows. The bias-corrected Cedar 2 flows are shown in Figure 8 with the SPU recreated flows. The bias-correction considerably improves the flows at Cedar 2, though there is still negative bias in the summer months when compared to SPU's recreated historic flows.

Figure 9 presents observed SWE at the SNOTEL site at Tinkham and DHSVM simulated SWE. The timing and SWE amounts are simulated well by the model, with some periods of positive bias, most noticeably the 1998 water year. Overall, the model matches well for SWE simulation. It is important to note that both the SNOTEL site and the DHSVM simulated SWE are for point locations and neither guarantee an accurate estimate of SWE in the entire basin.

Figure 10 presents observed and simulated monthly average flows. The observed and simulated flows match very well and show no signs of either over or under simulation of flows for any monthly period.

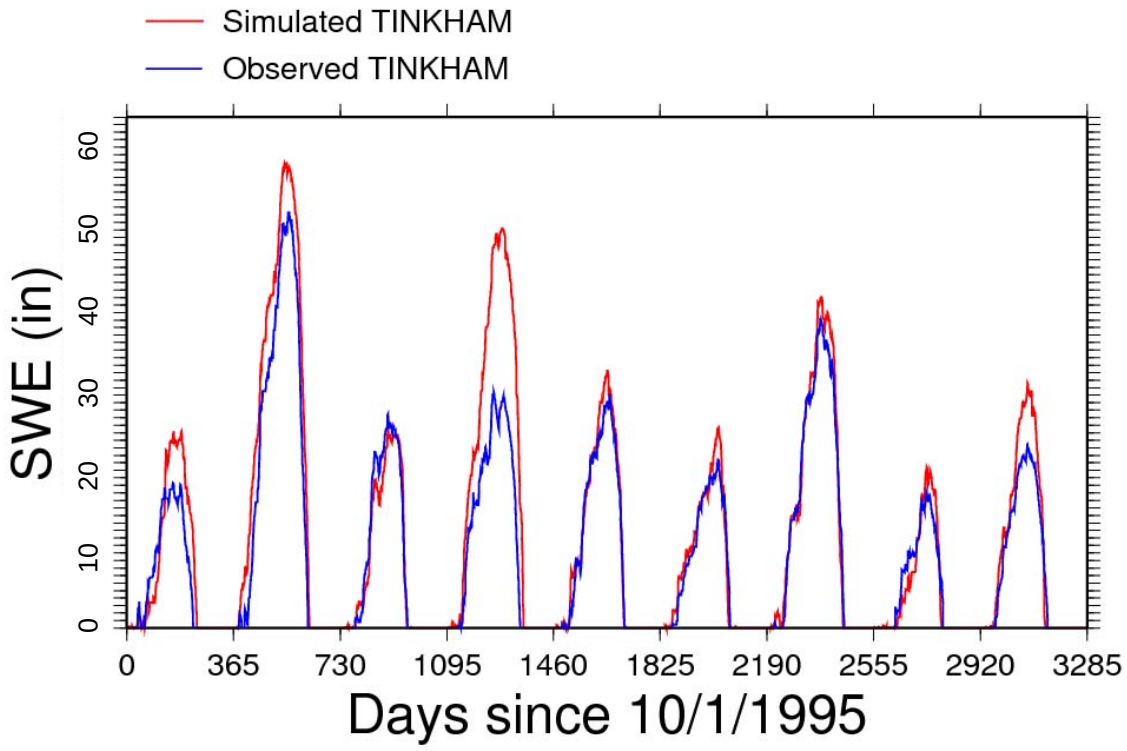

Figure 9: Observed and Simulated SWE at Tinkham SNOTEL site

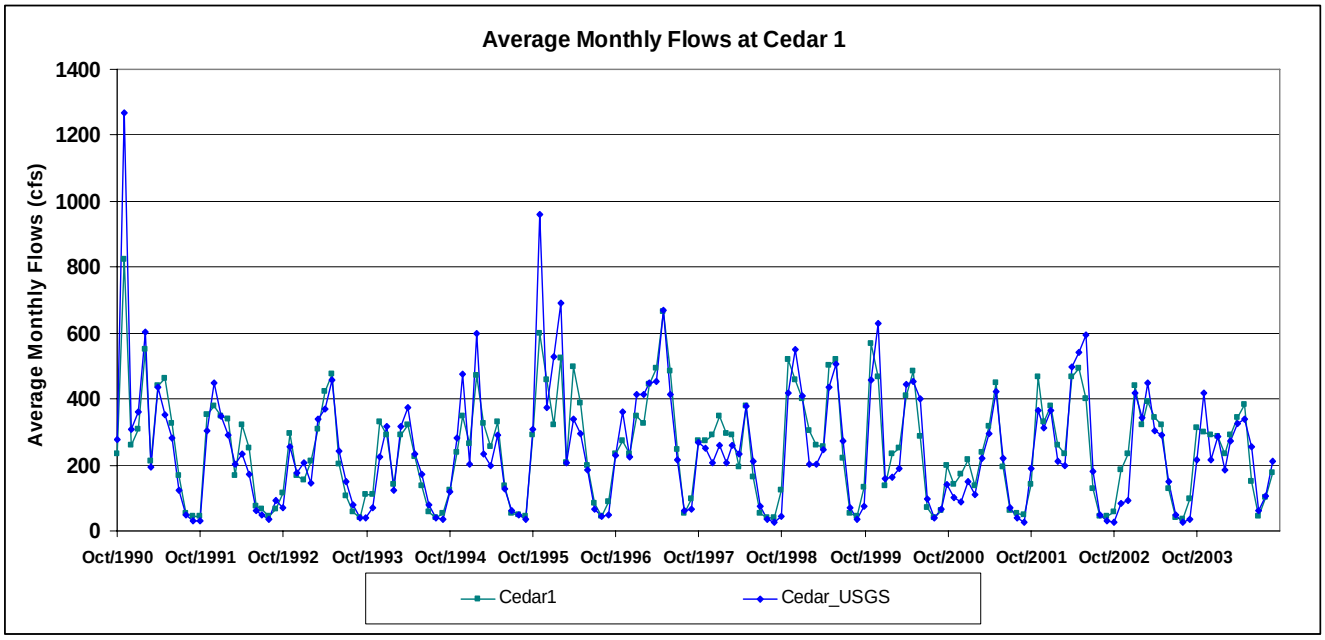

Figure 10: Simulated and Observed Average Monthly Flows at Cedar 1

Green River Simulation Results

Calibration of the Green River basin includes inflow points to the Howard Hanson Reservoir and naturalized flow above and below the reservoir (Figure 11). The red lines are mapped water courses while the blue lines are computer generated representations of the actual network. To evaluate the DHSVM model's ability to replicate the observed natural flows within the Green River, points upstream of the reservoir are used for the comparison. Once the model is initially calibrated, the recreated historic inflows are compared to the simulated inflows. Table 3 contains a listing of calibration points in the Green River Basin, the length of record, and the data source.

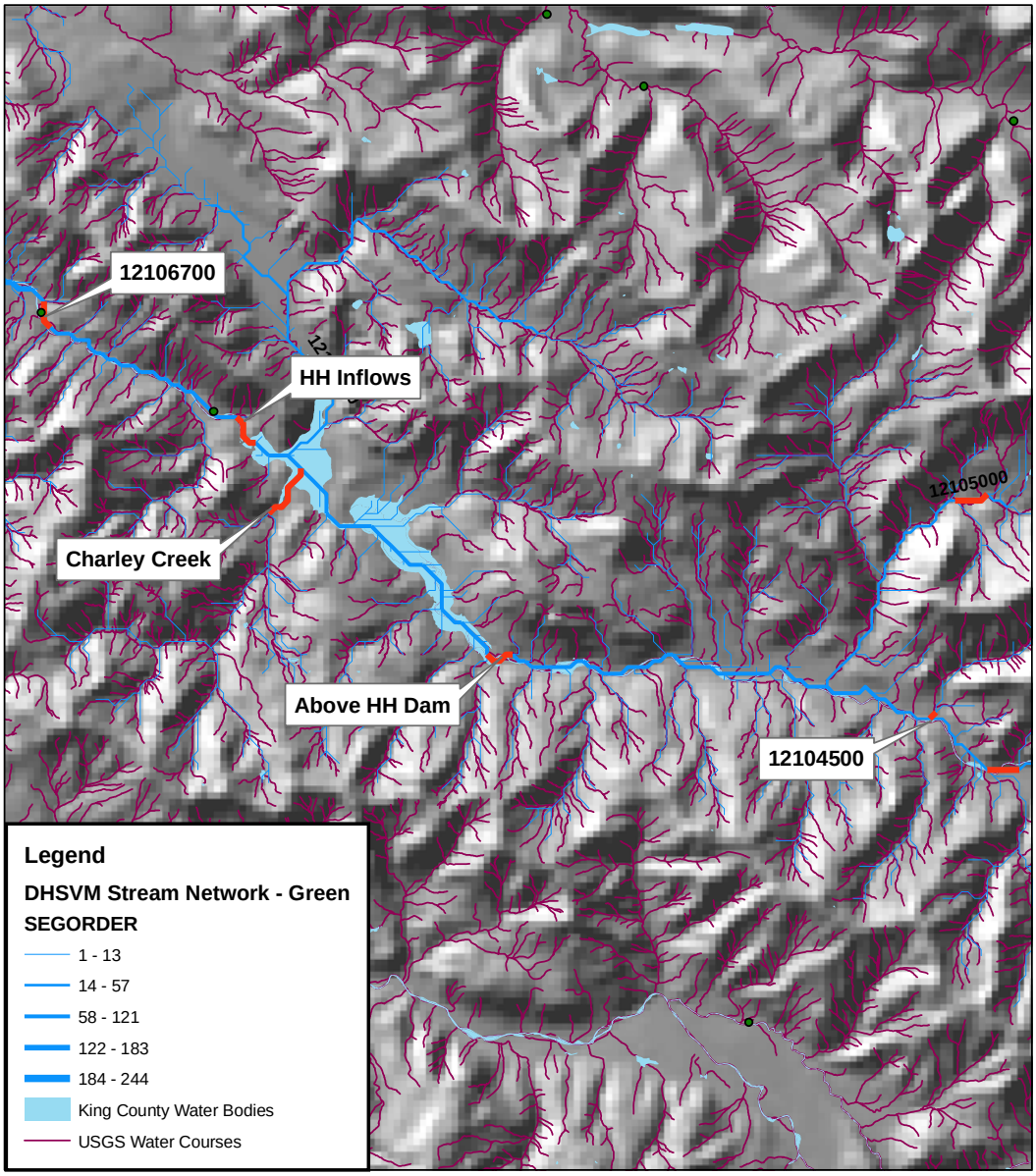

Figure 11: Howard Hanson Inflow Points

Table 3: Data Sources for Calibration (Green River)

Gage	Gage Names	Maintainer	Period of Record
12104500	Green River near Lester	USGS	10/1/1945 – 10/1/1993
HH Inflows	Inflows to Howard Hanson	USACE	10/1/1962 - Present
12106700	Green River at Purification Plant near Palmer	USGS	7/1/1963 - Present
12113000	Green River near Auburn	USGS	8/1/1936 - Present

Howard Hanson (HH) Inflows is the primary point of calibration as it represents the inflows into Howard Hanson. Two other important points for calibration are flows between USGS gages 12106700 and 12113000, more commonly known as the Palmer and Auburn gages. The flows between the Palmer and Auburn gages are important for the conservation storage used to augment flow for fish requirements.

The simulated flows at HH Inflow are greater in the late fall and mid-winter than those observed (Figure 13). Of note is the higher November and December flows. Figure 12 presents a mass curve diagram for at the HH Inflow. The higher flows are contributable to model bias and to the observed record for HH Inflow. Flows at HH Inflow are not gaged but calculated from reservoir levels for this location and may contain uncertainties when extrapolated to daily streamflows for a location. Some initial challenges with the model were properly accounting for rain shadow effects from Mount Rainier on this particular basin. It is possible that the remaining positive bias in the model is contributing to this.

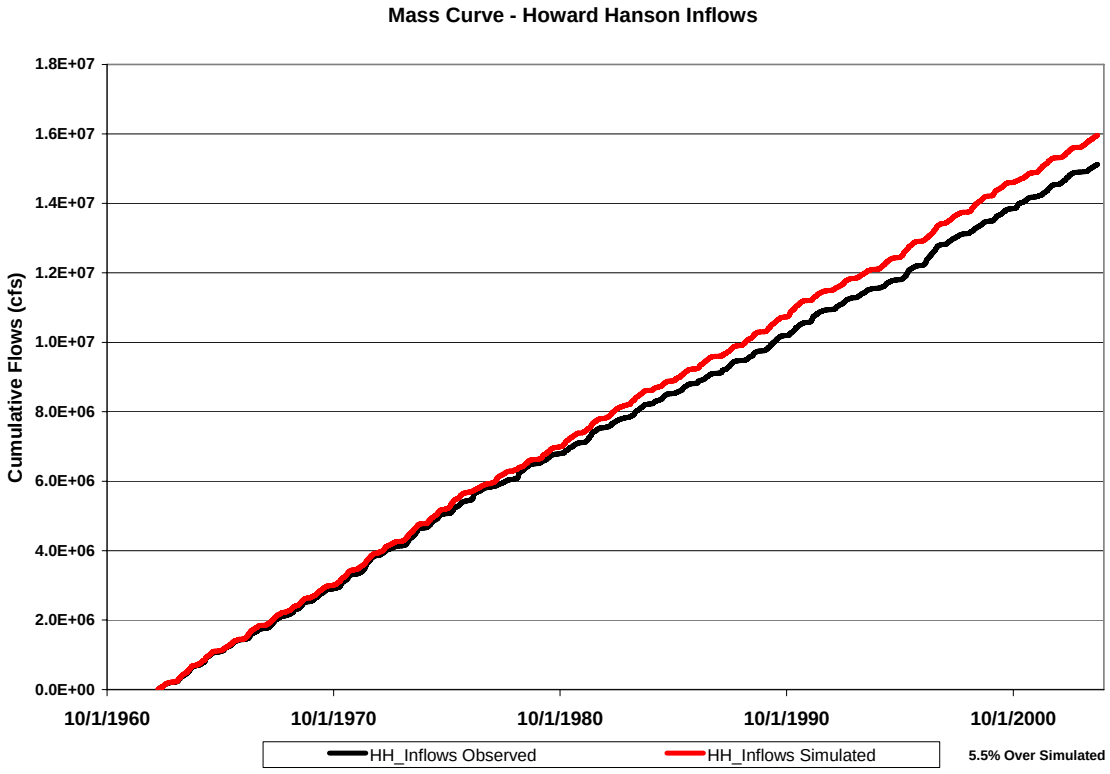

Figure 12: Mass Curve at HH Inflow

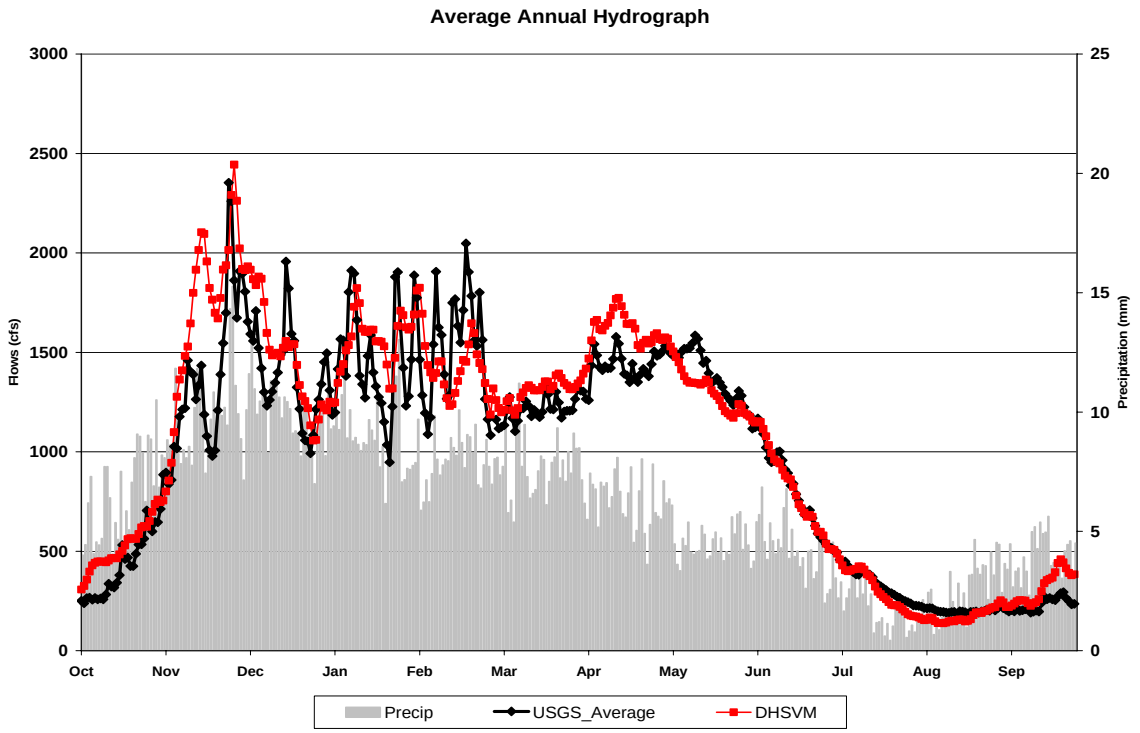

Figure 13: Average Annual Hydrograph at HH Inflow

Gage 12104500, located near Lester WA, is used for calibration in the upper portions of the watershed. The comparison shows a disparity over time, either due to gage or land use issues.

Figure 14 presents the annual average hydrographs for the HH Inflow point for a series of different time periods. Overall the model performs adequately, especially when representing summer flows. There tends to be a slightly larger peak for flow in April that diminishes in May, producing flow that approximates the observed record at HH Inflow. Figure 15 contains a time-series of flow observed between the Palmer and Auburn gages below Howard Hanson Dam. Assuming that the difference between the flow at the two gages removes dam operations and represents only natural flow entering from nearby drainage areas, the flow can be compared to DHSVM output, which only simulates naturalized flow. The naturalized observed flow and the modeled flow show good agreement in all seasons for this portion of the basin. The USGS record occasionally has spikes of near zero flow. This appears to be due to routing effects which are amplified in large storm events. The modeled flow was post-processed to account for the minor routing effects for these large storm events, essentially eliminating most of the near zero flows.

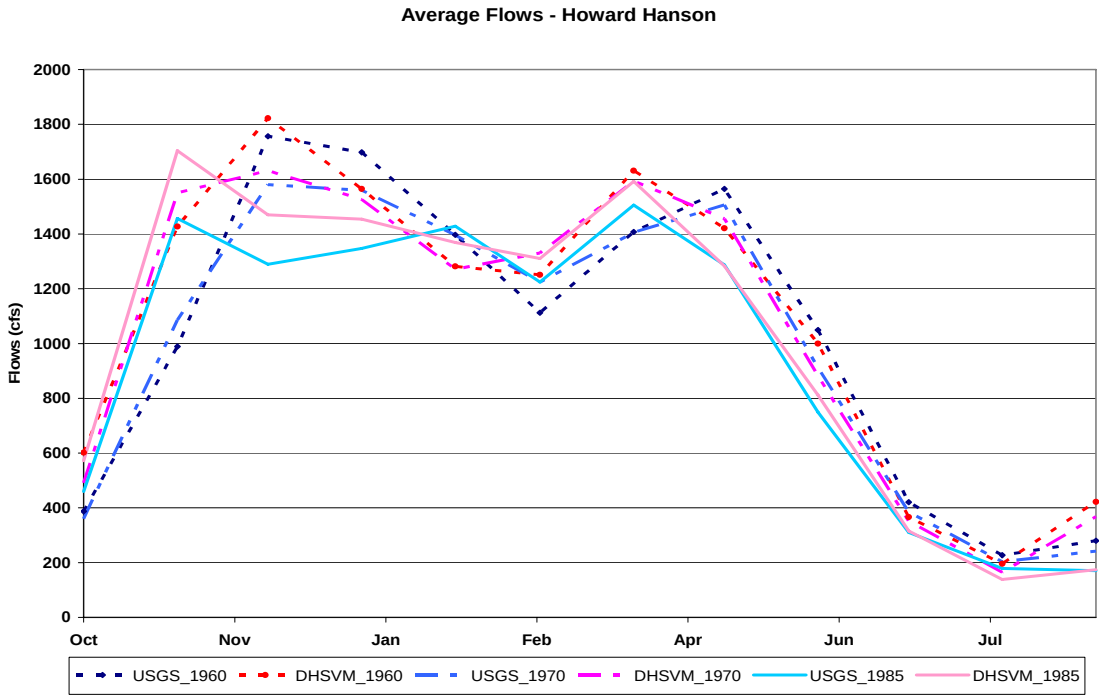

Figure 14: Average Annual Hydrograph at HH Inflows

To further evaluate the flows, the results of an existing operations model are presented (Figure 16 and Figure 17). There is good agreement between the recreated historic flows and the simulated flows, with closely matching refill and drawdown periods under the same operational rules.

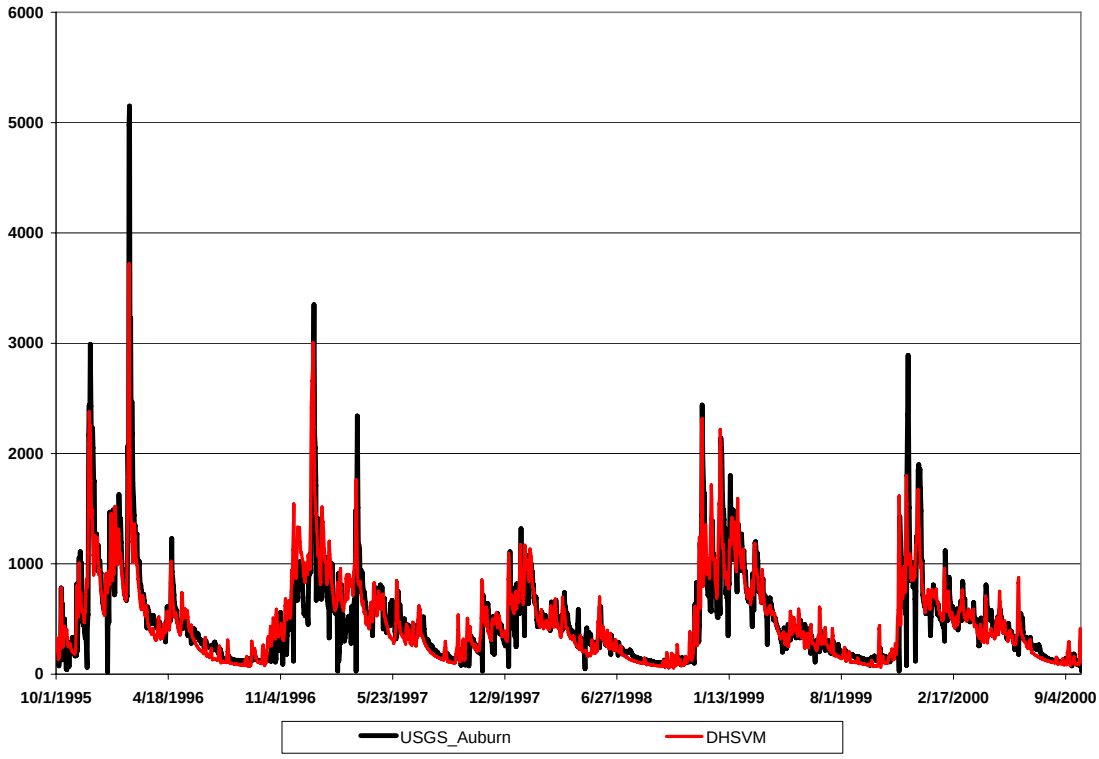

Figure 15: Difference of flow between Palmer and Auburn Gages

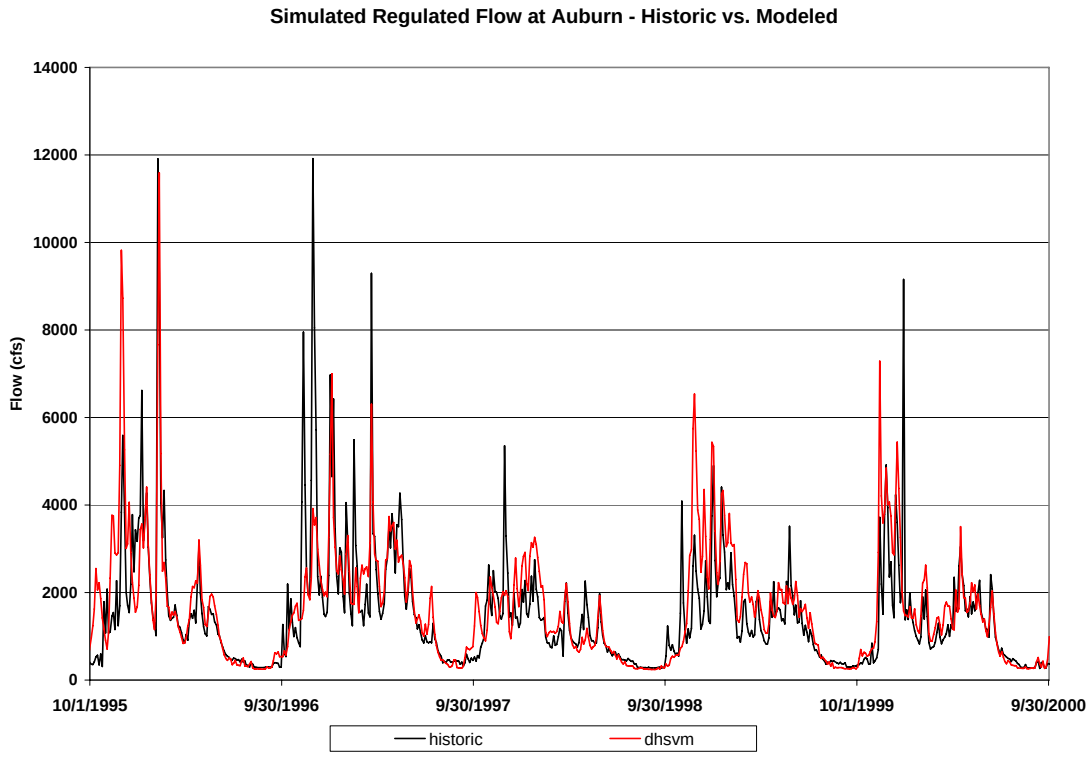

Figure 16 : Simulated Regulated Flows at Auburn

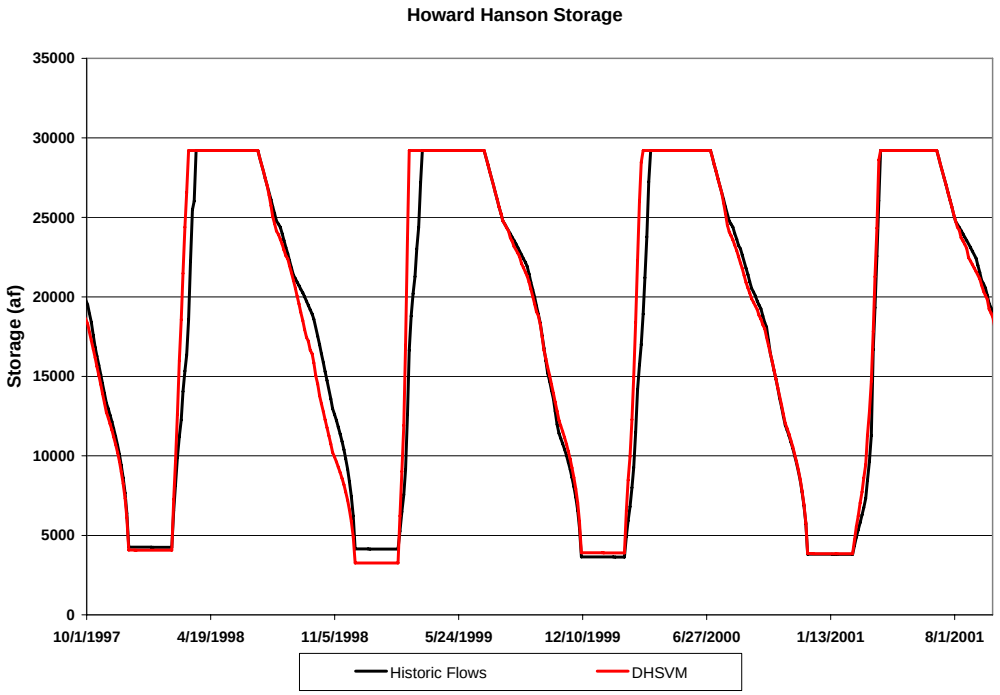

Figure 17: Simulated Storage for Howard Hanson

Figure 18 depicts SWE amounts at Meadows Pass SNOTEL and DHSVM simulated SWE. DHSVM simulated SWE mimics the observed SWE, with only one year slightly over simulated (1998). Both timing and amount appear to be in good agreement.

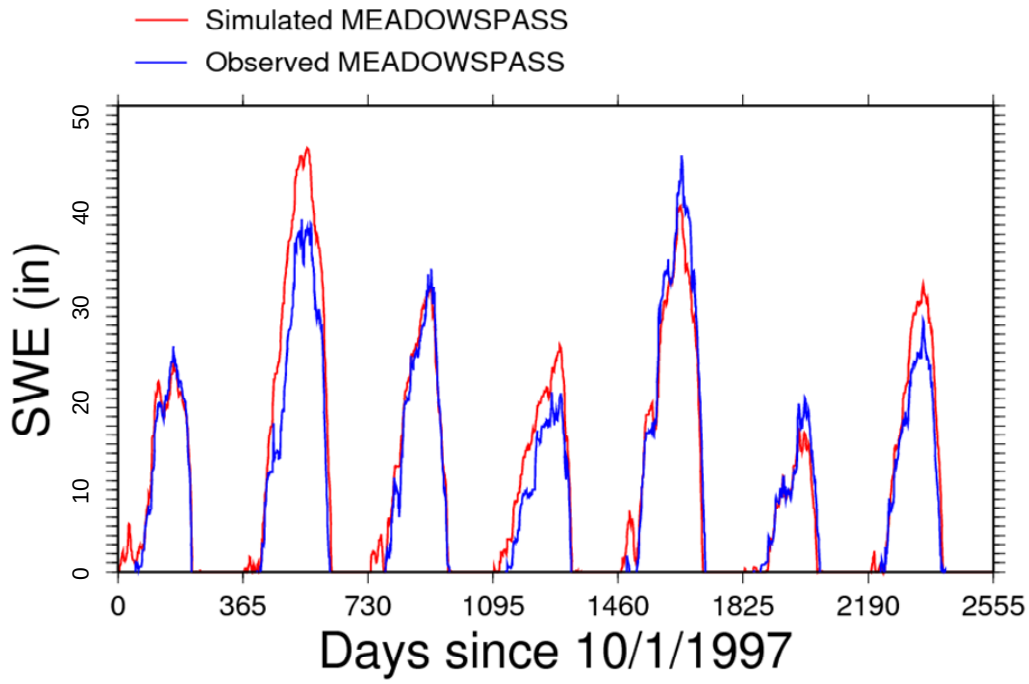

Figure 18: Simulated and Observed SWE at Meadows Pass SNOTEL site

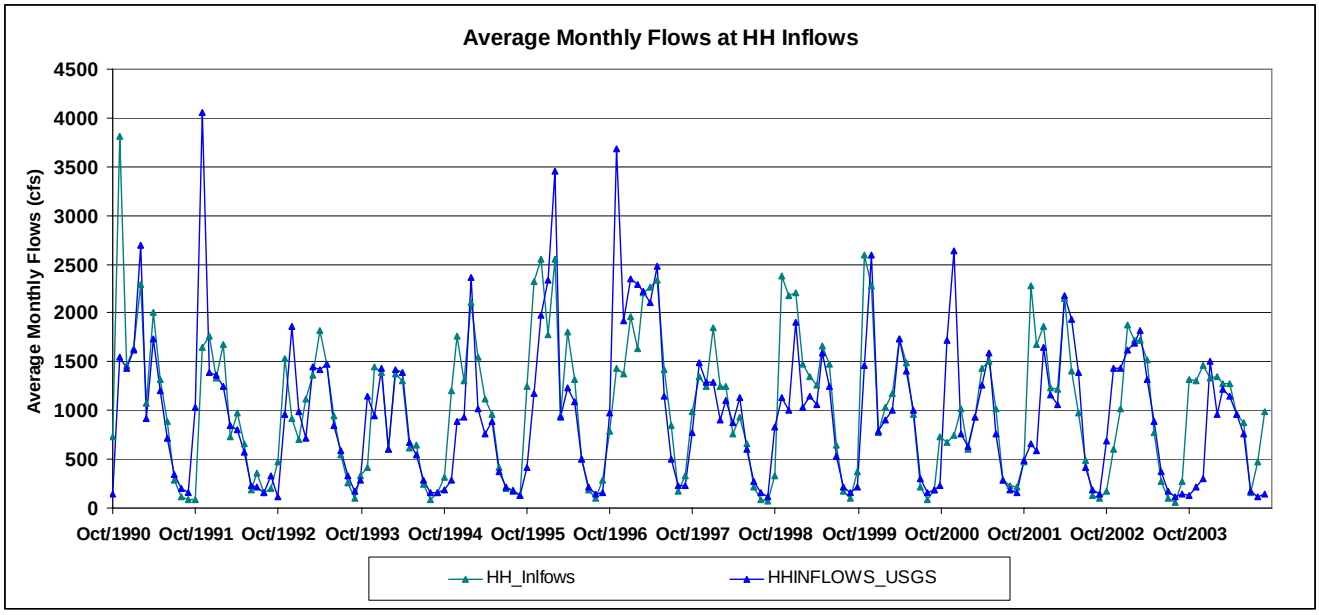

Figure 19: Simulated and Observed Average Monthly Flows at HH Inflow

Monthly observed and simulated flows are presented in Figure 19. It is evident from the plots that some of the flood peaks that are observed at HH Inflow are under simulated, but as previously noted, it is difficult to determine the amount of model bias in relation to biases introduced from the gage and record reconstruction. There are months in which flood peaks are simulated within the model, but no record exists in the observed and vice-verse. Despite issues related to representation of storms that arise for the fall months, the spring and summer flows match very well for every year, including the timing of return for fall rains.

Sultan/Tolt River Simulation Results

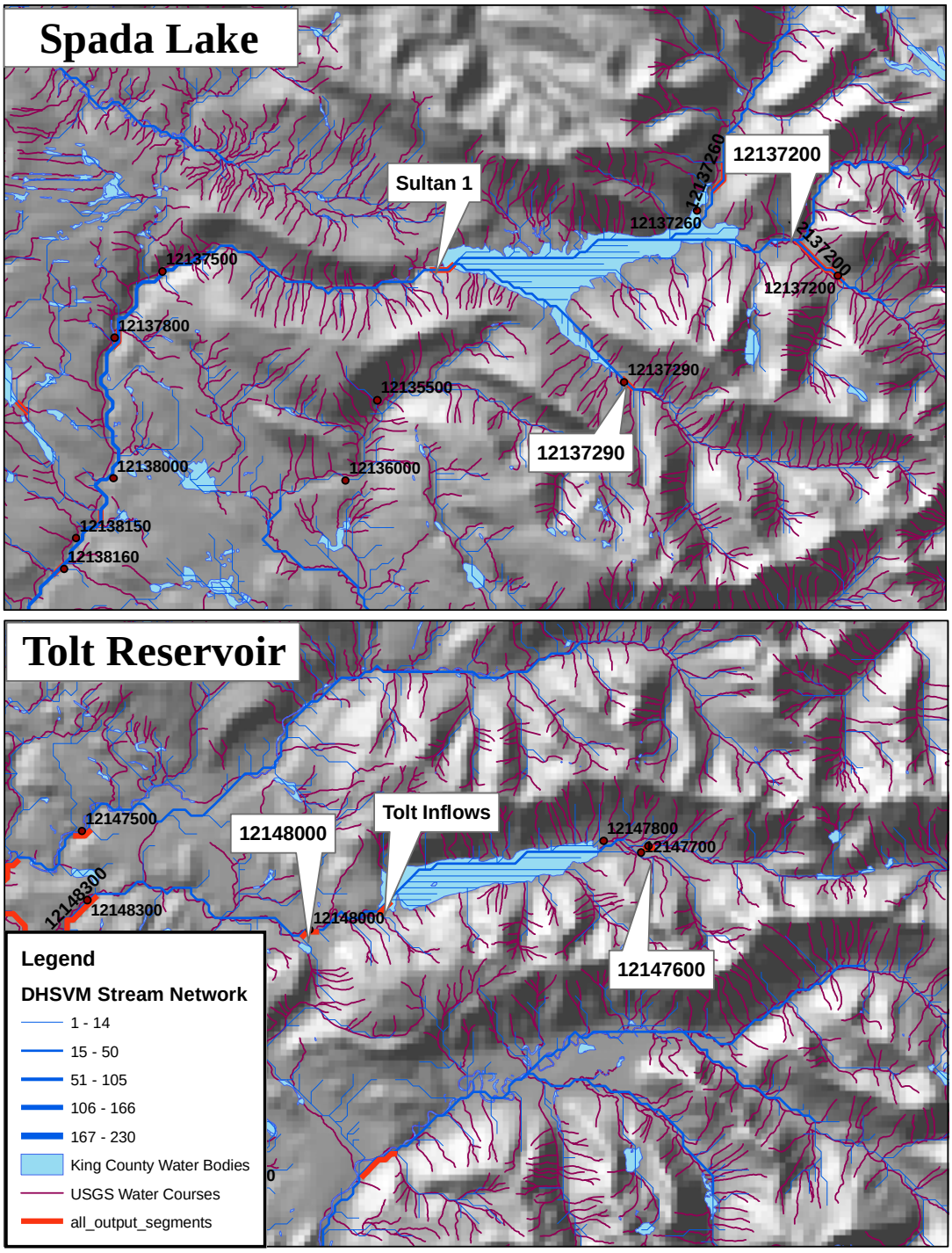

Figure 20: Sultan and Tolt System Calibration Points

The Tolt River and Sultan River are modeled using DHSVM. At each site, USGS gages are used as the calibration points. For the Tolt system, Gage 12147600 upstream of the reservoir and

Gage 12148000 downstream of the reservoir provide the majority of the observed information. Gage 12148000 has a very brief record (1952-1963) prior to the Tolt Dam being constructed.

Table 4: Data Sources for Calibration (Tolt and Sultan Rivers)

Gage	Gage Name	Maintainer	Period of Record
12147600	South Fork Tolt River near Index	USGS	10/1/1945 – 10/1/1993
12148000	South Fork Tolt near Carnation	USGS	10/1/1922 – 10/1/1963
12137290	South Fork Sultan River near Sultan	USGS	7/1/1963 - Present
12137200	Elk Creek near Sultan	USGS	8/1/1936 - Present

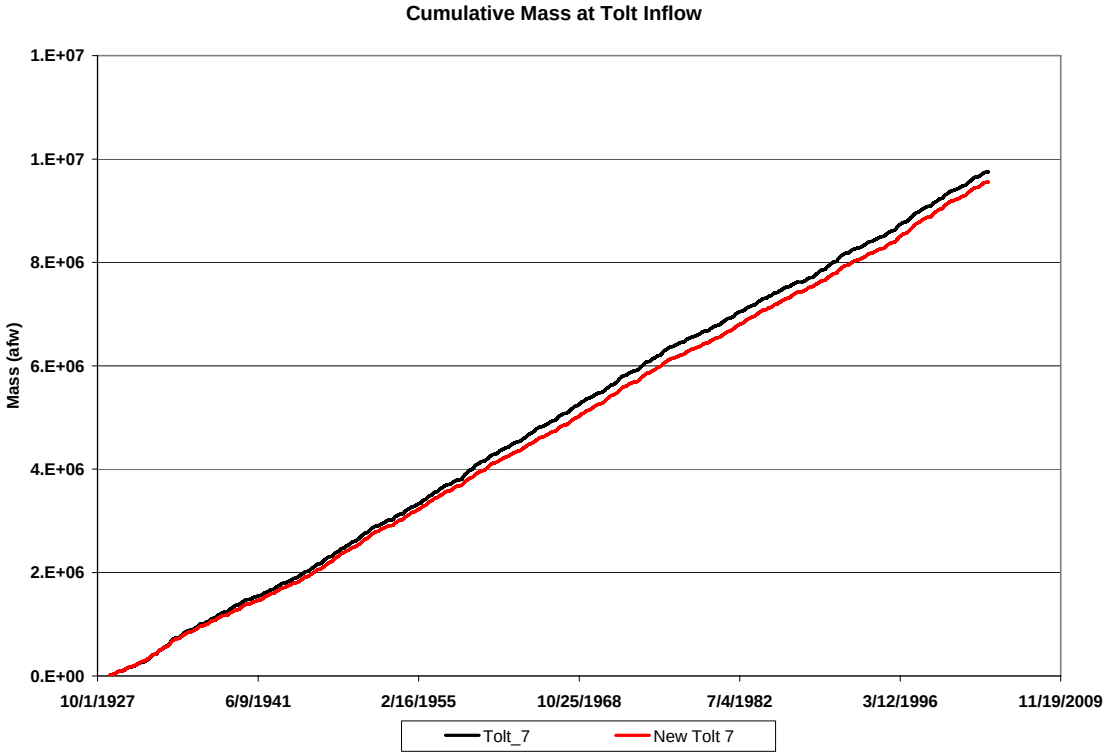

Figure 21: Mass Curve at Tolt Inflows

Figure 21 displays the cumulative mass at Tolt Inflow, which is the summation of SPU's recreated data point Tolt 7 (USGS gage 12147600) and Tolt 20. A comparison of mass with the USGS gage (not depicted) paints a similar picture. Total mass is negatively biased by approximately one percent. The annual hydrograph, depicted in Figure 22, compares observed flows at Gage 12147600 to the modeled flow. Overall the flows agree quite well, with modeled flows having slightly higher November flows and slightly lower summer flows than those observed. A time series depiction, found in Figure 23 also displays this good agreement at a more aggregate level, ie, on an acre-feet per week basis of flow.

Observed streamflow at Gage 12148000 is found in Figure 25. Only the years between 1952 and 1963 can be compared. The model replicates the observed flow adequately, though winter flows tend to be a slightly under simulated.

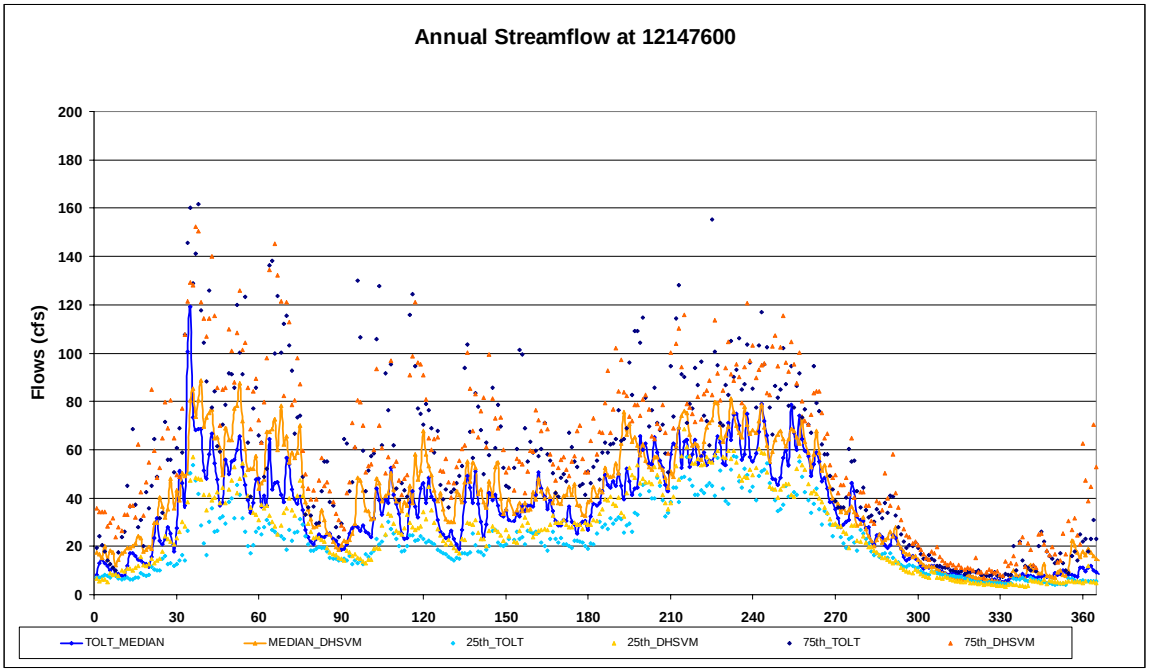

Figure 22 : Annual Hydrograph at 12147600

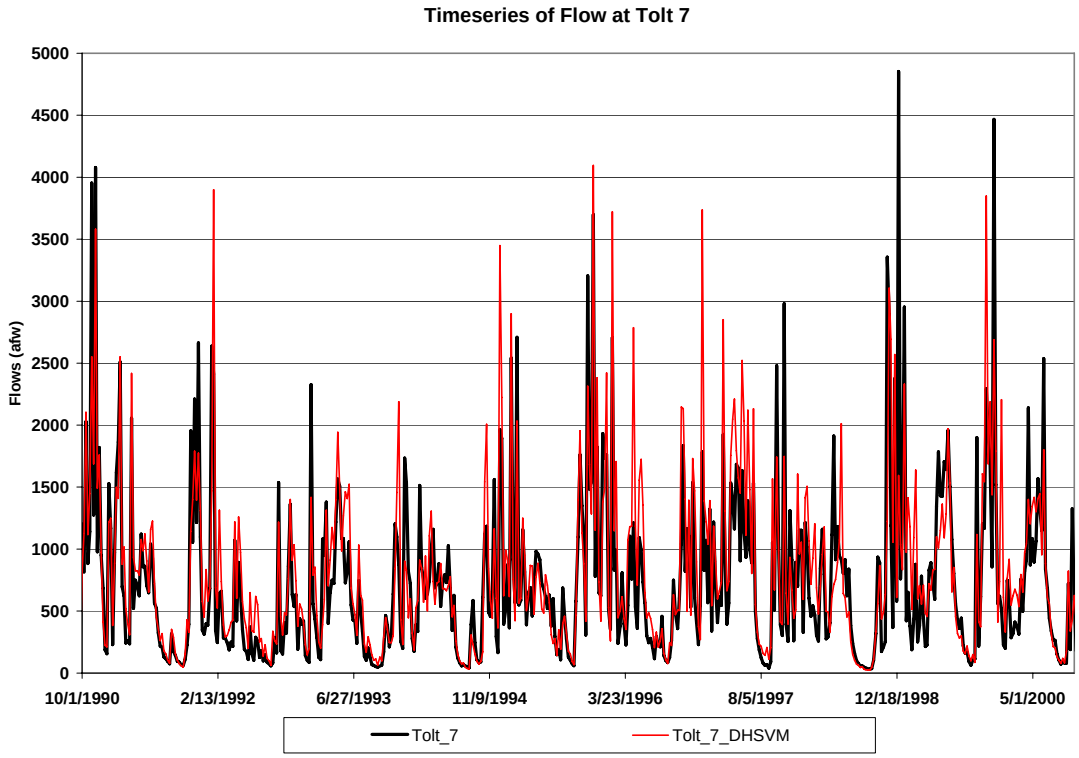

Figure 23: Time Series of Streamflow at Tolt 7

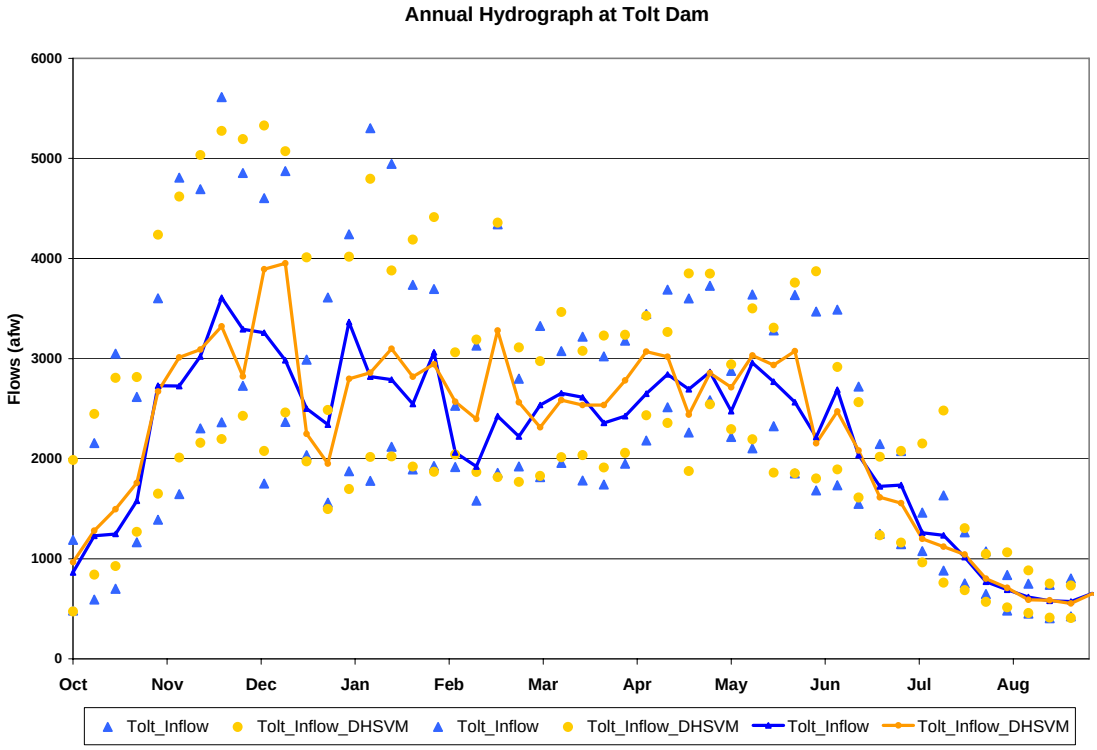

Figure 24: Annual Hydrograph at Tolt Inflow

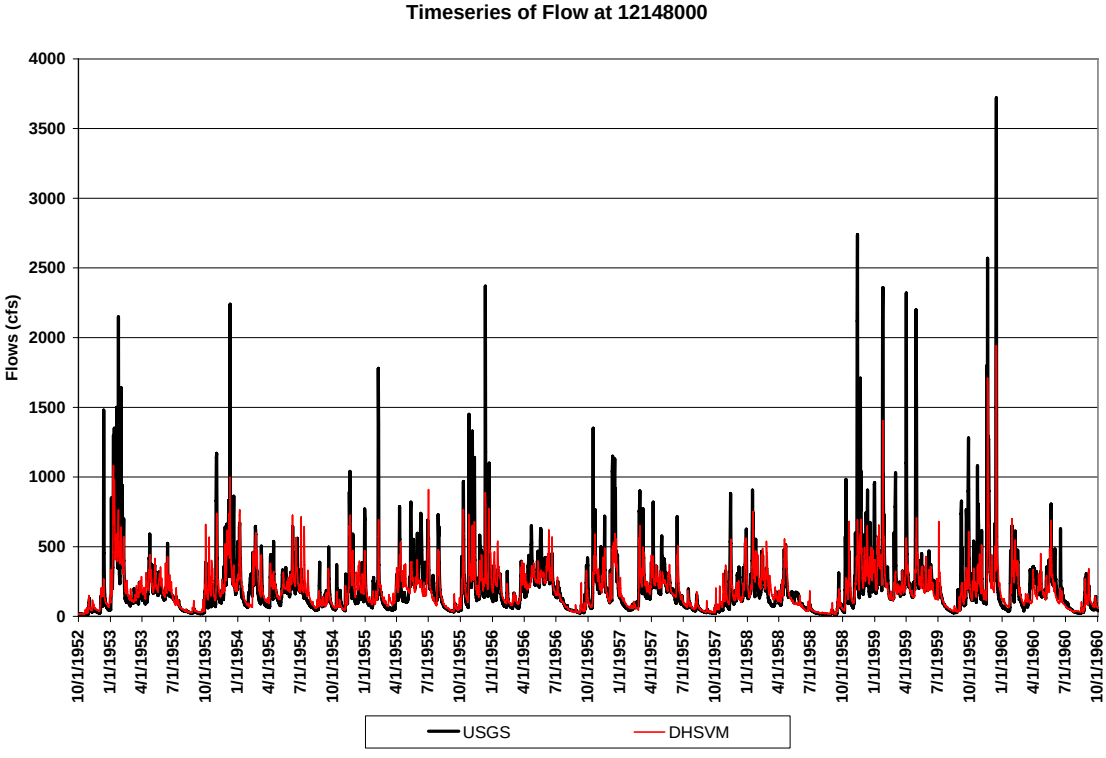

Figure 25: Time Series of Streamflow at 12148000

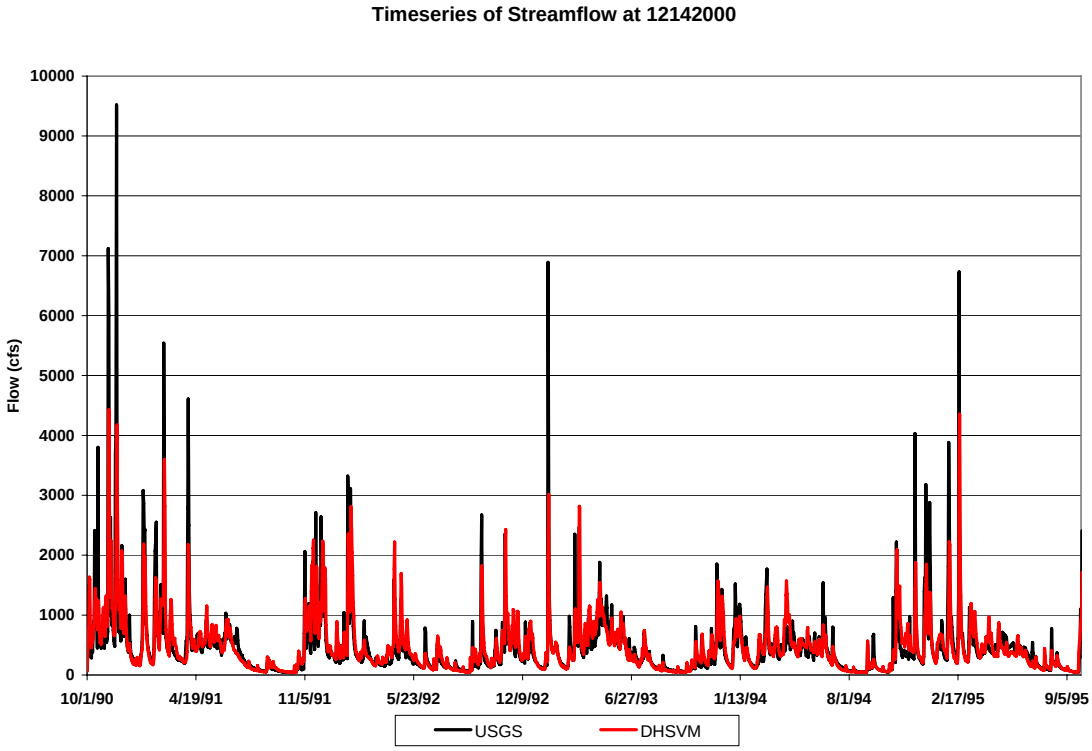

Figure 26: Time Series of Streamflow at 12142000

Figure 26 contains observed streamflow at Gage 12142000 compared to the modeled flow. This cursory evaluation is appropriate because of the close proximity of the gage even though it is located on the Snoqualmie River. This gage has a long historic record, (1929 to present). This gage is also the primary gage used to reconstruct streamflow below the Tolt Dam and to synthesize streamflow before the 1960's at Gage 12147600. As the time series indicates, DHSVM performs remarkably well in representing flows at this gaging station. The highest winter peaks are occasionally missed, but overall flows are modeled accurately. A positive bias of two percent exists for the cumulative mass difference between observed and modeled flow.

Figure 27 compares SWE at Skookum Creek SNOTEL to DHSVM simulated SWE. DHSVM over simulates for water year 2000. Other periods plotted are in good agreement between simulated and observed SWE for total SWE and timing of accumulation.

Average monthly simulated and observed flows at Tolt Inflow are displayed in Figure 28. There is good agreement between observed and simulated flows at Tolt Inflow. There is slight under estimation of some peak flows, but in general the simulation matches both the quantity and timing of observed flow. Spring and summer months are well simulated as is the timing of fall rain return.

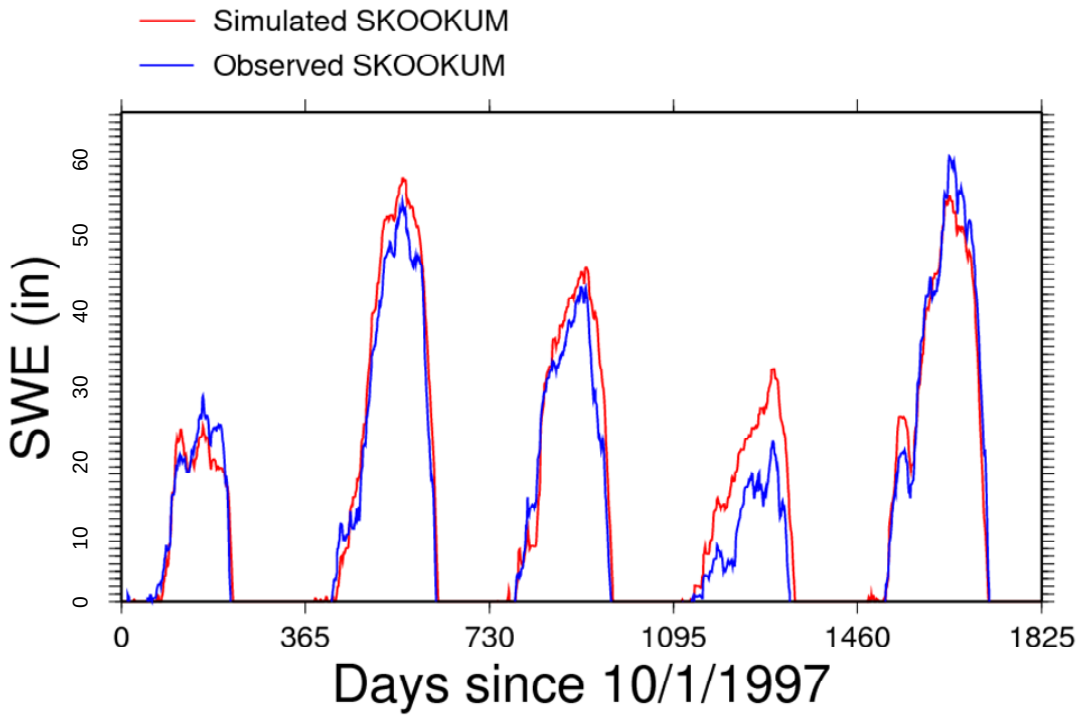

Figure 27: Simulated and Observed SWE at Skookum SNOTEL site

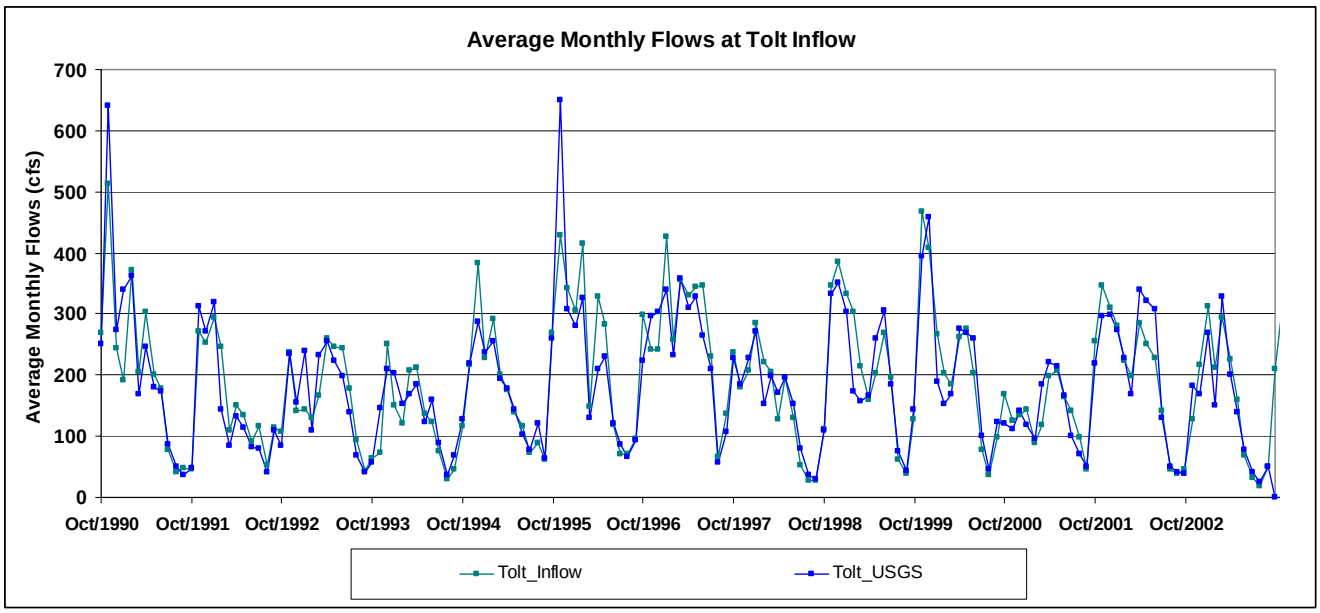

Figure 28: Simulated and Observed Average Monthly Flows at Tolt Inflow

The Sultan River system has two gages above Spada Lake for which model comparison is performed. Gage 12137290 is located on the South Fork Sultan River. The gage history is recent, starting in 1991 and continuing through the present. Gage 12137200 was located on Elk Creek and in service from 1976 to 1983.

Annual hydrographs for gages 12137290 and 12137200 are presented in Figure 29 and Figure 30. Although limited historic records are available, both annual hydrographs show good agreement between modeled and observed flows. There is a slight negative bias at 12137290 in July for median flows and lower 25th percentile flows. To examine how the model performs with large storms, a time series plot is presented in Figure 31. The winter peak flows are not always captured well, but in general, large flows are captured adequately. The modeled summer flows in Figure 31 match well with the observed streamflows at 12137290. Overall, the model appears to perform adequately for the Sultan River and Spada Lake.

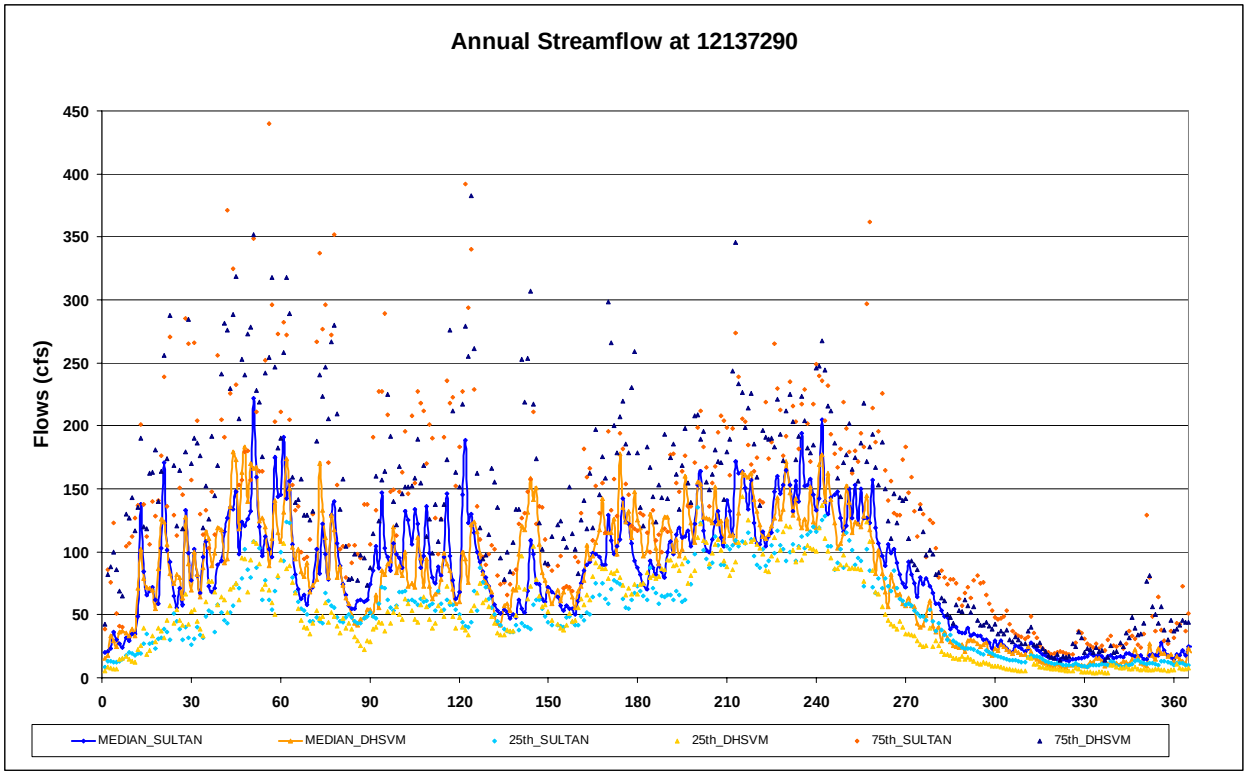

Figure 29: Annual Hydrograph at 12137290

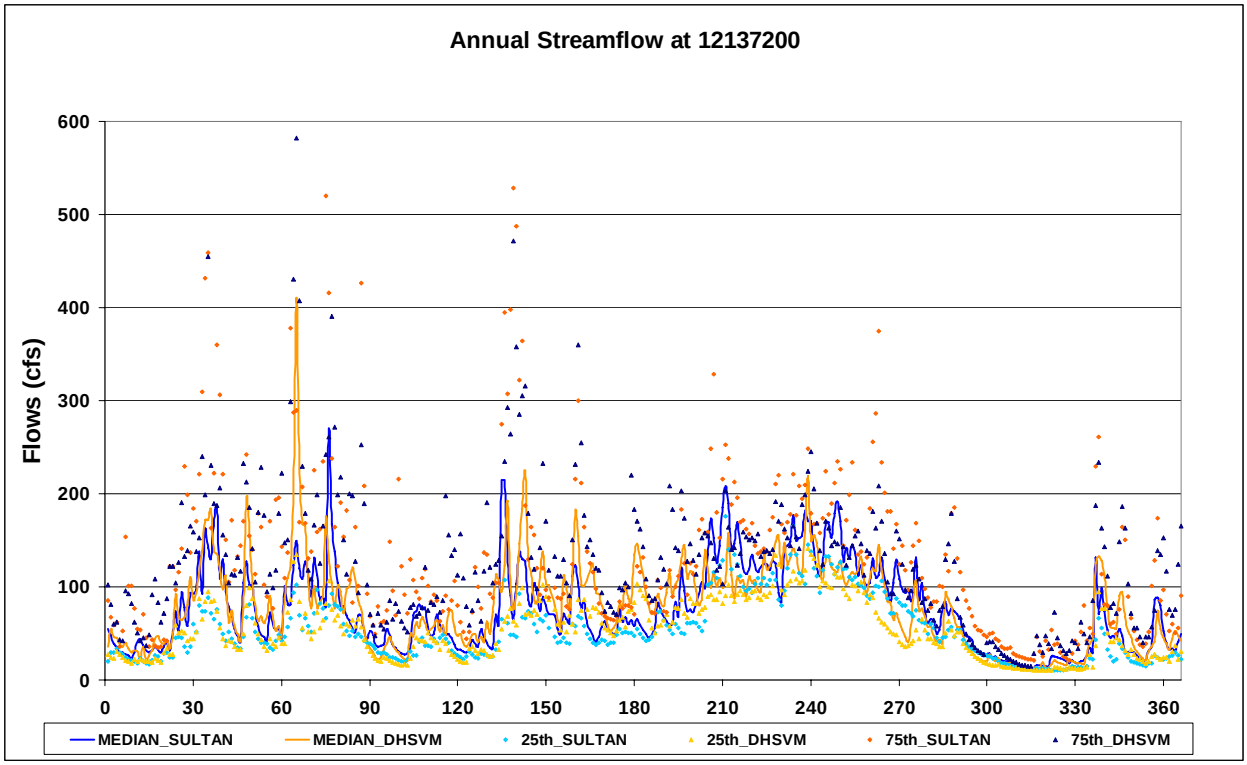

Figure 30: Annual Hydrograph at 12137200

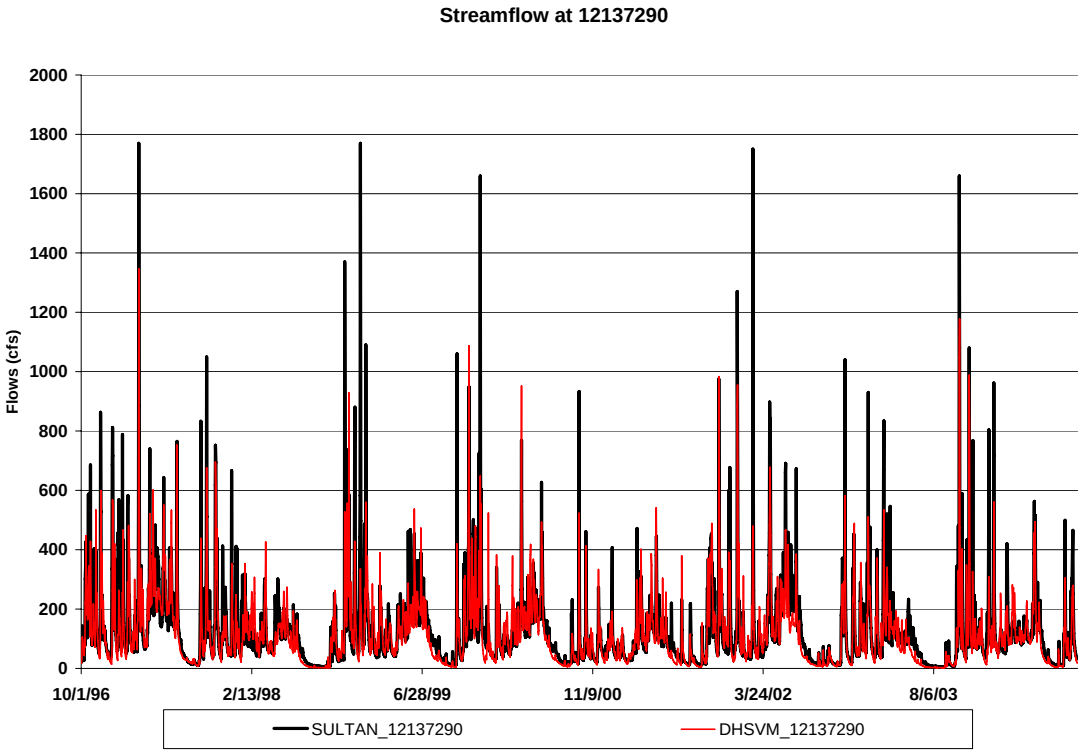

Figure 31: Time Series of streamflow at 12137290

Due to slight bias in simulation of winter flows, the same correction scheme used to augment Cedar 2 flows in the summer months is applied to the Sultan flows in the winter months. Figure 32 presents flows at Gage 12137290 after the correction scheme is applied. When compared to Figure 31 it is apparent that the correction scheme improves peak flow accuracy in the Sultan system. This is also noticeable in cumulative mass, where the correction improves the total mass to a one-percent under simulation of the observed flows over fourteen years.

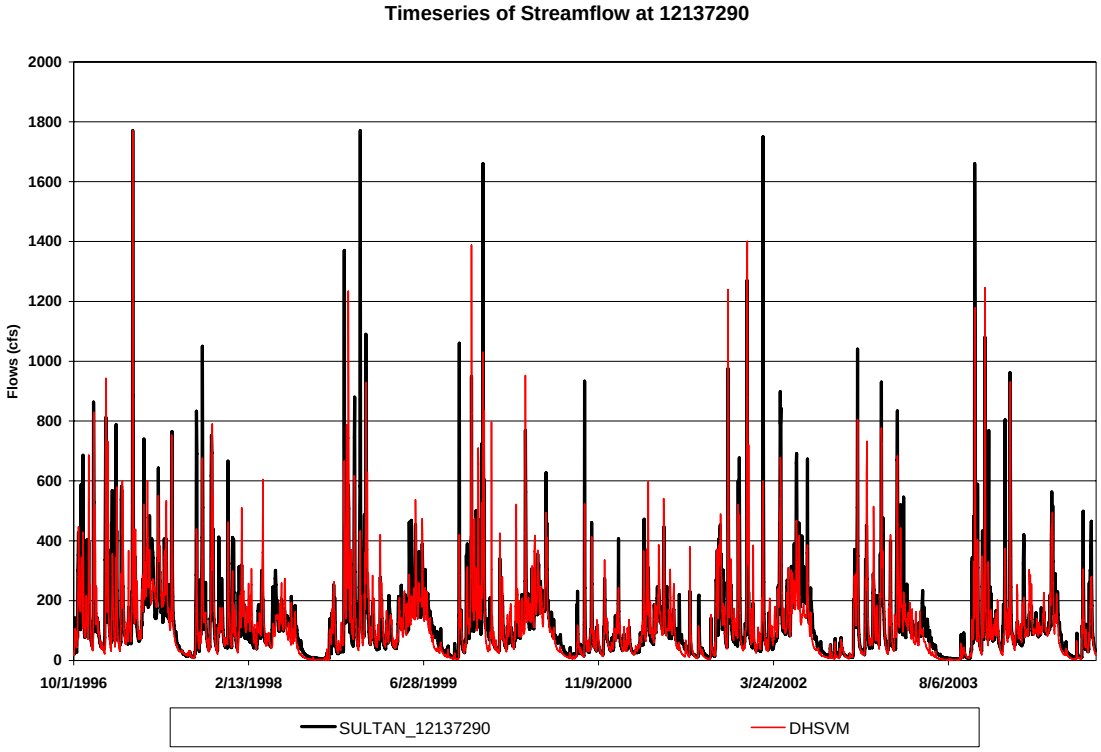

Figure 32: Time Series of Bias-Corrected Streamflow at 12137290

Figure 34 compares SWE at the Alpine Meadows SNOTEL site to DHSVM simulated SWE. The 1997 snowpack is under simulated, though other years show good results in both total amount and timing for SWE. Figure 35 contains corrected observed monthly and simulated flows at Sultan 1. The model simulates this basin well, with timing and monthly flow almost identical to the observed flows. In general, the model physics represent water cycling well within the Sultan basin, but small corrections are needed for peak winter flows due to model representation of storm systems. The spring and summer months, where no correction occurs are simulated well as are flows during the return of fall rains.

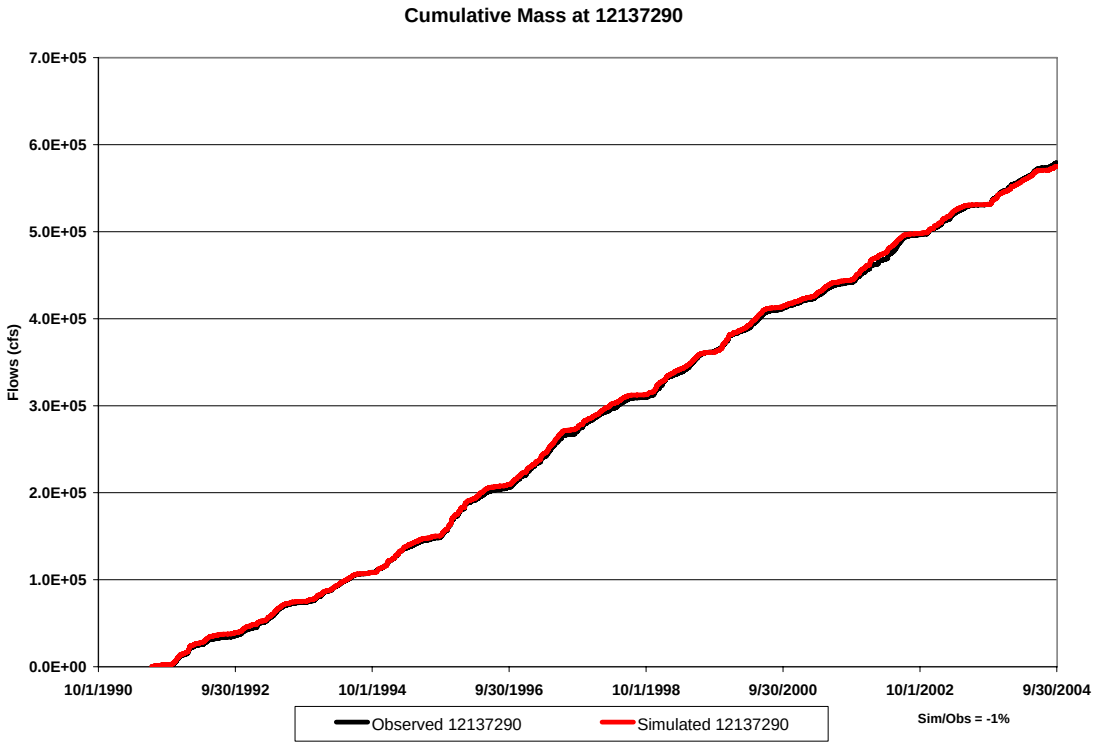

Figure 33: Cumulative Mass at 12137290 after Bias-Correction

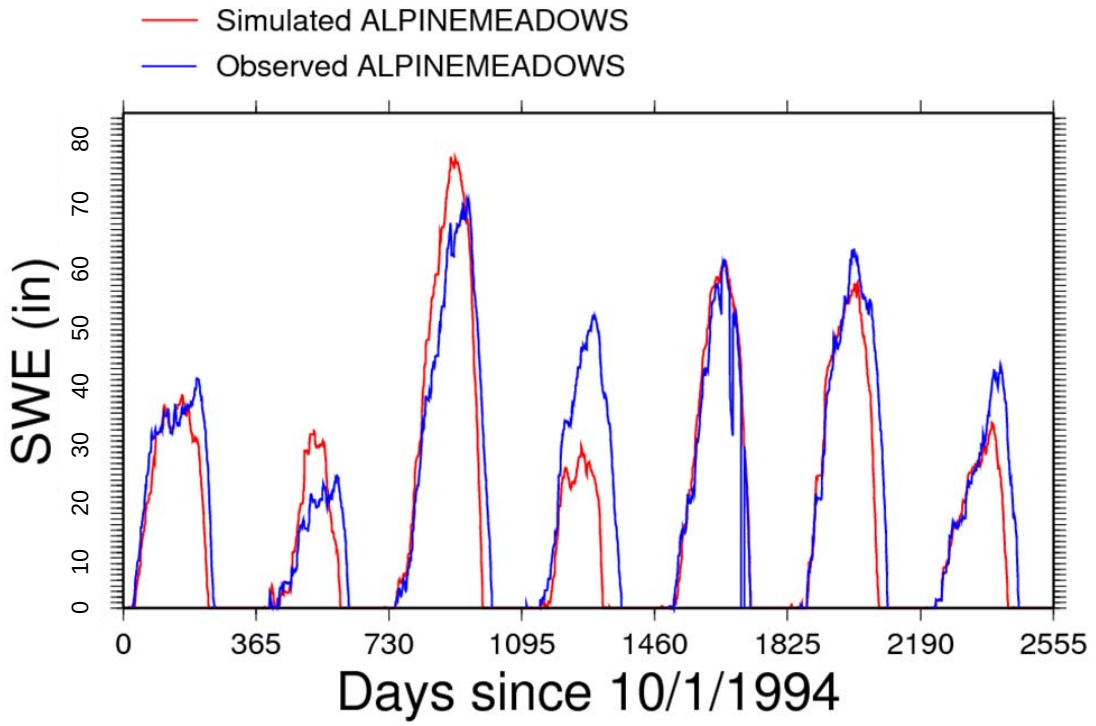

Figure 34: Simulated and Observed SWE at Alpine Meadows

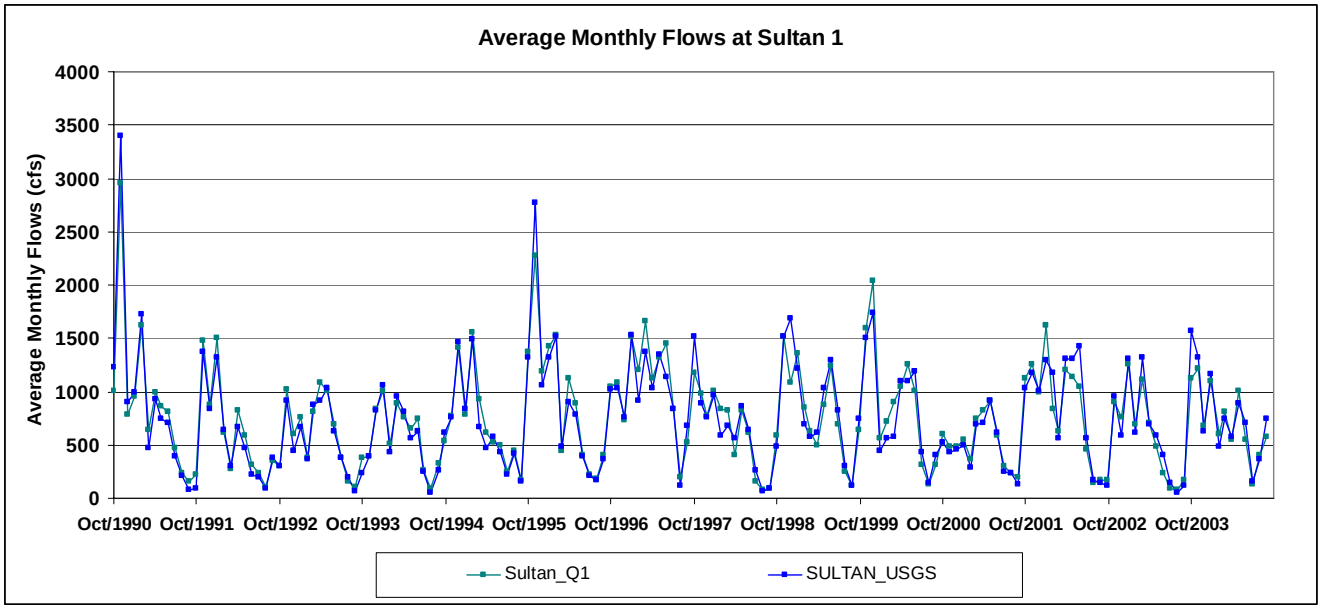

Figure 35: Simulated and Observed Average Monthly Flows at Sultan 1

White River Simulation Results

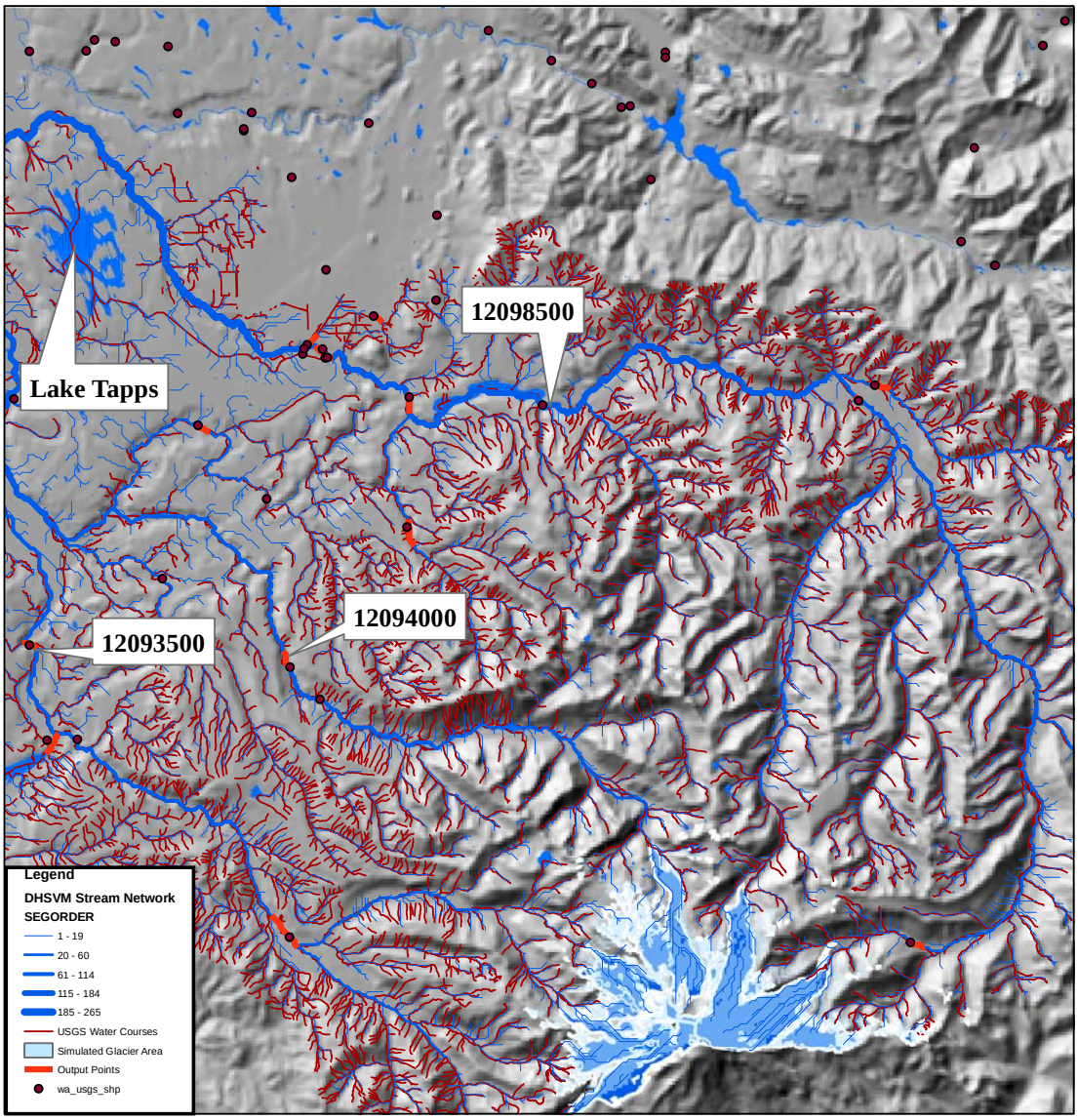

Figure 36: White - Puyallup River Calibration Points

The White and Puyallup River watershed model calibration uses three USGS gages, 12094000, 12093500, and 12098500. All gages have long records, though gage 12094000 has many gaps in the record. Figure 36 shows the location of the USGS gages. Gage 12094000 has missing records from 1977 – 1991, and gage 12098500 has little no records available from 1933 – 1938. Table 5 contains the period of record available for each gage.

Figure 37 contains the annual hydrograph for gage 12094000 on the Carbon River. The median simulate flow matches winter and summer flows of the observed record well, though some winter flows are slightly low.

Table 5: Data Sources for Calibration (White, Carbon, and Puyallup Rivers)

Gage	Gage Name	Maintainer	Period of Record
12098500	White River near Buckley	USGS	5/1/1928 – Present
12097000	White River at Greenwater	USGS	4/1/1929-10/17/1975
12094000	Carbon River near Fairfax	USGS	4/1/1929 – Present
12093500	Puyallup River near Orting	USGS	10/1/1931 - Present

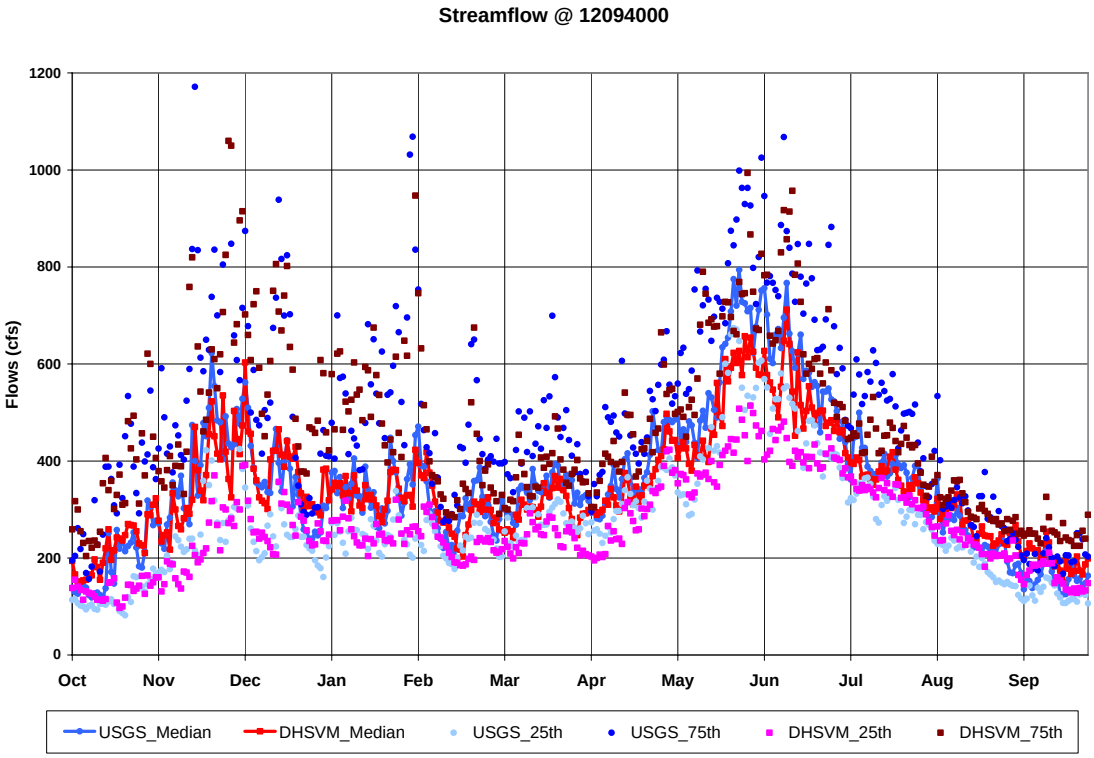

Figure 37: Annual Streamflow at 12094000

This is attributable to the challenge of accurately capturing peak flows in the winter and missing periods of record. Figure 38 presents the flows between 1995 and 2004. There is good agreement between flows in all seasons, though peak flows for the largest events are partly captured. For the years 1993 – 2004 the cumulative mass is close to observed, being negatively biased by approximately one percent.

Figure 39 presents the annual hydrograph for USGS Gage 12097000. The hydrograph has positive biases in the late summer months and autumn months but overall matches the historic record well. The period of record for this gage is through the 1970's, which may also be the cause of the discrepancy seen between the observed and modeled flows.

Modeled streamflows for the Puyallup River match the observed record well. Figure 40 contains the annual hydrograph for Gage 12093500. The flows at gage are negatively biased in the late summer months with modeled flows slightly less than those observed for the Puyallup.

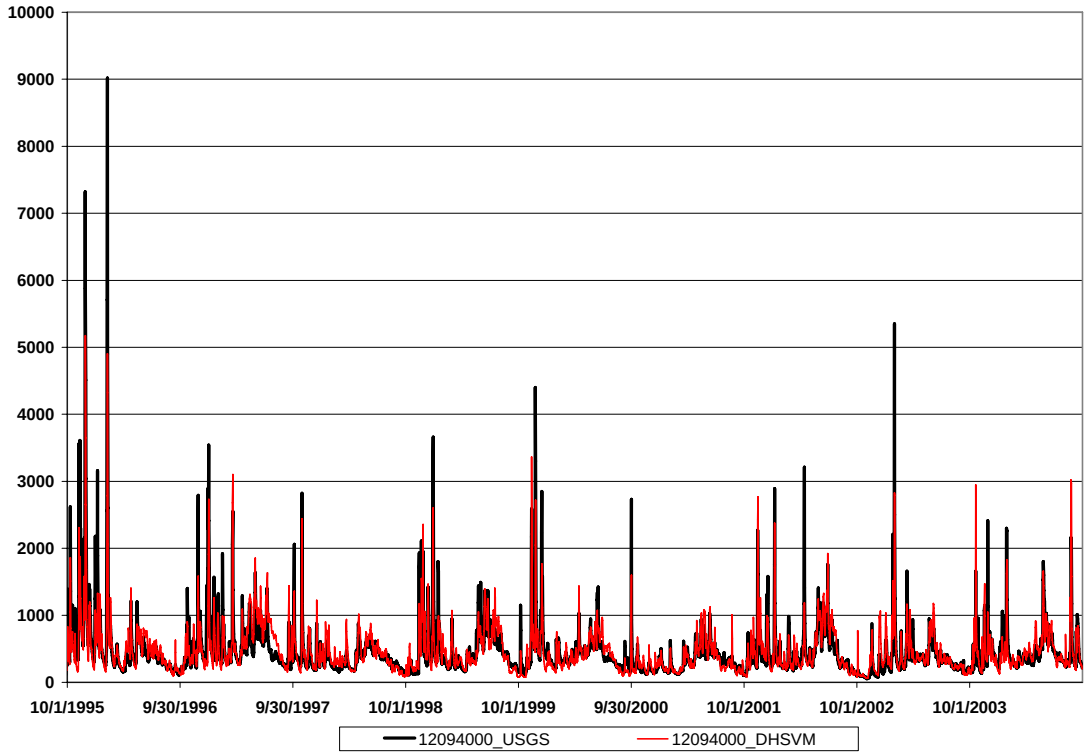

Figure 38: Time series at 12094000

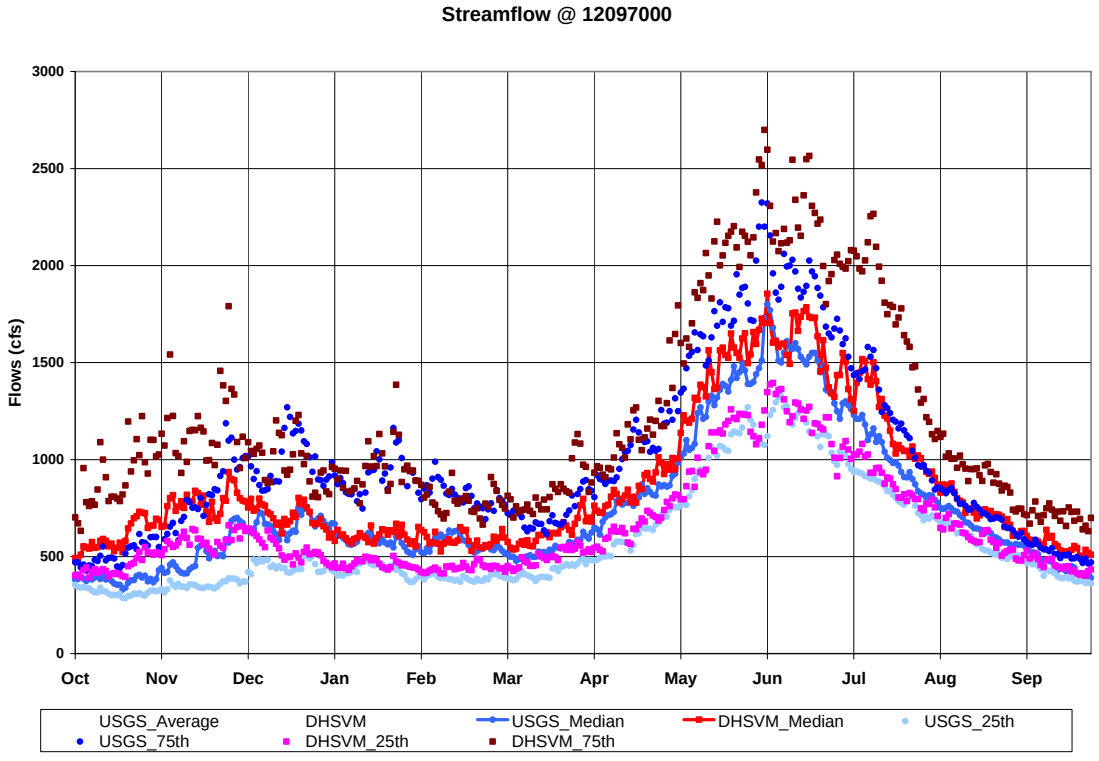

Figure 39: Annual Hydrograph at 12097000

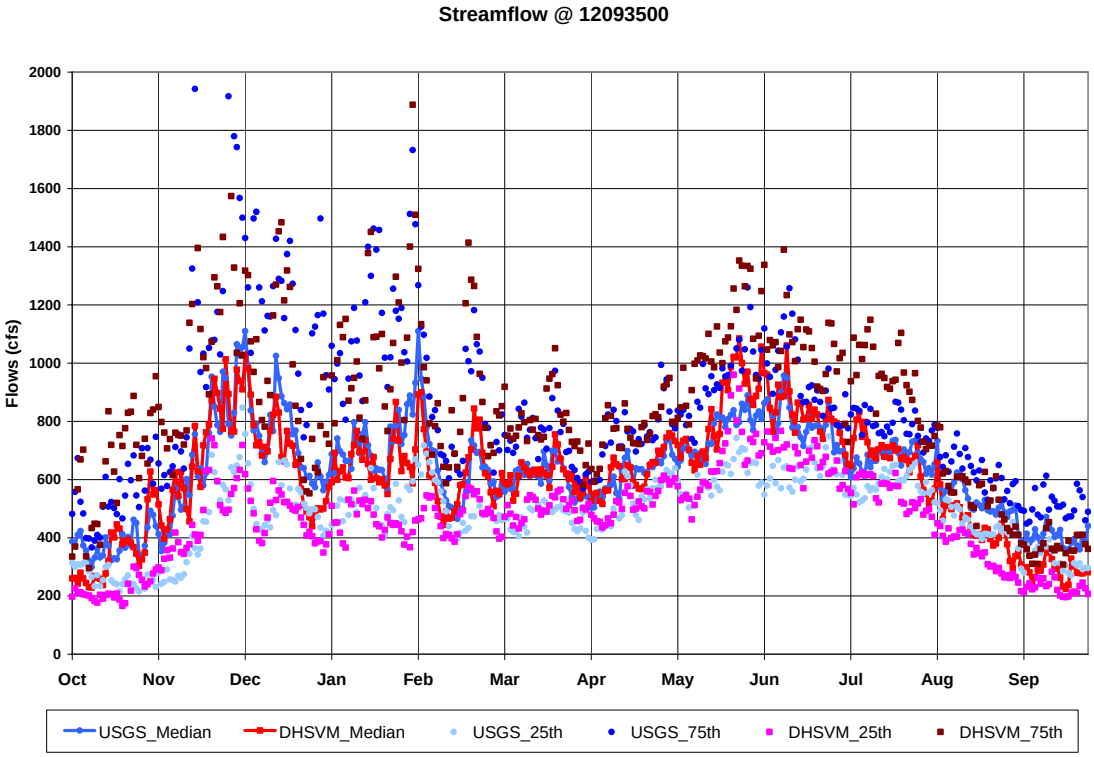

Figure 40: Annual Streamflow at 12093500

The initial flows generated for the White River were positively biased. This is caused by a stream-network error. Figure 41 highlights the incorrect routing in the White River. Flows in the South Prairie Creek were incorrectly routed as flowing into the White River Basin. This mistake was remedy to obtain the proper flows at USGS Gaging Station 12098500 using a two-phase approach. First, the incorrectly routed flows are subtracted from the main stem of the White River. This reduced much of the positive bias, though some positive bias still remained. Using the scheme developed to remove bias in the other basins, flows at USGS Gaging Station 12098500 were corrected for each month, removing the positive bias that existed in each month. Figure 42 and Figure 43 present the uncorrected and corrected flows for USGS Gaging Station 12098500. The correction scheme works well and has been applied to the climate impacted flows to remove the positive bias.

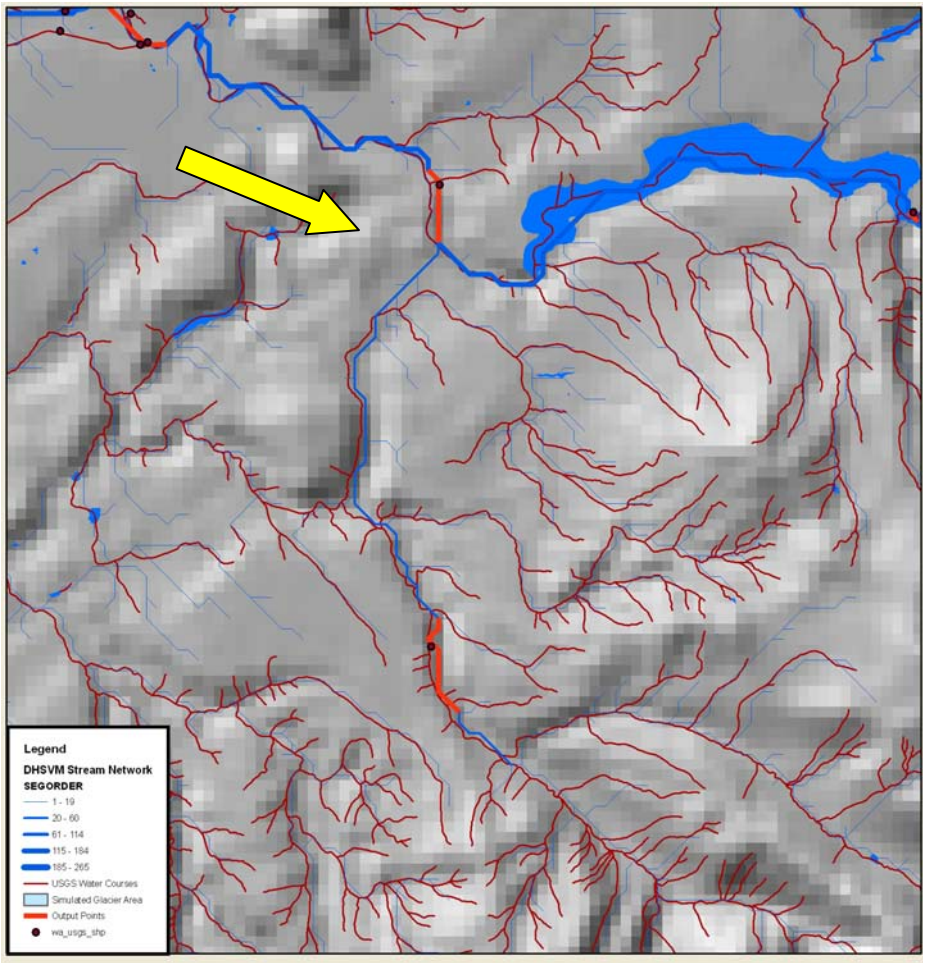

Figure 41: Model Stream Network Error for White River

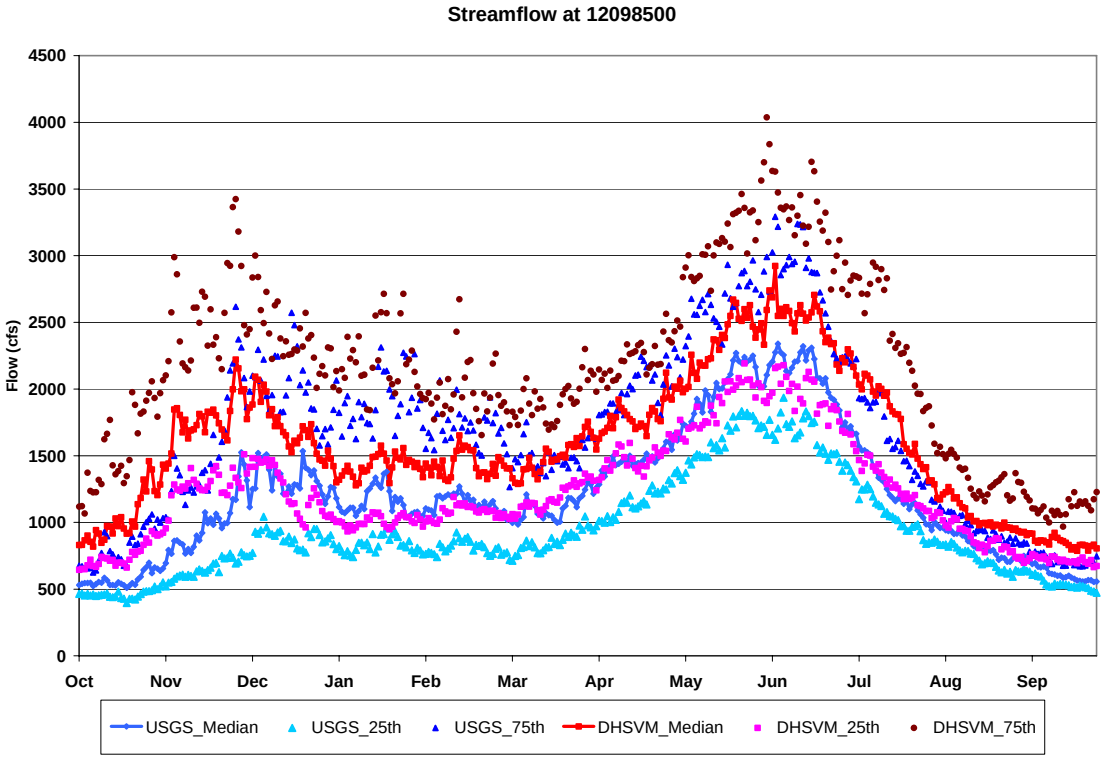

Figure 42: Annual Flows at 12098500 before correction

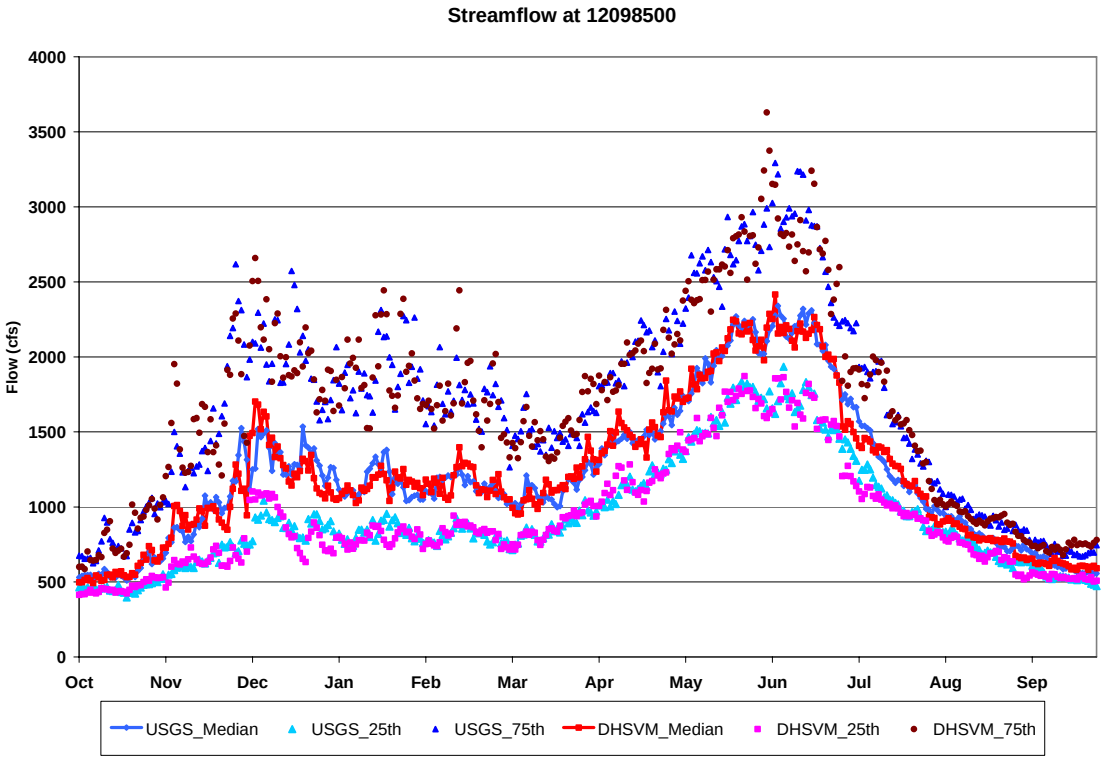

Figure 43: Annual Streamflow at 12098500

Glacier Discussion

Past DHVSM model formulations of this basin represented the glaciers as permanent snowpack. The new analysis done for this research contains a new glacier feature to DHSVM, where the accumulated snowpack is allowed to retreat or flow based on glacier physics. The ablating and accumulation processes remain the same as previous versions.

The motivation for the glacier movement component was to improve the ability to model the impacts of climate change in watersheds that contain significant quantities of glacial ice. This component allows the high altitude snow for a glacier to move down slope into the ablation zone where it can be melted. The glacier component is based upon the work of Patterson (1994). The equations are used to compute basal shear stress and average glacier velocity. The ice is then routed down slope according to the surface elevation. The primary equations used for glacier simulation are:

1) $\tau_b = -\rho g h \cdot \sin\theta$, where basal shear stress is a function of ice density, gravity, ice thickness, and hill slope, and
2) $\bar{u} = \frac{2A}{n+2} \cdot \tau_b^n \cdot h$, where average glacial velocity is a function of the Arrhenius value (A), Glen's Constant (n), ice thickness, and basal shear stress. The Arrhenius value (A) is defined as:
3) $A = A_\circ \cdot e^{-Q/RT}$, where R is the universal gas constant, T is the temperature of the ice, and Q is the activation energy for creep. Flux of ice per pixel during a DHSVM time-step is computed as:
4) Ice Flux $= \bar{u} \cdot h \cdot dx \cdot dt \cdot f$, where f is a fraction of SWE allowed to move.

The fraction of SWE flux parameter provides numerical stability and is a calibration parameter. Ice movement is constrained to move only when the basal shear stress exceeds atmospheric pressure, when this occurs; ice is routed as fractions of total flux towards eight different directions.

Figure 44 contrasts modeled glacier extent overlain on an aerial photo of Mount Rainier. The orange areas represent high (75-100 meter) accumulations of snow water equivalent (SWE). The blue area represents areas with 75 meters or less of SWE. Overall, the glaciers appear to closely match observed extents of the glaciers on Mount Rainier. One area which is over-simulated is the Emmons Glacier, which extends too far down valley. During the 77 year period though, the glacier recedes. Figure 44 is only a snapshot in time of glacier extent. Glaciers are dynamic making period by period comparisons difficult. This is compounded by the lack of glacier monitoring records for Mount Rainer.

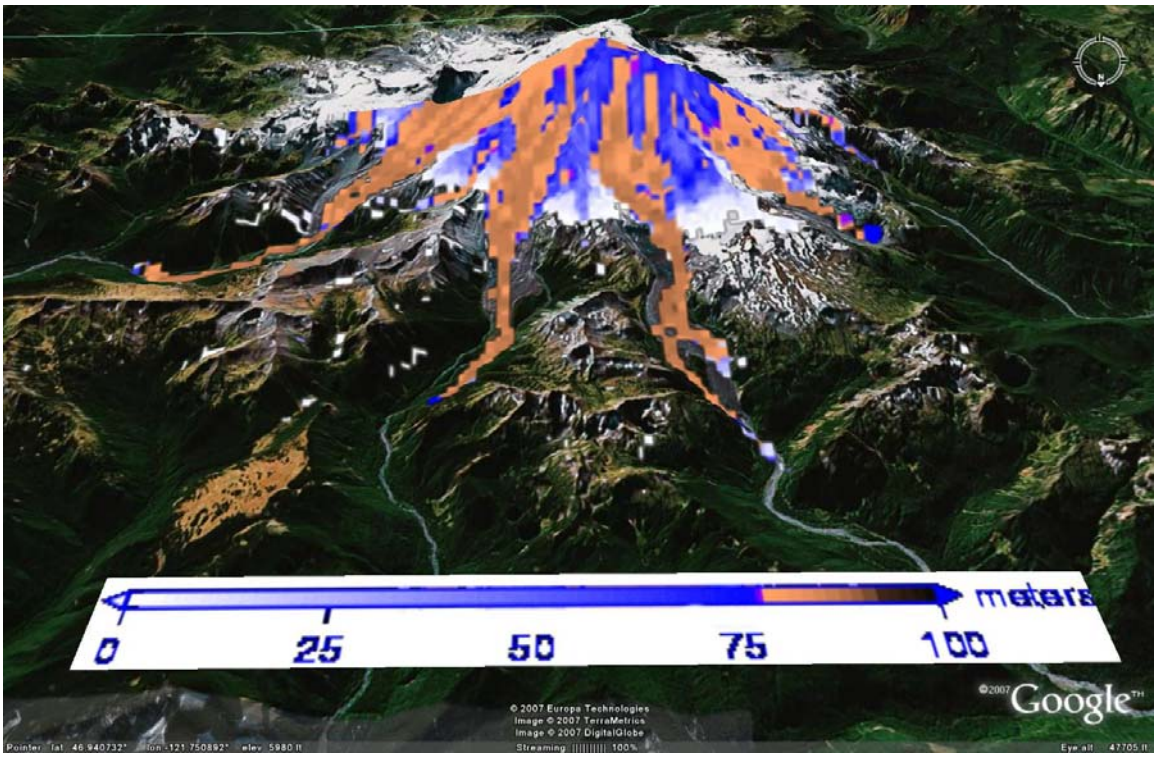

Figure 44: Modeled Glacier Extent

The current model is an improvement over previous model versions for this region because it includes the ability for ablation and accumulation in glacier dominated regions. Figure 45 and Figure 46 show a comparison between disabling and enabling glacier physics within DHSVM after 25 years of simulation. SWE levels are depicted as depths from five to two-hundred meters, ranging from dark brown to the light copper color. Without the glacier model, there is an unrealistic positive accumulation of SWE atop Mount Rainier as seen in Figure 45. The SWE map in Figure 46 displays SWE when allowed to move down slope, thereby removing the massive accumulation at the summit, and creating a glacier pattern that more closely matches that actually pattern found on the mountain.

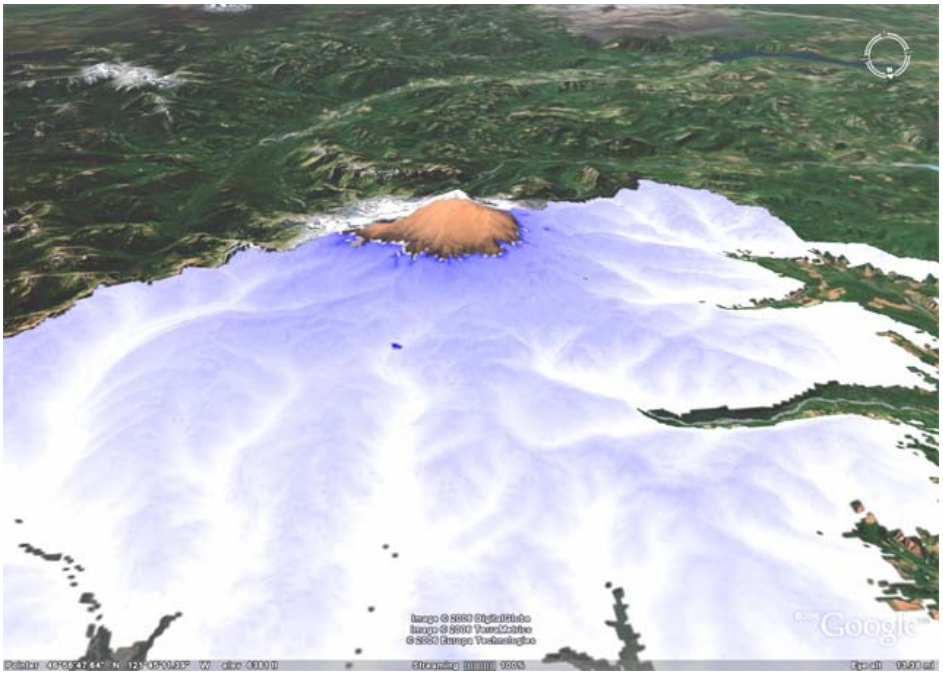

Figure 45: Modeling of SWE on Mount Rainer without Glacier Model enabled

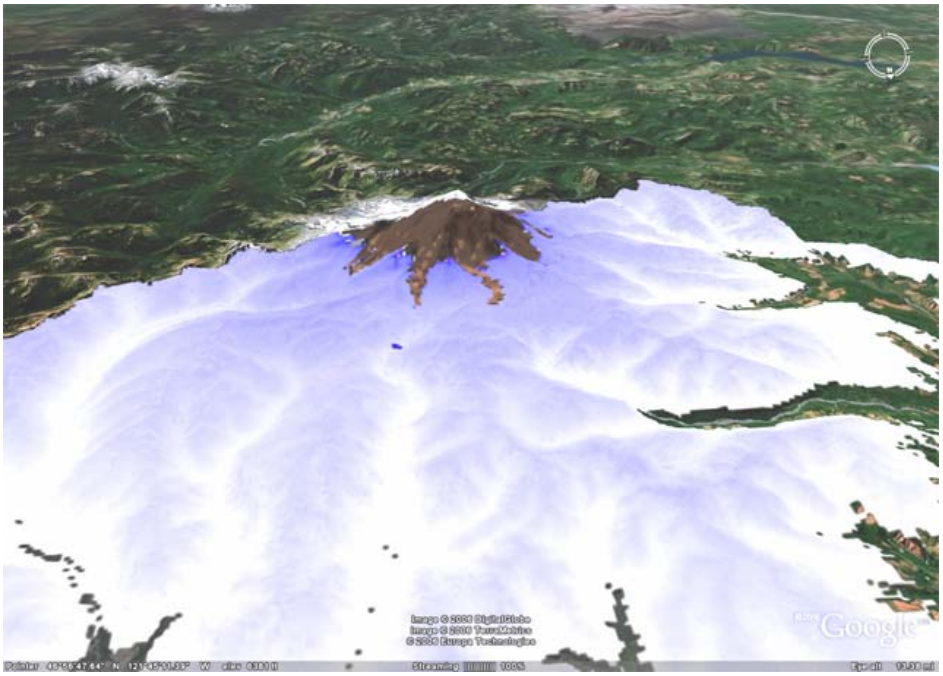

Figure 46: Modeling of SWE on Mount Rainier with Glacier Model enabled

Comparison of Simulated Historic to Climate Impacted Futures

DHSVM simulated historic streamflows serve as a basis of comparison for the DHSVM simulated streamflows generated given potential future climate conditions. This comparison provides insight as to the magnitude and timing of changes to streamflow patterns that may occur in future climate change scenarios.

Sultan River Climate Impacts Simulation Results

Figure 47 displays the impacts to Q1 streamflows, or the inflows to the Sultan Reservoir, associated with each climate scenario (ECHAM5_A2, GISS_B1, IPSL_A2) during each of the four periods of interest (2000, 2025, 2050, 2075).

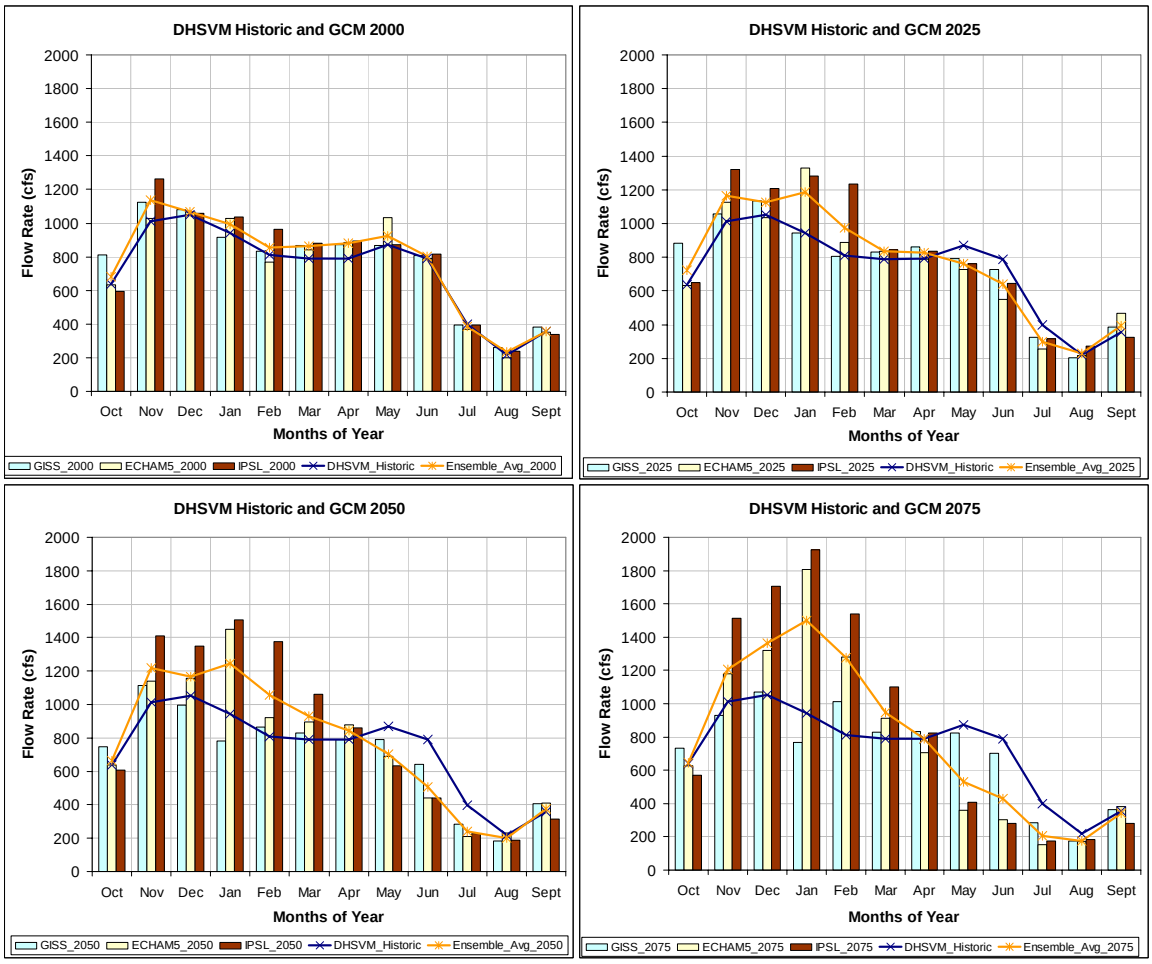

Figure 47: Simulated 2000, 2025, 2050, and 2075Projected Annual Average Streamflows at Q1

The ensemble average 2000 streamflows are slightly greater than the simulated historic flows year-round. The most significant increase in flow between the two periods occurs during winter and spring, though all values are within 10% (

Table 6). On an annual basis, the 2000 ensemble results in 6.0% more flow at the Q1 location than in the simulated historic record.

Table 6: Change in Forecasted Q1 Streamflows: Ensemble Average vs. DHSVM Historic

	Spring (MAM)	Summer (JJA)	Fall (SON)	Winter (DJF)	Annual
Ensemble_2000	9.0%	1.2%	8.3%	4.0%	6.0%
Ensemble_2025	-1.1%	-16.8%	13.6%	17.1%	5.6%
Ensemble_2050	0.9%	-32.6%	12.6%	23.6%	5.5%
Ensemble_2075	-7.6%	-42.4%	9.2%	47.4%	8.3%

The ensemble suggests that total annual flow at Q1 will remain relatively constant throughout the 21st century. All four simulation periods feature total annual inflows between 5.5% and 8.3% greater than those indicated by the simulated historic record.

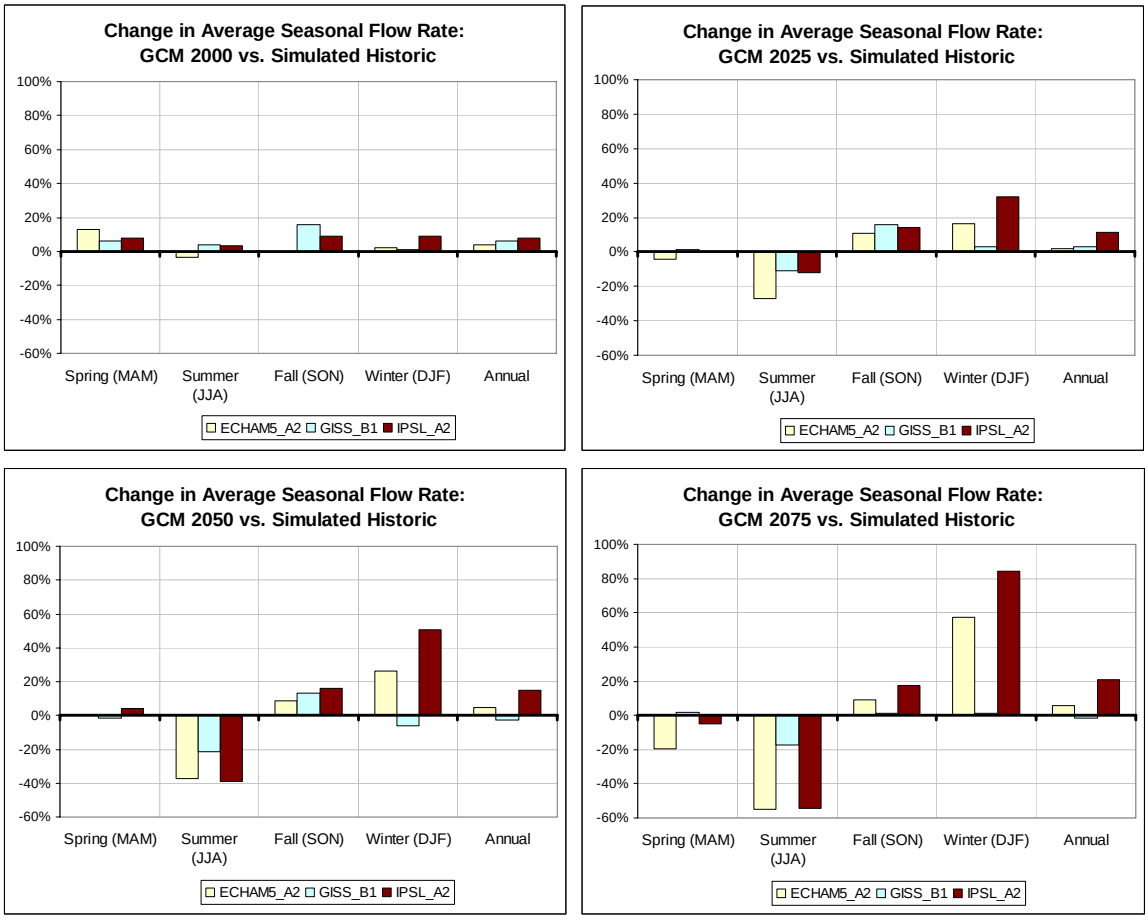

Figure 48: Projected Q1 Seasonal Streamflows for Each GCM Scenario

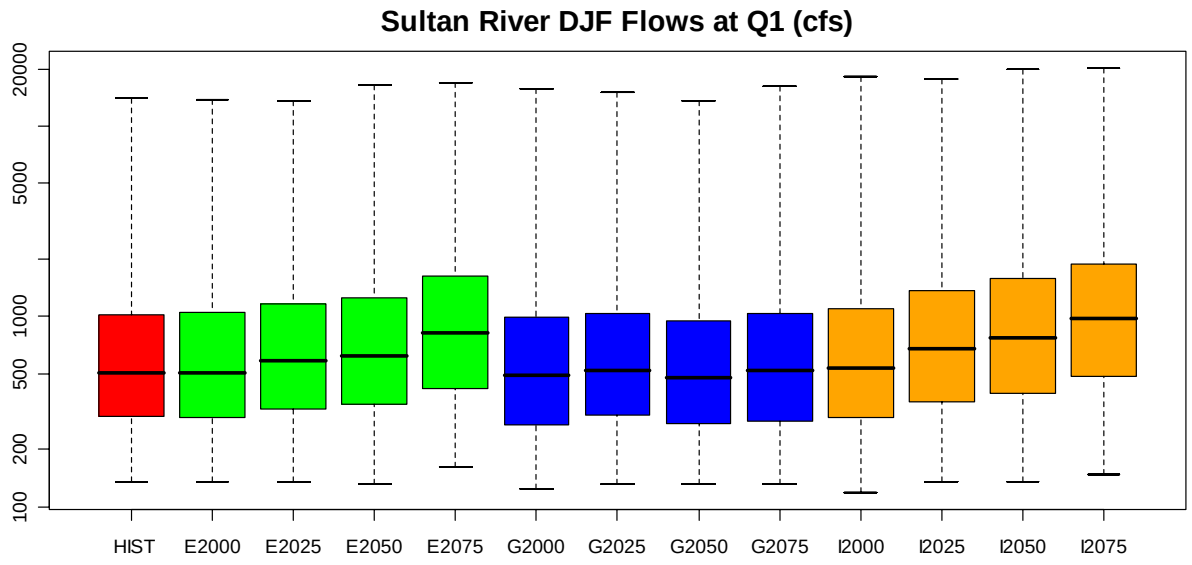

Figure 49: Boxplots of Projected Flows at Q1 for DJF

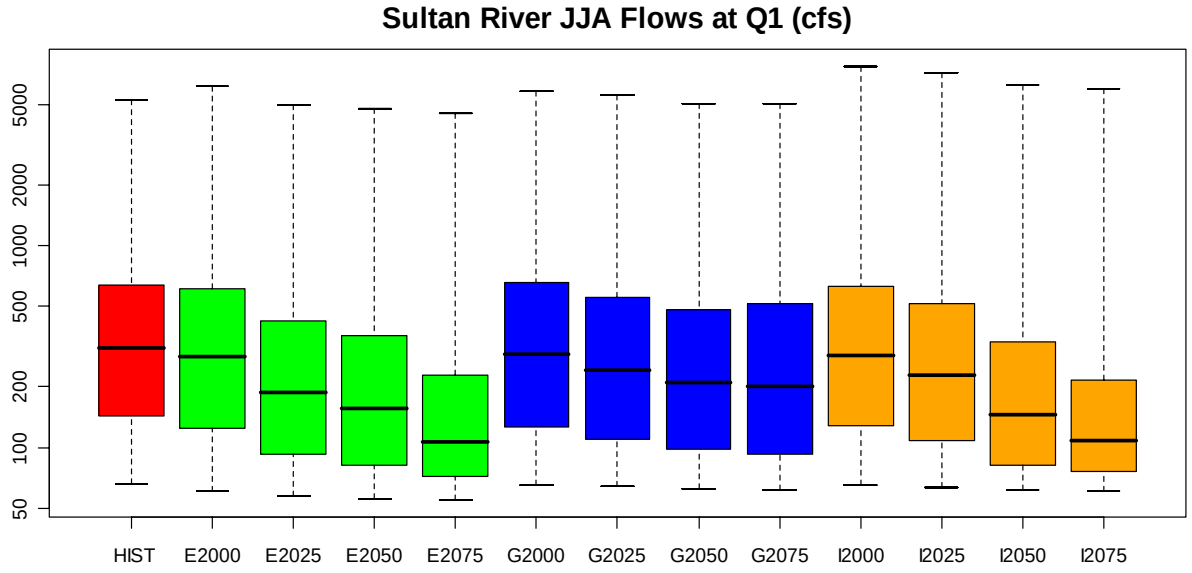

Figure 50: Boxplots of Projected Flows at Q1 for JJA

Despite this consistency in total annual mass, the ensemble indicates that there will be substantial changes in the distribution of flows. Winter ensemble flows during the 2050 period are 23.6% greater than in the historic record, while summer flows in the same time period are 32.6% lower. This is illustrated in Figure 48, Figure 49, and Figure 50. In particular, both the ECHAM5_A2 and IPSL_A2 models forecast consistently increasing winter streamflows and declining summer flows (Figure 48). Alternatively, the GISS_B1 model reflects only moderate changes, with slightly higher fall flows and moderately decreased summer flows. According to the ensemble, 2050 fall flows at Q1 are 12.6% greater than the simulated historic record. While spring streamflows are within 1% of the simulated historic flows, it should be noted that shifts during this season are largely masked by averaging, due to the cancelling effect of increasing March flows and decreasing May flows.

Cedar River Climate Impacts Simulation Results

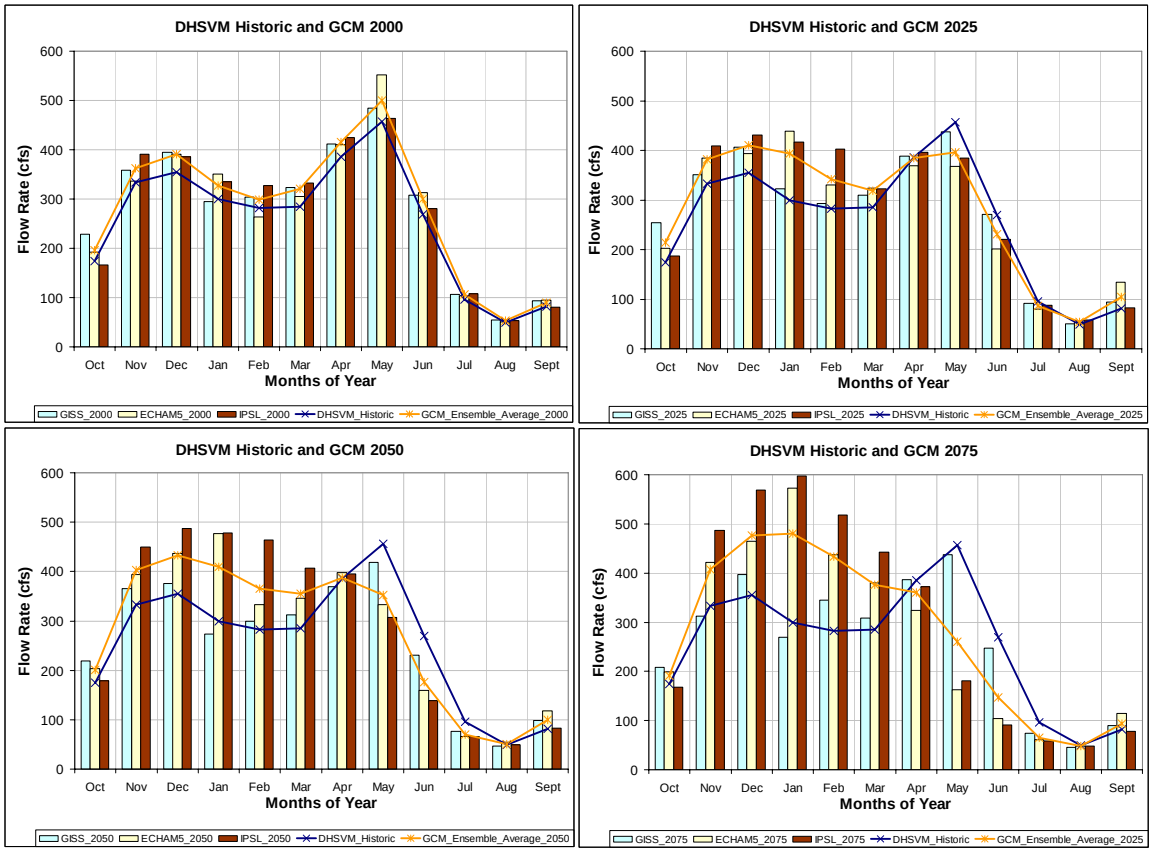

Figure 51: Simulated 2000, 2025, 2050, and 2075 Projected Annual Average Streamflow at Cedar 1

Figure 51 shows the change in Cedar 1 streamflows, the inflows to the Cedar Reservoir, associated with each climate scenario and period of interest. The 2000 ensemble flows are almost uniformly greater (as a percentage increase) than simulated historic flows in all seasons, resulting in 9.5% more discharge annually.

Table 7: Change in Forecasted Cedar 1 Streamflows: Ensemble Average vs. DHSVM Historic

	Spring (MAM)	Summer (JJA)	Fall (SON)	Winter (DJF)	Annual
Ensemble_2000	9.7%	10.8%	9.8%	8.5%	9.5%
Ensemble_2025	-2.4%	-10.5%	18.9%	22.3%	8.0%
Ensemble_2050	-2.9%	-28.4%	19.2%	28.9%	7.5%
Ensemble_2075	-11.6%	-37.2%	17.5%	48.2%	8.7%

The ensemble suggests that total annual flow at Cedar 1 will remain relatively constant between 2000 and 2075 periods. All periods feature total annual streamflows between 7.5% and 9.5% greater than that indicated by the historic record.

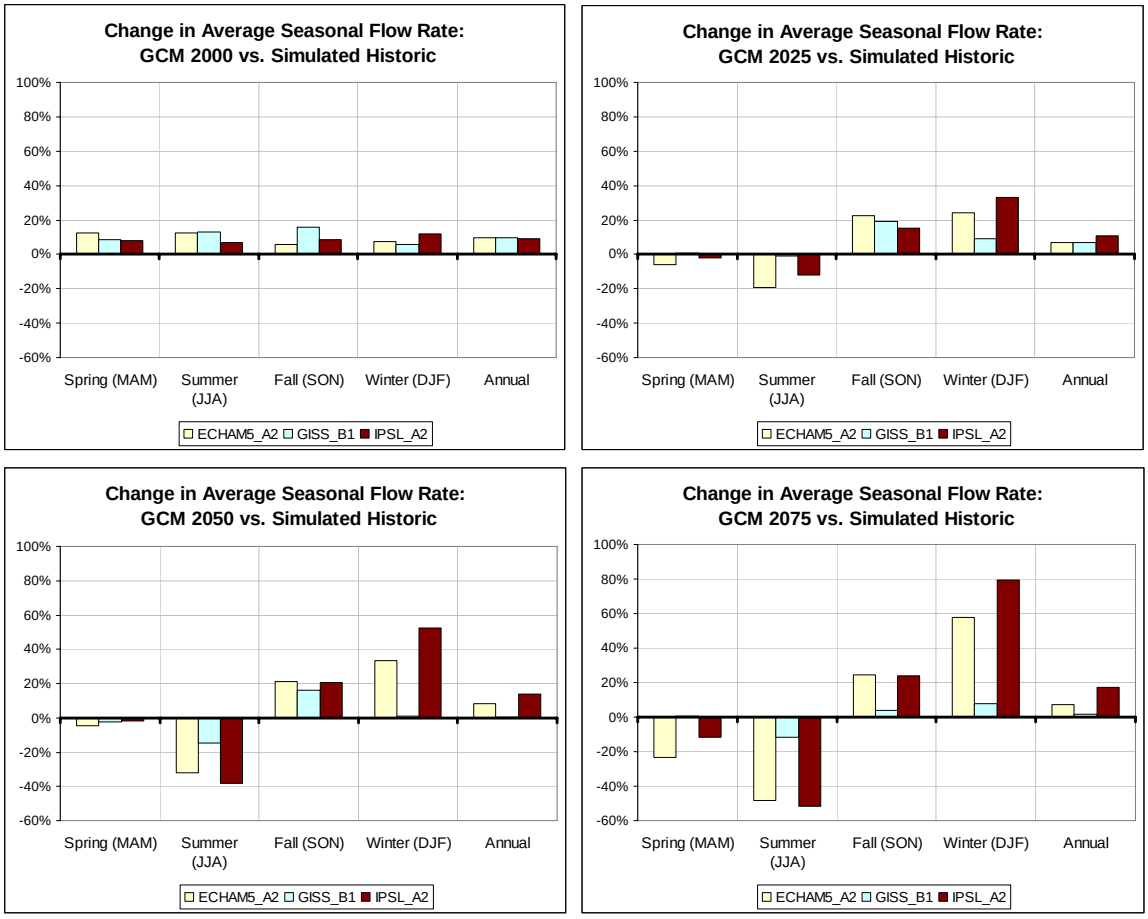

Figure 52: Projected Cedar 1 Seasonal Streamflows for Each GCM Scenario

Despite this relatively constant rate of average annual flows, the ensemble suggests increasing fall and winter flows and decreasing spring and summer flows. Winter ensemble flows during the 2050 period are 28.9% greater than in the historic record, while summer flows in the same time period are 28.4% lower. In particular, both the ECHAM5_A2 and IPSL_A2 models forecast consistently increasing winter streamflows and declining summer flows (Figure 52). This is apparent in Figure 53 and Figure 54, where not only average streamflows are shifted, but large changes in the median and quartiles result as well. Alternatively, the GISS_B1 model reflects only modest changes, with moderately higher fall flows and lower summer flows, with climate impacts affecting total distribution of summer flows more so than winter (Figure 54). According to the ensemble, 2050 fall flows at Cedar 1 are 19.2% greater than in the historic record, while spring flows are only slightly less than those of the historic dataset due to substantially higher March flows masking decreases in April and May flows.

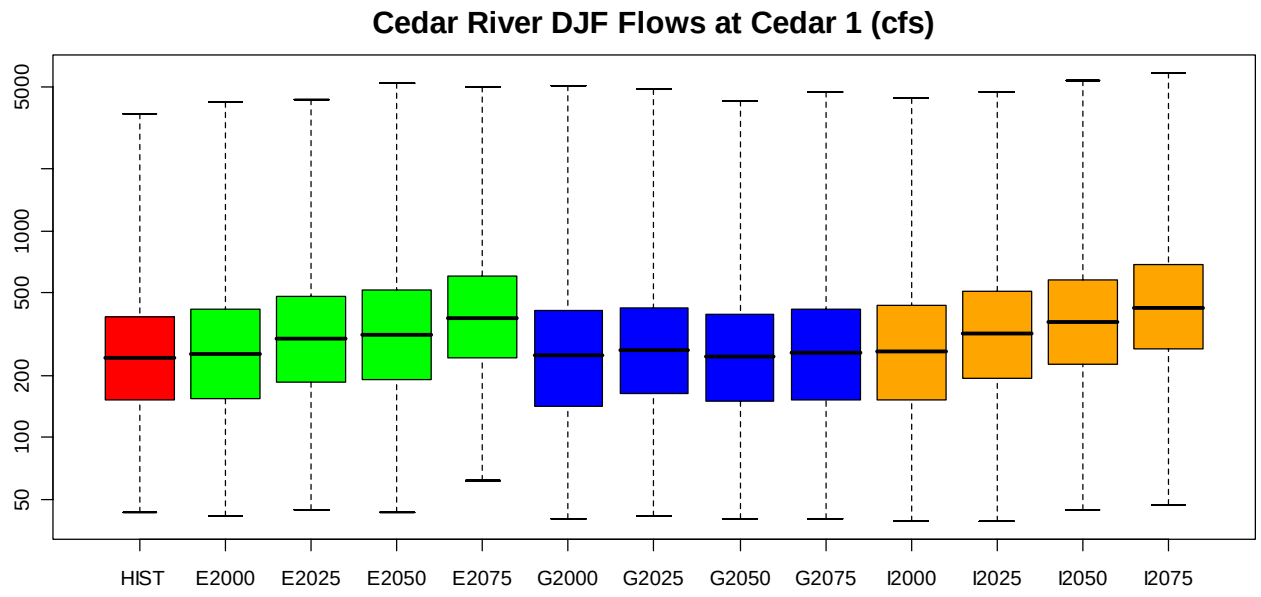

Figure 53: Boxplots of Projected Flows at Cedar 1 for DJF

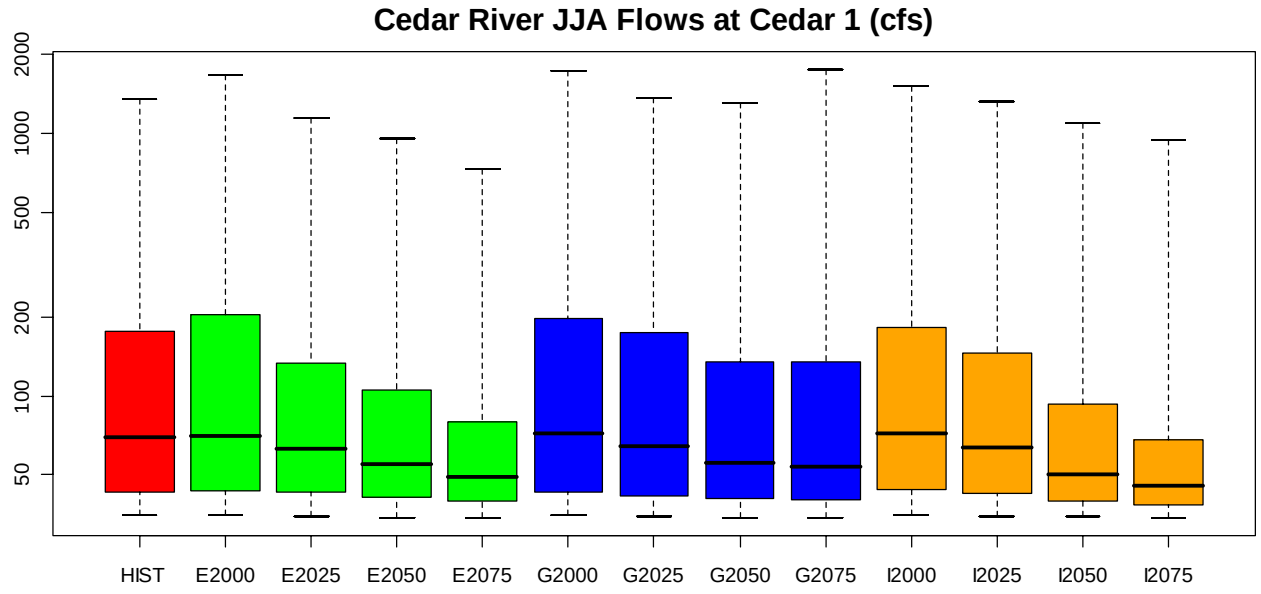

Figure 54: Boxplots of Projected Flows at Cedar 1 for JJA

Tolt River Climate Impacts Simulation Results

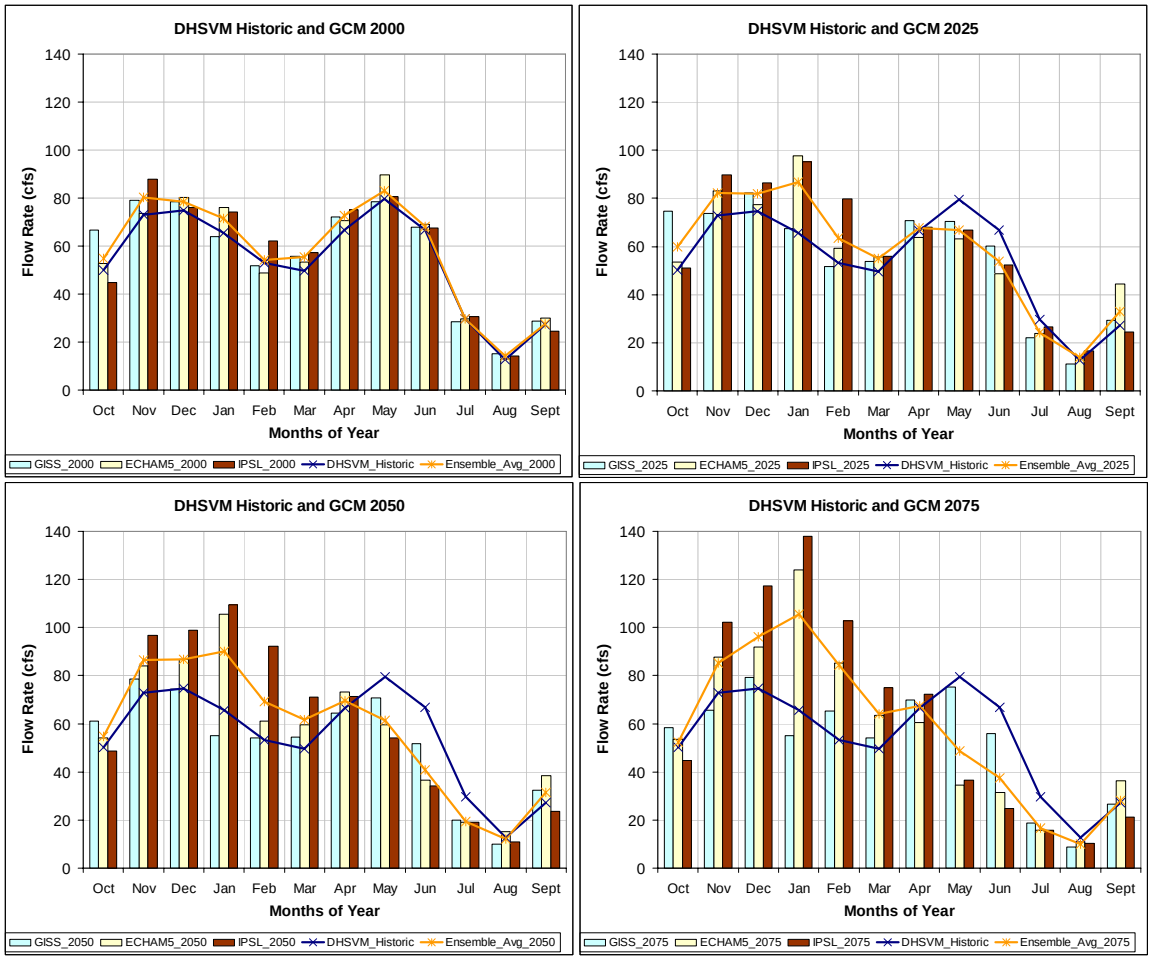

Figure 55: Simulated 2000, 2025, 2050, and 2075 Projected Annual Average Streamflow for Tolt 7

Figure 55 displays the climate impacts to Tolt 7 streamflows, the inflows to the Tolt Reservoir, which are associated with each climate scenario and period of interest. The ensemble again shows modestly increased flows, particularly during spring and fall. Increases of 2.6% – 8.2% in each of the four seasons result in 6.4% more flow annually, relative to simulated historic streamflows (Table 8).

Table 8: Change in Forecasted Tolt 7 Streamflows: Ensemble Average vs. DHSVM Historic

	Spring (MAM)	Summer (JJA)	Fall (SON)	Winter (DJF)	Annual
Ensemble_2000	7.8%	2.6%	8.2%	5.5%	6.4%
Ensemble_2025	-3.2%	-15.7%	16.4%	20.2%	6.2%
Ensemble_2050	-1.6%	-33.8%	14.7%	27.0%	5.3%
Ensemble_2075	-7.9%	-41.1%	10.1%	47.7%	7.2%

The ensemble suggests that total annual inflow mass will remain relatively constant between 2000 and 2075 periods. All periods feature annual streamflows between 5.3% and 7.2% greater than those indicated by the historic dataset.

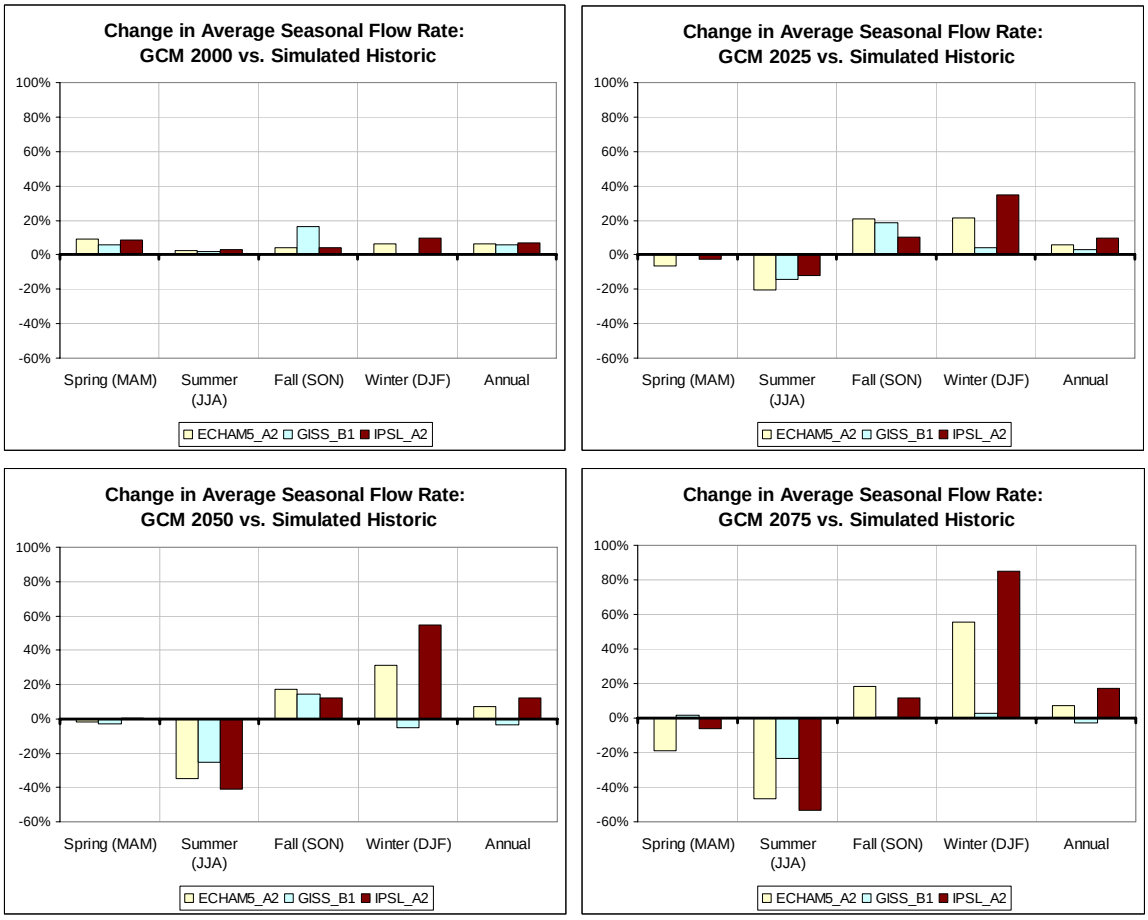

Figure 56: Tolt 7 Projected Seasonal Streamflows for Each GCM Scenario

Despite this relatively constant rate of average annual flows, the GCM Ensemble suggests increasing winter flows and decreasing spring and summer flows. Winter ensemble flows during the 2050 period are 27.0% greater than in the historic record, while summer flows in the same time period are 33.8% lower. In particular, both the ECHAM5_A2 and IPSL_A2 models forecast consistently increasing winter streamflows and declining summer flows (Figure 56). The distribution of does not become more skewed as the case for the Cedar River. Instead, a translation of flow occurs, with higher winter and lower summer flows becoming the norm in the future periods for ECHAM and IPSL models. Alternatively, the GISS_B1 model reflects only modest changes, with moderately higher fall flows and lower summer flows. Ensemble fall flows during the 2050 period are 14.7% greater than historic fall flows.

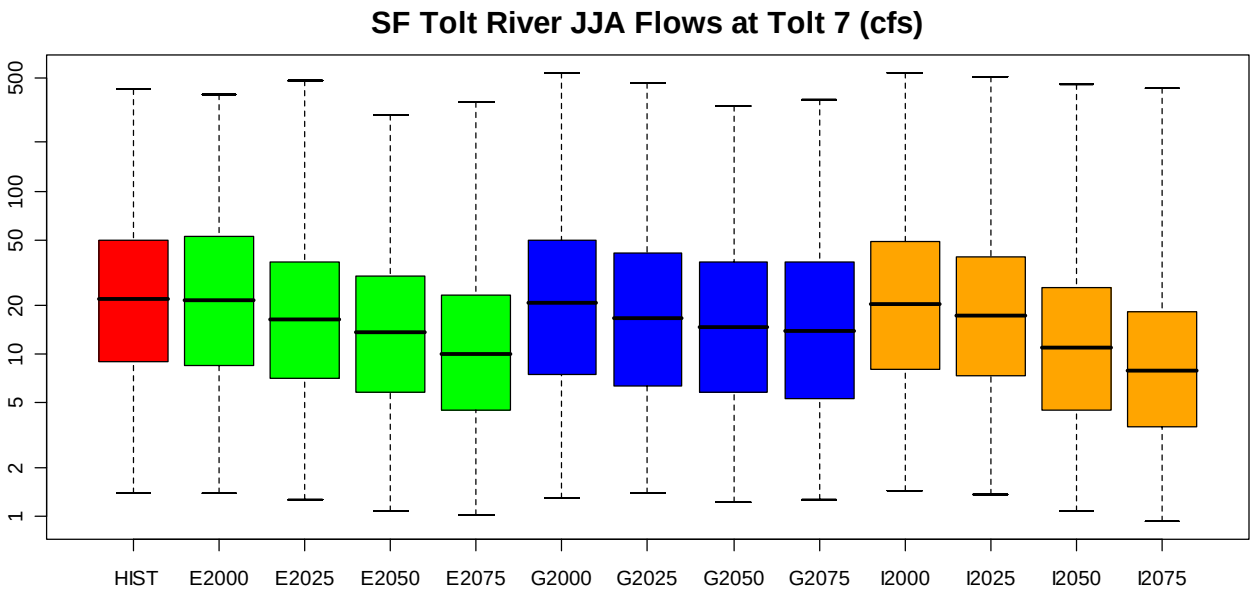

Figure 57: Boxplots of Projected Flows at Tolt 7 for JJA

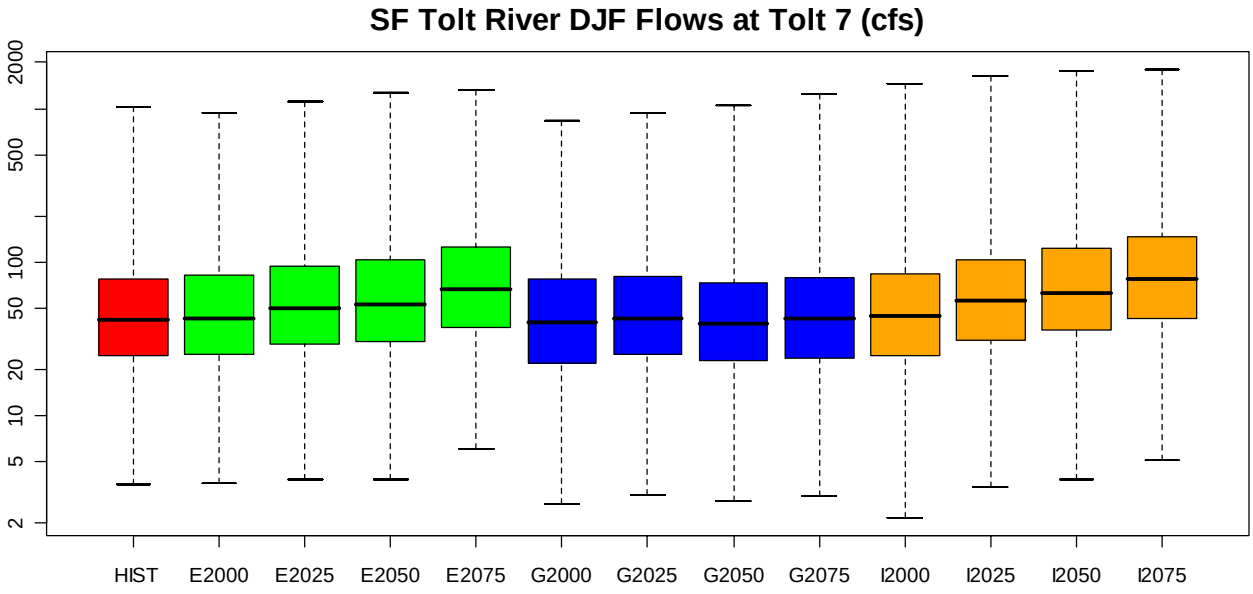

Figure 58: Boxplots of Projected Flows at Tolt 7 for DJF

Green River Climate Impacts Simulation Results

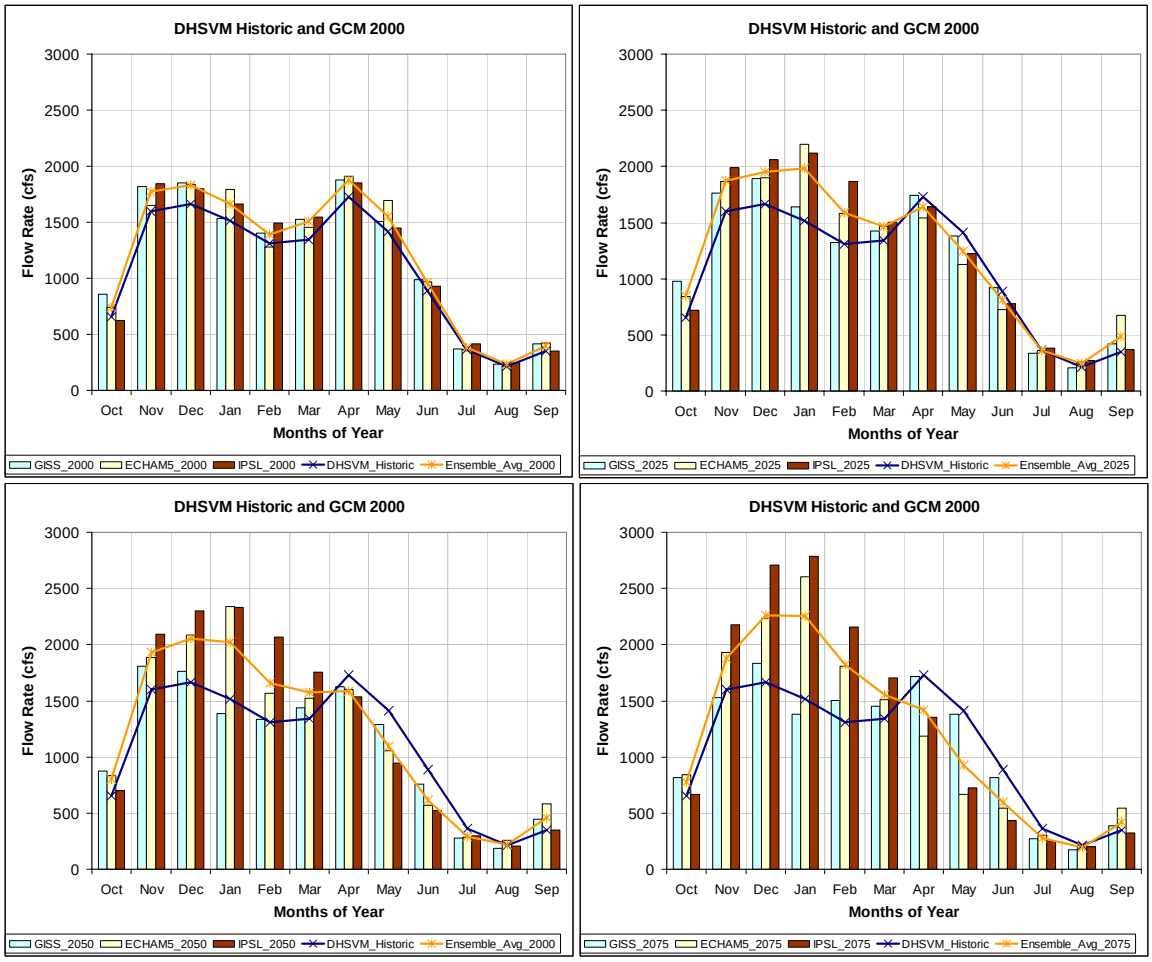

Figure 59: Simulated 2000, 2025, 2050, and 2075 Projected Annual Average Streamflow for HH Inflows

Figure 59 shows the impact to HH Inflows, or the inflows to the Howard Hanson Reservoir, associated with each climate scenario and period of interest. In the first panel, the ensemble forecast for the year 2000 suggests a nearly uniform increase over simulated historic values of 7.5% – 11.6% in all seasons (Table 9). On an annual basis, the 2000 ensemble features flows that are 9.7% higher than historic annual flows.

Table 9: Change in Forecasted HH Inflow Streamflows: Ensemble Average vs. DHSVM Historic

	Spring (MAM)	Summer (JJA)	Fall (SON)	Winter (DJF)	Annual
Ensemble_2000	10.1%	7.5%	11.6%	8.9%	9.7%
Ensemble_2025	-3.0%	-3.6%	23.2%	23.1%	11.1%
Ensemble_2050	-5.1%	-23.1%	22.6%	27.7%	9.6%
Ensemble_2075	-13.1%	-26.7%	18.0%	41.3%	10.2%

The ensemble suggests that total annual inflow to the Howard Hanson Reservoir will remain relatively constant between 2000 and 2075 periods. All periods feature total annual inflow mass between 9.6% and 11.1% greater than that indicated by the historic record.

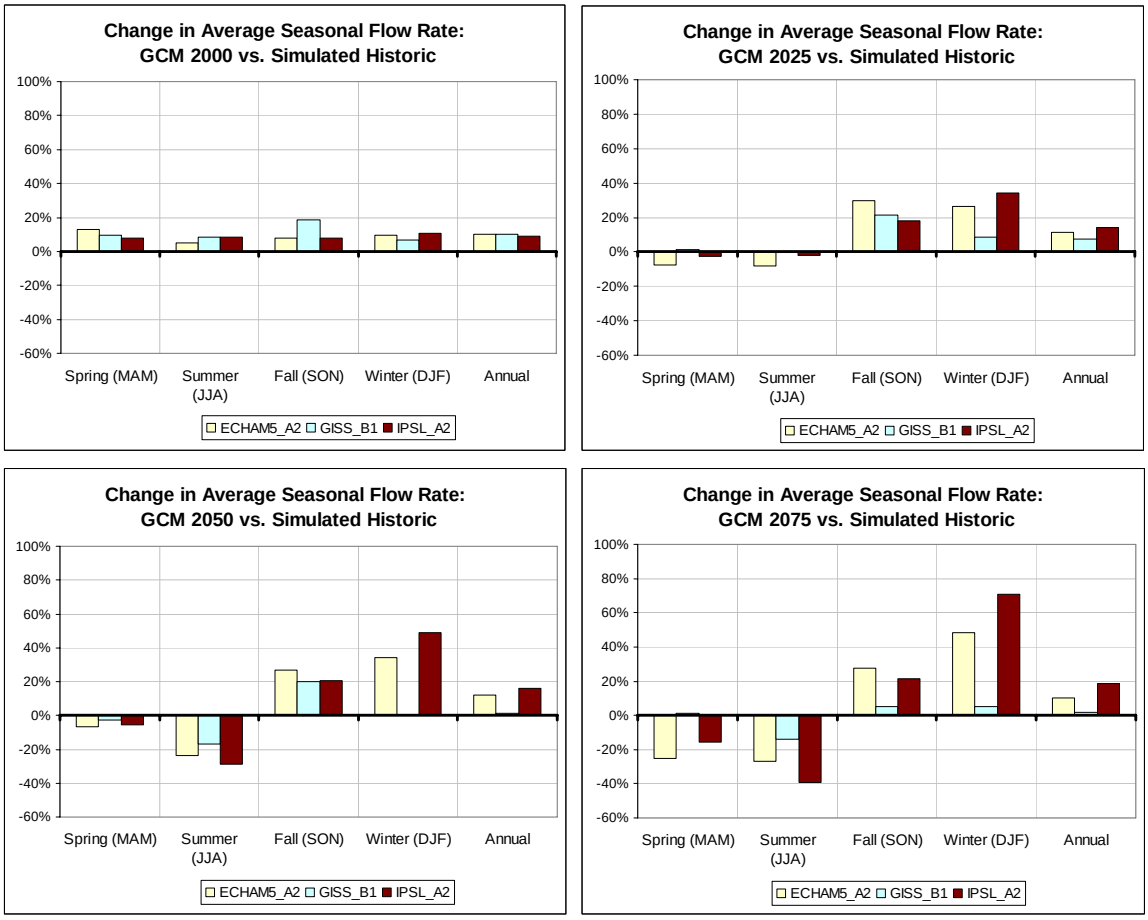

Figure 60: HH Inflows Projected Seasonal Streamflows for Each GCM Scenario

Despite this relatively constant rate of average annual flows, the ensemble also suggests increasing winter flows and decreasing spring and summer flows. Winter ensemble flows during the 2050 period are 27.7% greater than in the historic record, while summer flows in the same time period are 23.1% lower. In particular, both the ECHAM5_A2 and IPSL_A2 models forecast consistently increasing winter streamflows and declining summer flows (Figure 60). Figure 61 and Figure 62 illustrate the pattern of shifting flow magnitude and distribution of flows. Although winter flows increase in magnitude, the distribution remains relatively unchanged whereas summer flows undergo substantial decreases in magnitude and develop a smaller variance band with increased warming. Alternatively, the GISS_B1 model reflects only modest changes, with moderately higher fall flows and lower summer flows. According to the ensemble, 2050 fall flows at HH Inflows show a 22.6% increase over historic flows.

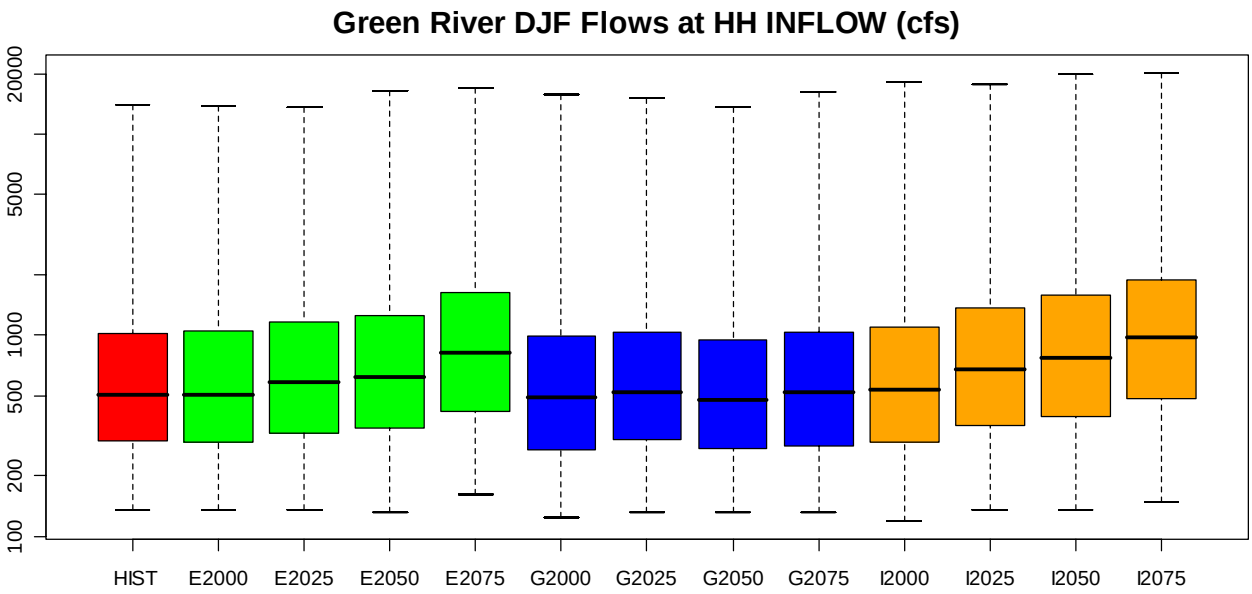

Figure 61: Boxplots of Projected Flows at HH Inflow for DJF

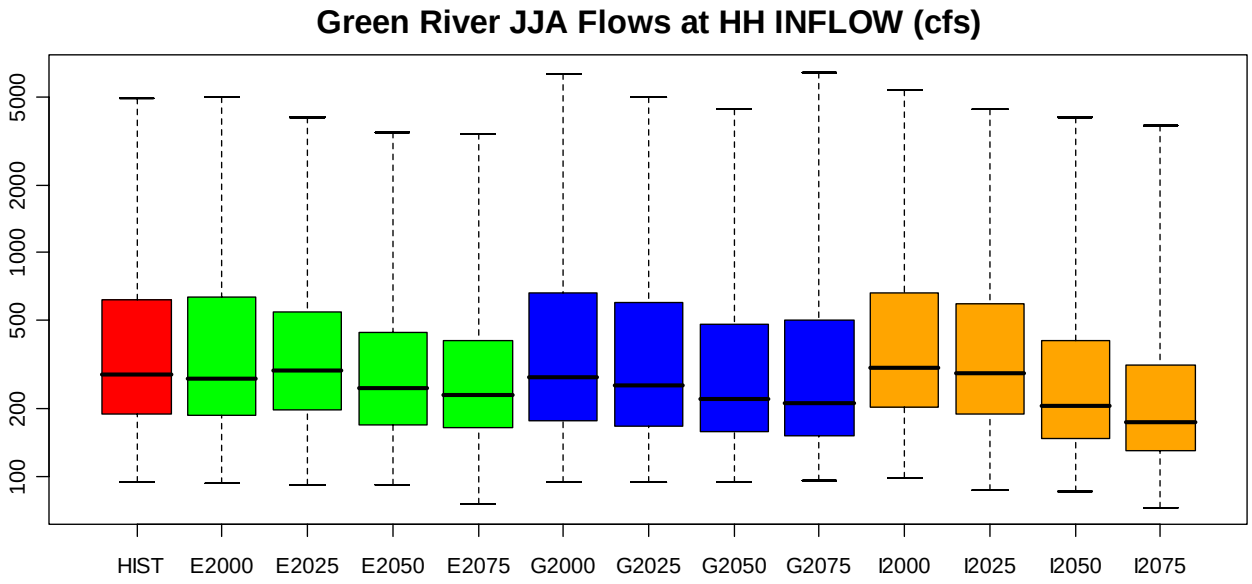

Figure 62: Boxplots of Projected Flows at HH Inflow for JJA

White River Climate Impacts Simulation Results

Figure 63 presents the impact to flows in the White River associated with each climate scenario and period of interest. In the first panel, the ensemble forecast for the year 2000 suggests a increase over simulated historic values in the winter, spring, and fall seasons (Table 10) and a slight decrease in summer flow. The annual 2000 ensemble feature flows that are 9.1% higher than historic annual flows.

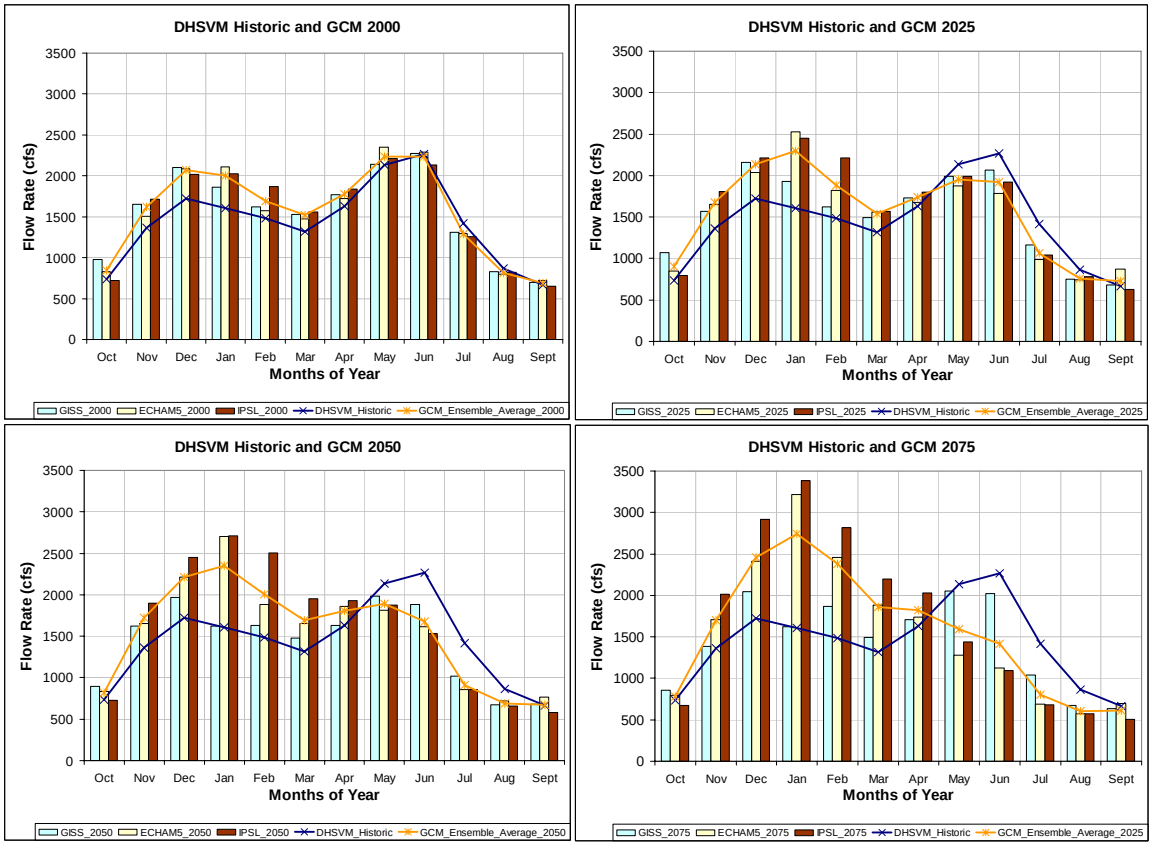

Figure 63: Simulated 2000, 2025, 2050, and 2075 Projected Annual Average Streamflow for 12098500

Table 10: Change in Forecasted 12098500 Streamflows: Ensemble Average vs. DHSVM Historic

	Spring (MAM)	Summer (JJA)	Fall (SON)	Winter (DJF)	Annual
Ensemble_2000	8.8%	-4.8%	14.2%	19.6%	9.1%
Ensemble_2025	2.8%	-17.8%	19.7%	31.3%	8.0%
Ensemble_2050	6.1%	-28.1%	16.3%	36.3%	7.0%
Ensemble_2075	3.7%	-38.0%	11.7%	57.1%	8.8%

Despite this relatively constant rate of average annual flows, the ensemble also suggests increasing winter flows and decreasing summer flows. Winter ensemble flows during the 2050 period are approximately 36.3% greater than in the historic record, while summer flows in the same time period are approximately 28% lower. In particular, both the ECHAM5_A2 and IPSL_A2 models forecast consistently increasing winter streamflows and declining summer flows (Figure 64). Figure 65 and Figure 66 illustrate the pattern of shifting flow magnitude and distribution of flows. Although winter flows increase in magnitude, the distribution remains

relatively unchanged whereas summer flows undergo substantial decreases in magnitude and variance with increased warming. Alternatively, the GISS_B1 model reflects only modest changes, with moderately higher fall and winter flows and slightly lower summer flows. The change in streamflow is primarily attributable to the loss of glacier mass and an increase in available area for runoff. Because the White River is glacier fed, loss in total glacier mass in the future reduces available water stored for summer flows.

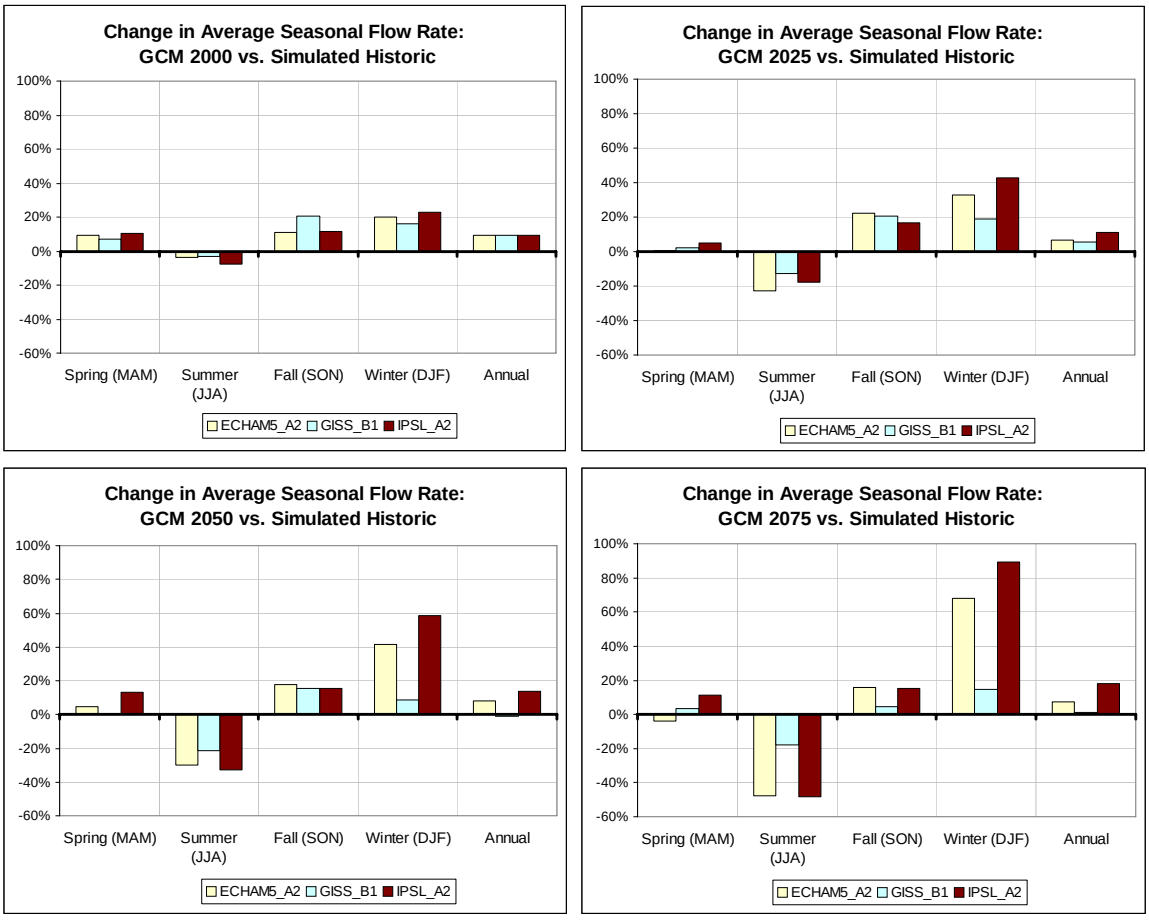

Figure 64: 12098500 Projected Seasonal Streamflows for Each GCM Scenario

The changing distribution of flow occurring with increasing temperatures indicates a decrease SWE, that is, year to year variability of flow in the summer is dominated by the amount of SWE available for melting, as this the total mass diminishes in a warmed climate, there is less opportunity to have large variations in flow.

Figure 67 provides evidence for this. The color gradient (from white to blue) represents SWE values from 0 to 75 meters. The orange color represents SWE in excess of 75 meters. As temperatures warm in the ECHAM model, large reductions in glacial mass on the north side of Mount Rainier occur. These glaciers are particularly sensitive to warming because of their low elevation. An explanation is that the reduction in mass results when the warmer summers diminish the mass at a rate faster than can be replaced in the winter months. Warmer winters affect how precipitation falls, converting what would normally be snow to rain, which is more likely to runoff as opposed to accumulate in the lower regions of the glacier. Warmer winters

also compound the melt off at lower elevations, as areas that may have once froze during winter months are now warmer, and thus contribute to increased melt off of the glacier.

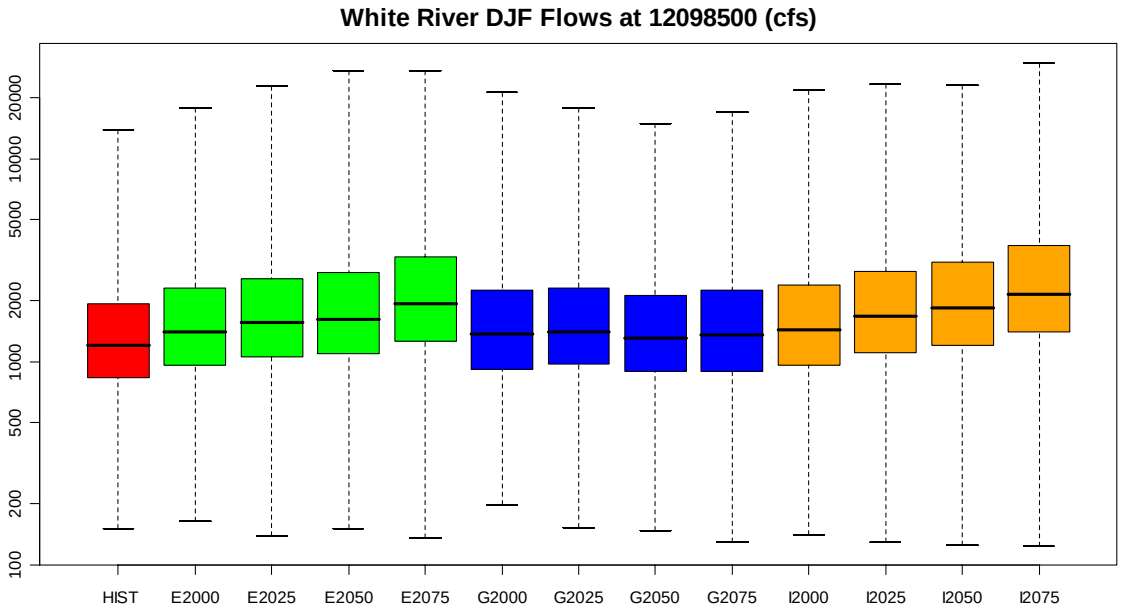

Figure 65: Boxplots of Projected Streamflows at 12098500 for DJF

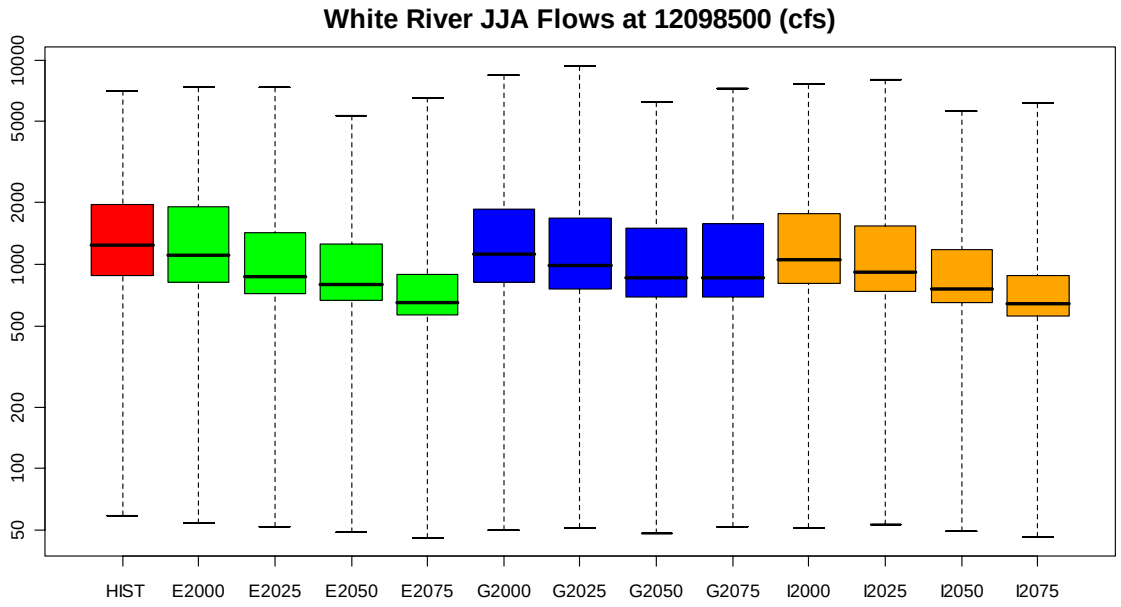

Figure 66: Boxplots of Projected Streamflows at 12098500 for JJA

Another issue that may cause a more significant reduction in the model is that the glacier is subjected to steady-state increase in temperatures, that is, the glacier in the year 2075 experiences constant 2075 temperatures, which may cause more melting than may be seen if a transient approach is taken. Warming developing over time may allow for periods of equilibration or a chance for the glacier to regain mass, whereas the time series used to represent 2075 is consistently warmer for extended periods of time causing substantial reductions in mass.

One alternative for evaluating glacial loss would be to force DHSVM with a transient time series of warming for each GCM and compare that to the current results obtained, though streamflow results from such an exercise are of shortened length compared to the quasi steady-state approach.

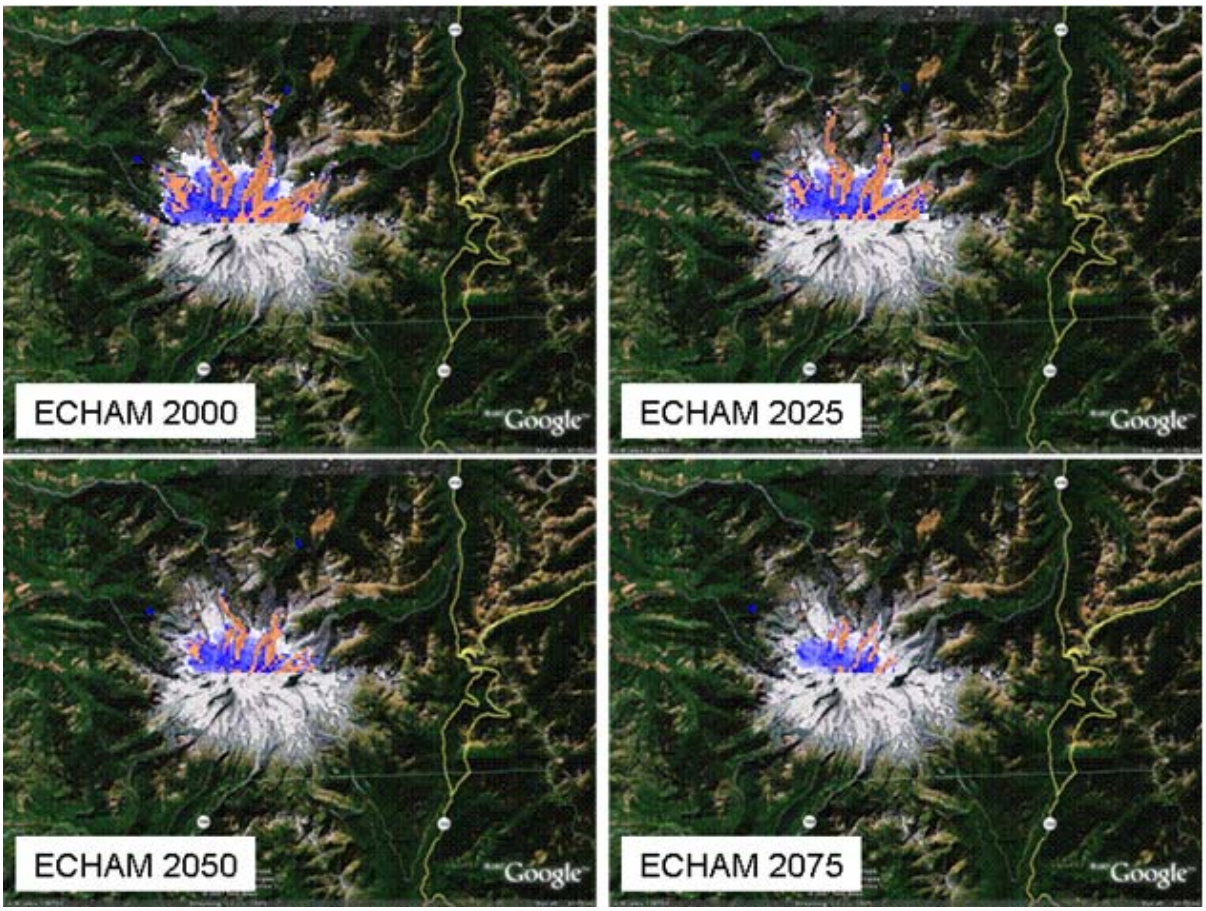

Figure 67: Changing Glacier Mass on Mount Rainier for the ECHAM GCM

References

Paterson, W. S. B., 1994, /The physics of glaciers/: Oxford, United Kingdom, Pergamon Press, 480 p.

Polebitski, A., M.W. Wiley, and R.N. Palmer. 2007. “Technical Memorandum #2: Methodology for Downscaling Meteorological Data for Evaluating Climate Change.” A report prepared by the Climate Change Technical Subcommittee of the Regional Water Supply Planning Process, Seattle, WA.

Wigmosta, M.S., Vail, L.W., Lettenmaier, D.P., 1994. A distributed hydrology-vegetation model for complex terrain. Water Resources Research 30 (6), 1665-1679.

Appendix 1: Listing of Meteorological Stations Used

Meteorological Stations Used for WRIA 7: Snohomish

Station Name 1 = CEDAR
North Coordinate 1 = 5251568.
East Coordinate 1 = 593818.
Elevation 1 = 475.

Station Name 2 = BREMERTON
North Coordinate 2 = 5267969.000000
East Coordinate 2 = 523844.937500
Elevation 2 = 34.000000

Station Name 3 = CLEARWATER
North Coordinate 3 = 5270591.000000
East Coordinate 3 = 402245.031250
Elevation 3 = 24.000000

Station Name 4 = BUCKLEY
North Coordinate 4 = 5224259
East Coordinate 4 = 575534
Elevation 4 = 208.8

Station Name 5 = CUSHMAN_POWER
North Coordinate 5 = 5245706.500000
East Coordinate 5 = 487389.906250
Elevation 5 = 6.000000

Station Name 6 = ELMA
North Coordinate 6 = 5205023.000000
East Coordinate 6 = 469589.312500
Elevation 6 = 21.000000

Station Name 7 = ELWHA
North Coordinate 7 = 5319950.500000
East Coordinate 7 = 456538.093750
Elevation 7 = 110.000000

Station Name 8 = EVERETT
North Coordinate 8 = 5314552.000000
East Coordinate 8 = 560965.937500
Elevation 8 = 18.000000

Station Name 9 = KENT
North Coordinate 9 = 5249682.500000
East Coordinate 9 = 557876.500000
Elevation 9 = 9.000000

Station Name 10 = MCMILLIN
North Coordinate 10 = 5220023.000000
East Coordinate 10 = 555589.687500
Elevation 10 = 177.000000

Station Name 11 = SEATAC
North Coordinate 11 = 5257032.500000
East Coordinate 11 = 551473.000000
Elevation 11 = 122.000000

Station Name 12 = WAUNA
North Coordinate 12 = 5245736.500000
East Coordinate 12 = 522652.093750
Elevation 12 = 5.000000

Station Name 13 = ABERDEEN20NNE
North Coordinate 13 = 5234817.500000
East Coordinate 13 = 447046.156250
Elevation 13 = 133.000000

Station Name 14 = LANDSBURG
North Coordinate 14 = 5247282.
East Coordinate 14 = 577191.
Elevation 14 = 161.

Station Name 15 = PALMER
North Coordinate 15 = 5239681.
East Coordinate 15 = 586740.
Elevation 15 = 276.

Station Name 16 = SNOQUALMIE
North Coordinate 16 = 5265727.0
East Coordinate 16 = 587525.0
Elevation 16 = 134.1

Station Name 17 = SFTOLT
North Coordinate 17 = 5282935.75
East Coordinate 17 = 598485.0
Elevation 17 = 609

Station Name 18 = DARRINGTON
North Coordinate 18 = 5345924.0
East Coordinate 18 = 603642.0
Elevation 18 = 167.64

Station Name 19 = MONROE
North Coordinate 19 = 5345924.0
East Coordinate 19 = 603642.0
Elevation 19 = 167.64

Station Name 20 = CULMBACK
North Coordinate 20 = 5314180.5
East Coordinate 20 = 598320.0
Elevation 20 = 442

Station Name 21 = STARTUP
North Coordinate 21 = 5302278.
East Coordinate 21 = 595976.
Elevation 21 = 52.0

Station Name 22 = FORKS
North Coordinate 22 = 5311428.500000
East Coordinate 22 = 397926.906250
Elevation 22 = 107.000000

Station Name 23 = OLYMPIA
North Coordinate 23 = 5201246.000000
East Coordinate 23 = 507607.968750
Elevation 23 = 63.000000

Station Name 24 = PORTANGELES
North Coordinate 24 = 5330978.500000
East Coordinate 24 = 470238.312500
Elevation 24 = 27.000000

Station Name 25 = PORTTOWNSEND
North Coordinate 25 = 5329078.500000
East Coordinate 25 = 518607.375000
Elevation 25 = 31.000000

Station Name 26 = QUILCENE
North Coordinate 26 = 5295622.8
East Coordinate 26 = 507370.5
Elevation 26 = 38.000000

Meteorological Stations Used for WRIA 8: Cedar- Sammamish

Station Name 1 = CEDAR
North Coordinate 1 = 5251568.
East Coordinate 1 = 593818.
Elevation 1 = 475.

Station Name 2 = BREMERTON
North Coordinate 2 = 5267969.000000
East Coordinate 2 = 523844.937500
Elevation 2 = 34.000000

Station Name 3 = BUCKLEY
North Coordinate 3 = 5224259
East Coordinate 3 = 575534
Elevation 3 = 208.8

Station Name 4 = CUSHMAN_POWER
North Coordinate 4 = 5245706.500000
East Coordinate 4 = 487389.906250
Elevation 4 = 6.000000

Station Name 5 = EVERETT
North Coordinate 5 = 5314552.000000
East Coordinate 5 = 560965.937500
Elevation 5 = 18.000000

Station Name 6 = KENT
North Coordinate 6 = 5249682.500000
East Coordinate 6 = 557876.500000
Elevation 6 = 9.000000

Station Name 7 = MCMILLIN
North Coordinate 7 = 5220023.000000
East Coordinate 7 = 555589.687500
Elevation 7 = 177.000000

Station Name 8 = PORTTOWNSEND
North Coordinate 8 = 5329078.500000
East Coordinate 8 = 518607.375000
Elevation 8 = 31.000000

Station Name 9 = QUILCENE
North Coordinate 9 = 5295622.8
East Coordinate 9 = 507370.5
Elevation 9 = 38.000000

Station Name 10 = SEATAC
North Coordinate 10 = 5257032.500000
East Coordinate 10 = 551473.000000
Elevation 10 = 122.000000

Station Name 11 = WAUNA
North Coordinate 11 = 5245736.500000
East Coordinate 11 = 522652.093750
Elevation 11 = 5.000000

Station Name 12 = ABERDEEN20NNE
North Coordinate 12 = 5234817.500000
East Coordinate 12 = 447046.156250
Elevation 12 = 133.000000

Station Name 13 = LANDSBURG
North Coordinate 13 = 5247282.
East Coordinate 13 = 577191.
Elevation 13 = 161.

Station Name 14 = PALMER
North Coordinate 14 = 5239681.
East Coordinate 14 = 586740.
Elevation 14 = 276.

Station Name 15 = SNOQUALMIE
North Coordinate 15 = 5265727.0
East Coordinate 15 = 587525.0
Elevation 15 = 134.1

Station Name 16 = SFTOLT
North Coordinate 16 = 5282935.75
East Coordinate 16 = 598485.0
Elevation 16 = 609

Station Name 17 = DARRINGTON
North Coordinate 17 = 5345924.0
East Coordinate 17 = 603642.0
Elevation 17 = 167.64

Station Name 18 = MONROE
North Coordinate 18 = 5345924.0
East Coordinate 18 = 603642.0
Elevation 18 = 167.64

Station Name 19 = CULMBACK
North Coordinate 19 = 5314180.5
East Coordinate 19 = 598320.0
Elevation 19 = 442

Station Name 20 = STARTUP
North Coordinate 20 = 5302278.
East Coordinate 20 = 595976.
Elevation 20 = 52.0

Meteorological Stations Used for WRIA 9: Duwamish- Green

Station Name 1 = CEDAR
North Coordinate 1 = 5251568.
East Coordinate 1 = 593818.
Elevation 1 = 475.

Station Name 2 = BREMERTON
North Coordinate 2 = 5267969.000000
East Coordinate 2 = 523844.937500
Elevation 2 = 34.000000

Station Name 3 = BUCKLEY
North Coordinate 3 = 5224259
East Coordinate 3 = 575534
Elevation 3 = 208.8

Station Name 4 = CUSHMAN_POWER
North Coordinate 4 = 5245706.500000
East Coordinate 4 = 487389.906250
Elevation 4 = 6.000000

Station Name 5 = EVERETT
North Coordinate 5 = 5314552.000000
East Coordinate 5 = 560965.937500
Elevation 5 = 18.000000

Station Name 6 = KENT
North Coordinate 6 = 5249682.500000
East Coordinate 6 = 557876.500000
Elevation 6 = 9.000000

Station Name 7 = MCMILLIN
North Coordinate 7 = 5220023.000000
East Coordinate 7 = 555589.687500
Elevation 7 = 177.000000

Station Name 8 = PORTTOWNSEND
North Coordinate 8 = 5329078.500000
East Coordinate 8 = 518607.375000
Elevation 8 = 31.000000

Station Name 9 = QUILCENE
North Coordinate 9 = 5295622.8
East Coordinate 9 = 507370.5
Elevation 9 = 38.000000

Station Name 10 = SEATAC
North Coordinate 10 = 5257032.500000
East Coordinate 10 = 551473.000000
Elevation 10 = 122.000000

Station Name 11 = WAUNA
North Coordinate 11 = 5245736.500000
East Coordinate 11 = 522652.093750
Elevation 11 = 5.000000

Station Name 12 = ABERDEEN20NNE
North Coordinate 12 = 5234817.500000
East Coordinate 12 = 447046.156250
Elevation 12 = 133.000000

Station Name 13 = LANDSBURG
North Coordinate 13 = 5247282.
East Coordinate 13 = 577191.
Elevation 13 = 161.

Station Name 14 = PALMER
North Coordinate 14 = 5239681.
East Coordinate 14 = 586740.
Elevation 14 = 276.

Station Name 15 = SNOQUALMIE
North Coordinate 15 = 5265727.0
East Coordinate 15 = 587525.0
Elevation 15 = 134.1

Station Name 16 = SFTOLT
North Coordinate 16 = 5282935.75
East Coordinate 16 = 598485.0
Elevation 16 = 609

Station Name 17 = DARRINGTON
North Coordinate 17 = 5345924.0
East Coordinate 17 = 603642.0
Elevation 17 = 167.64

Station Name 18 = MONROE
North Coordinate 18 = 5345924.0
East Coordinate 18 = 603642.0
Elevation 18 = 167.64

Station Name 19 = CULMBACK
North Coordinate 19 = 5314180.5
East Coordinate 19 = 598320.0
Elevation 19 = 442

Station Name 20 = STARTUP
North Coordinate 20 = 5302278.
East Coordinate 20 = 595976.
Elevation 20 = 52.0

Meteorological Stations Used for WRIA 10: Puyallup- White

Station Name 1 = CEDAR
North Coordinate 1 = 5251568.
East Coordinate 1 = 593818.
Elevation 1 = 475.

Station Name 2 = BREMERTON
North Coordinate 2 = 5267969.000000
East Coordinate 2 = 523844.937500
Elevation 2 = 34.000000

Station Name 3 = BUCKLEY
North Coordinate 3 = 5224259
East Coordinate 3 = 575534
Elevation 3 = 208.8

Station Name 4 = CUSHMAN_POWER
North Coordinate 4 = 5245706.500000
East Coordinate 4 = 487389.906250
Elevation 4 = 6.000000

Station Name 5 = EVERETT
North Coordinate 5 = 5314552.000000
East Coordinate 5 = 560965.937500
Elevation 5 = 18.000000

Station Name 6 = KENT
North Coordinate 6 = 5249682.500000
East Coordinate 6 = 557876.500000
Elevation 6 = 9.000000

Station Name 7 = MCMILLIN
North Coordinate 7 = 5220023.000000
East Coordinate 7 = 555589.687500
Elevation 7 = 177.000000

Station Name 8 = SEATAC
North Coordinate 8 = 5257032.500000
East Coordinate 8 = 551473.000000
Elevation 8 = 122.000000

Station Name 9 = WAUNA
North Coordinate 9 = 5245736.500000
East Coordinate 9 = 522652.093750
Elevation 9 = 5.000000

Station Name 10 = ABERDEEN20NNE
North Coordinate 10 = 5234817.500000
East Coordinate 10 = 447046.156250
Elevation 10 = 133.000000

Station Name 11 = LANDSBURG
North Coordinate 11 = 5247282.
East Coordinate 11 = 577191.
Elevation 11 = 161.

Station Name 12 = PALMER
North Coordinate 12 = 5239681.
East Coordinate 12 = 586740.
Elevation 12 = 276.

Station Name 13 = SNOQUALMIE
North Coordinate 13 = 5265727.0
East Coordinate 13 = 587525.0
Elevation 13 = 134.1

Station Name 14 = SFTOLT
North Coordinate 14 = 5282935.75
East Coordinate 14 = 598485.0
Elevation 14 = 609

Station Name 15 = DARRINGTON
North Coordinate 15 = 5345924.0
East Coordinate 15 = 603642.0
Elevation 15 = 167.64

Station Name 16 = MONROE
North Coordinate 16 = 5345924.0
East Coordinate 16 = 603642.0
Elevation 16 = 167.64

Station Name 17 = CULMBACK
North Coordinate 17 = 5314180.5
East Coordinate 17 = 598320.0
Elevation 17 = 442

Station Name 18 = STARTUP
North Coordinate 18 = 5302278.
East Coordinate 18 = 595976.
Elevation 18 = 52.0

Station Name 19 = LONGMIRE
North Coordinate 19 = 5177757
East Coordinate 19 = 590747
Elevation 19 = 841.9

Station Name 20 = STAMPEDE
North Coordinate 20 = 5238885
East Coordinate 20 = 625723
Elevation 20 = 1206.

Station Name 21 = PARADISE
North Coordinate 21 = 5181914
East Coordinate 21 = 595986
Elevation 21 = 1654

Station Name 22 = FORKS
North Coordinate 22 = 5311428.500000
East Coordinate 22 = 397926.906250
Elevation 22 = 107.000000

Station Name 23 = ELWHA
North Coordinate 23 = 5319950.500000
East Coordinate 23 = 456538.093750
Elevation 23 = 110.000000

Station Name 24 = ELMA
North Coordinate 24 = 5205023.000000
East Coordinate 24 = 469589.312500
Elevation 24 = 21.000000

Appendix 2 – Methodology for Streamflow Correction

The accuracy of a hydrology model in recreating past events can be impacted by a variety of factors. For the type of distributed hydrology model used in this research, inaccuracies occur primarily from:

1. Incomplete or inaccurate representation of soils and geology,
2. Incomplete or inaccurate representation of vegetation,
3. A paucity of reliable precipitation and temperature data,
4. Erroneous past streamflow measurements,
5. Incomplete information about temperature lapse rates,
6. Static land-use maps (when land use has actually changed over time), and
7. Simplified representation of the groundwater/surface water interactions.

Challenges in modeling rainfall/runoff events in a watershed occur even when good data are generally available but when a storm event deposits considerable amounts in rainfall in an area that is not represented in the rainfall gaging network.

When a model consistently under-calculates or over-calculates the runoff for a basin, this is often referred to as a systematic bias. For the water resource systems discussed in this study, a systematic bias might involve overestimating the runoff in the month of March or underestimating the runoff in July. Systematic biases are typically due to simplifications in models made to allow their formulation and execution, incompleteness in our understanding of a physical process, an error in the mathematical representation of a physical process, or inaccurate mathematical algorithms.

The hydrology model used in this study (DHSVM) has been applied in many settings and its conceptual approach and mathematical accuracy have been evaluated in the past. However, when consistent biases in the model output are noted, it is appropriate to develop a correction scheme for removing these biases. This appendix describes the processes that were used when such bias was observed in developed streamflow data. Although various methods exist for correcting flows, for work performed for the Climate Change Technical Committee; a process similar to quantile-mapping as described in Technical Memorandum 2 (Polebitski et al., 2007) is used.

The systematic bias correction technique that was used has three primary steps that are described in this appendix. They are:

1. Rank the observed historic record and compare this record to the ranked simulated record (from the hydrology model). Develop return percentiles using an accepted ranking technique (such as the Weibull or Cunnane method).
2. Create adjustment factors that relate (or map) flows at specified probability levels in the historic record to flows at specified probability levels in the generated record. This is done on a monthly time-step.
3. Create adjusted simulated flows by applying the monthly correction factors.

It is important to note the bias correction was used as sparingly as possible. Each basin model was exhaustively calibrated. Streamflows generated for the Climate Change Technical Committee in general have been left unaltered. Four streamflow sites had bias corrections:

1. Cedar River – Site noted as Cedar 2
2. Green River – Howard Hanson Inflows
3. Sultan River – Sultan River 1, and
4. White River - Associated with USGS 12098500 – which had minor corrections.

Technical Memorandum 5 includes graphics of streamflows "before" and "after" correction. For HH Inflows, Sultan 1, and Cedar 2, the correction scheme was applied to remove a negative bias (the generated flows were too low). For the White River, the correction scheme was applied to remove a general bias associated with the annual flows. Cedar 2 was bias corrected for May-October, HH Inflow was bias corrected for July-October, and Sultan 1 is corrected for November-March. At Cedar 2, the streamflows primarily associated with lower flows needed correction. This is likely, in part, due to record reconstruction (Cedar 2 is below the dam face) and groundwater moraine issues that were not possible to incorporate into the model. The peak flows were for Sultan 1 were, in general, under-simulated every winter resulting in the total annual inflow being underestimated. The sparse gaging network likely created this problem.

The correction routine relies heavily on observed flows of nearby gages. For Cedar 2, a mapping of flows between simulated and observed flows at USGS Gage 12117000 (Taylor Creek) is used. Observed and simulated streamflow at USGS Gage 12137290 (South Fork Sultan River) creates the reference point for Sultan 1. Historic simulated streamflow is used in this process, generating a corrected sequence of streamflows. This is compared to the observed record to ensure consistent statistics and time series properties. Once the historic streamflow sequence has been validated, the climate impacted streamflows are processed and validated. A monthly evaluation is performed, where the observed record, the raw climate impacted series, and the corrected climate impacted series are examined to ensure the correction has not resulted in uncharacteristic flows. The corrected climate impacted data should have similar maximum flows to the historic record.

Figure 68 indicates that the simulated historic flows match well with flows at Sultan 1, with the exception of the most extreme flows, i.e. those less than ten-percent probability. The red line represents the corrected flow, which is closer to the observed than the unadjusted flows. To examine how future flows are corrected at the most extremes peak flows, the raw and corrected flows are plotted for the 2075 period in Figure 69. Relative to the raw historic, the extreme flows increase significantly in the future, mostly due to little snow accumulation and increased runoff. Assuming that this relationship is appropriate for the future climate, the adjustment is reasonable. Although the most extreme events do not increase, there is a general increase in the lower probability events, most noticeably in the one to five percent range.

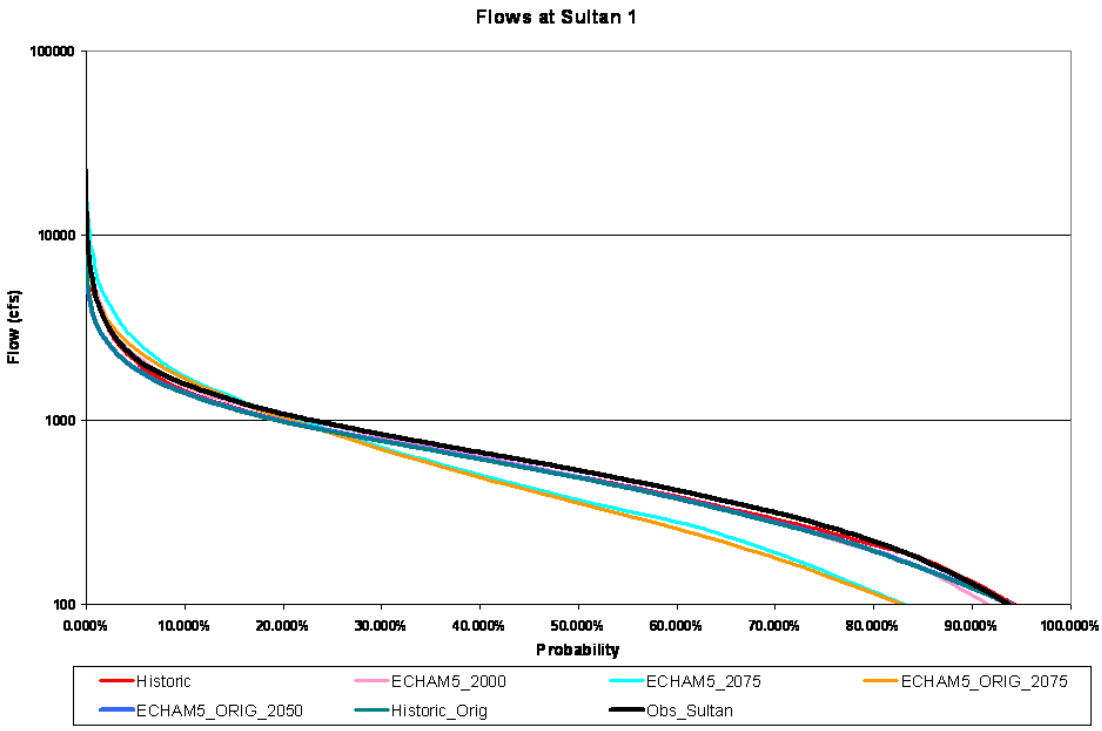

Figure 68: Example of Bias Correction Process for Sultan 1

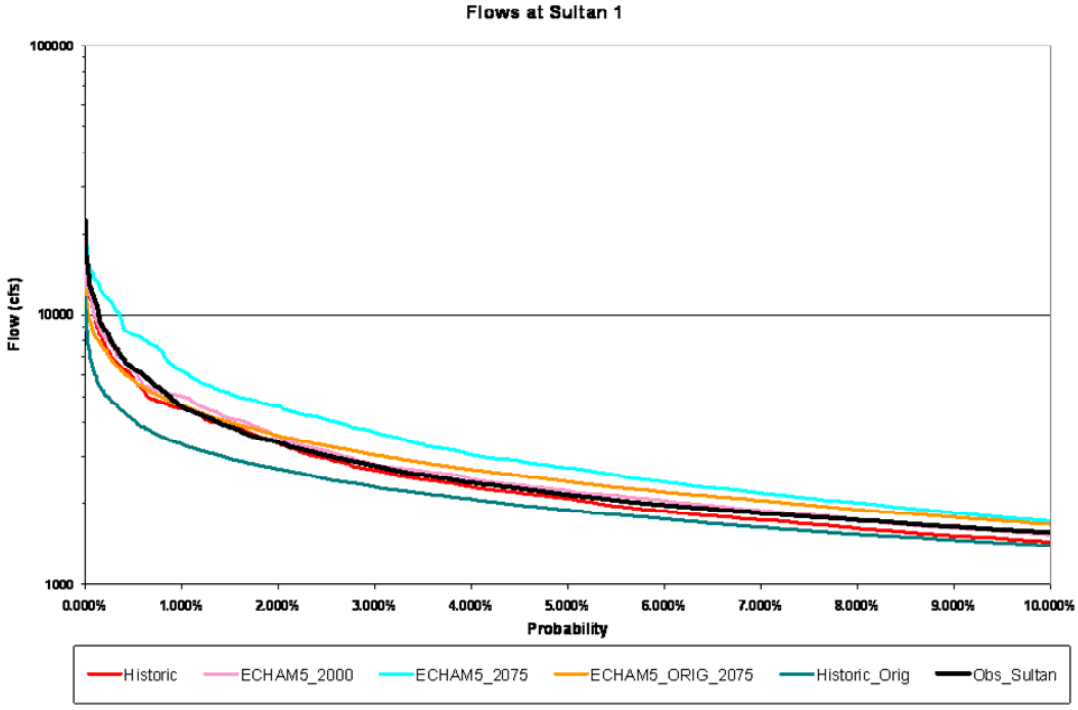

Figure 69: Simulated Streamflows at Sultan 1 for 2075 period

For the Green River, chronic low flows and a small number of extremely low flows were exhibited in summer in the modeled flows. To correct these low flows, the steps listed above were applied. A mapping of simulated flows at HH Inflows and observed historic flows are used to create the adjustment factors. The correction routine addresses the lower percentiles of the CDF. Figure 70 presents the observed (black), unaltered (green), and corrected (red) streamflow at HH Inflow. For the low flows during summer there is an improvement after the correction scheme is applied to the simulated flows. Because of the overall improvement seen in summer flows after adjustment, the correction scheme was applied to all simulated flows at HH Inflow.

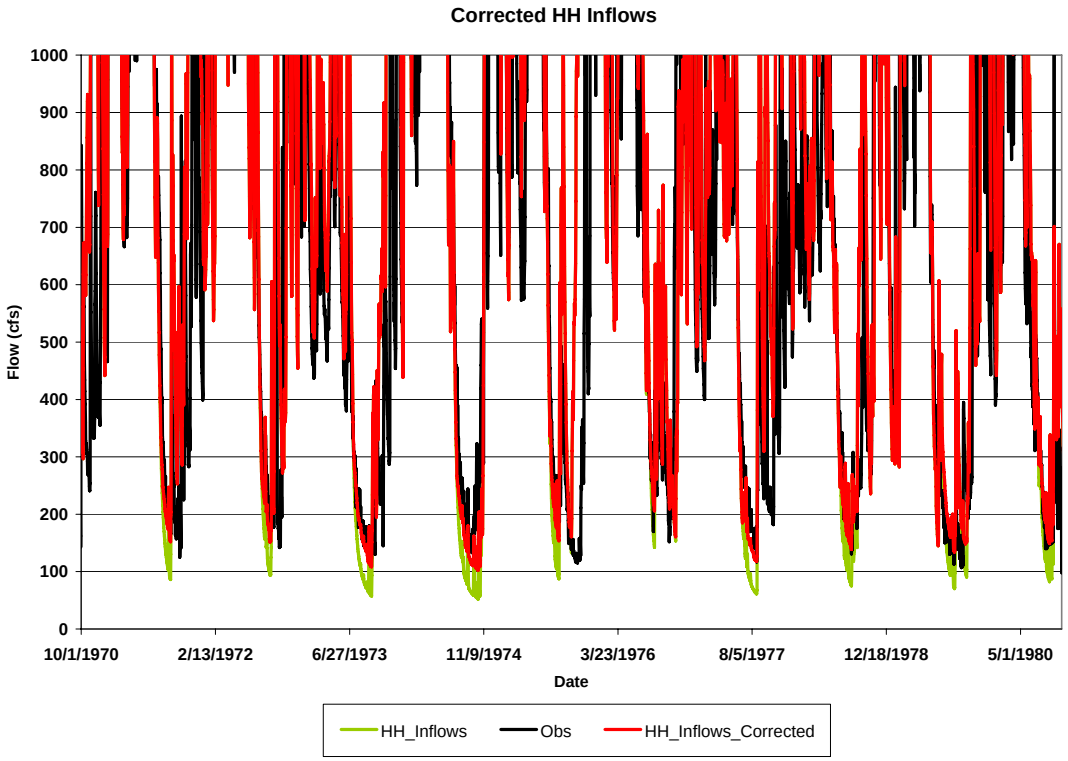

Figure 70: Corrected and Raw Simulated Flows at HH Inflows

In the White River, bias is introduced due to the mapping of the stream network. Figure 71 displays the model stream network in blue lines and the USGS mapped streams in red. The yellow arrow indicates where flow is incorrectly being routed from a subbasin of the Carbon into the White River. To address this issue, the incorrectly routed simulated flow is removed from the simulated main stem of the White River. Because not all of the incorrect flow entering the White could be removed using this arithmetic approach, and some positive bias is exhibited solely from the modeling of the basin, the correction scheme is applied to adjust streamflow below Mud Mountain Dam. Keeping with the steps detailed above, adjustment factors were created using the simulated and observed flows at USGS Gage 12098500. The correction factors are applied by month to the simulated flow.

Once the correction is complete, the corrected streamflow is evaluated for consistency in mass curves and time series evaluations. Figure 72 and Figure 73 provide a comparison of the simulated flows at USGS Gage 12098500 prior to and after applying the adjustment factors.

Figure 73 shows very good agreement between the simulated and observed flows in both median and quartile events.

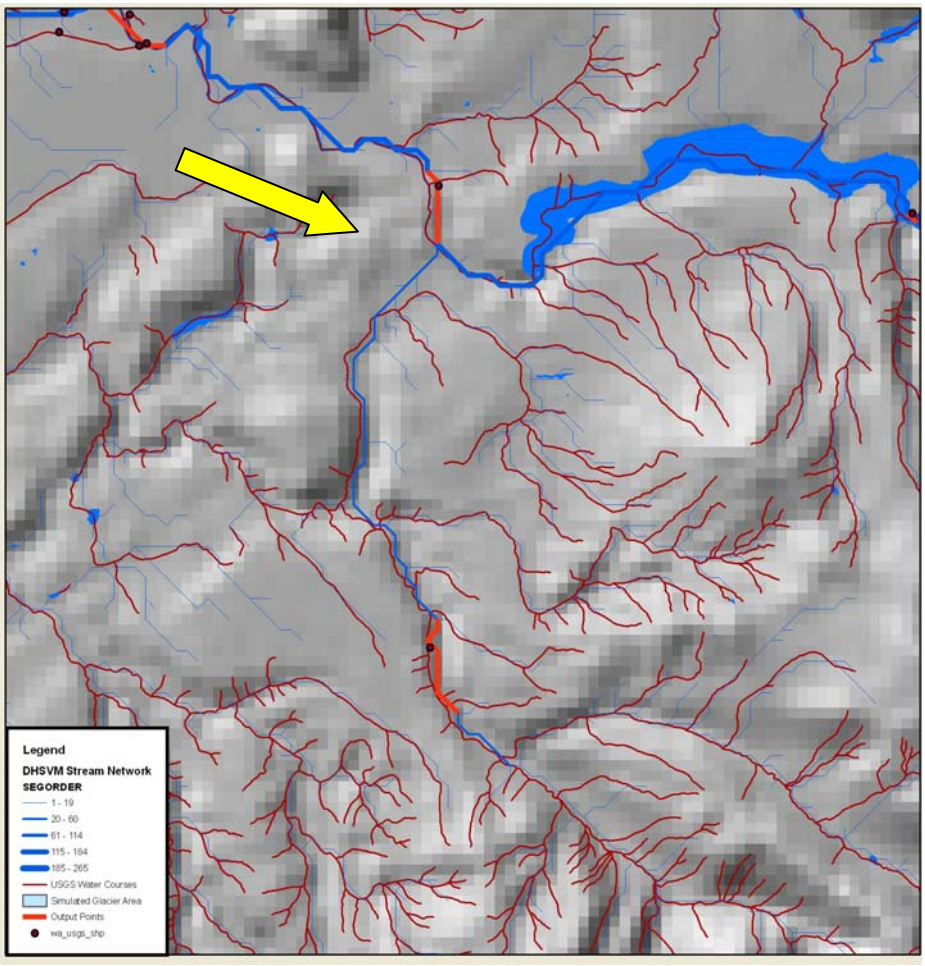

Figure 71: Location of Incorrect Stream Network

Overall, the correction scheme removes the model error within DHSVM exhibited primarily in the summer months and extreme winter events. Bias correct of some form is very common when forecasting or simulating streamflow. The correction scheme is used sparingly, only at four points out of the many modeled in each basin. Correction of positive bias using the quantile mapping scheme for the White River works well, with the positive bias being removed and the time series kept intact. Correction of negative bias in the Green, Sultan, and Cedar Rivers prevents unrealistic low flows while keeping the simulated time series intact.

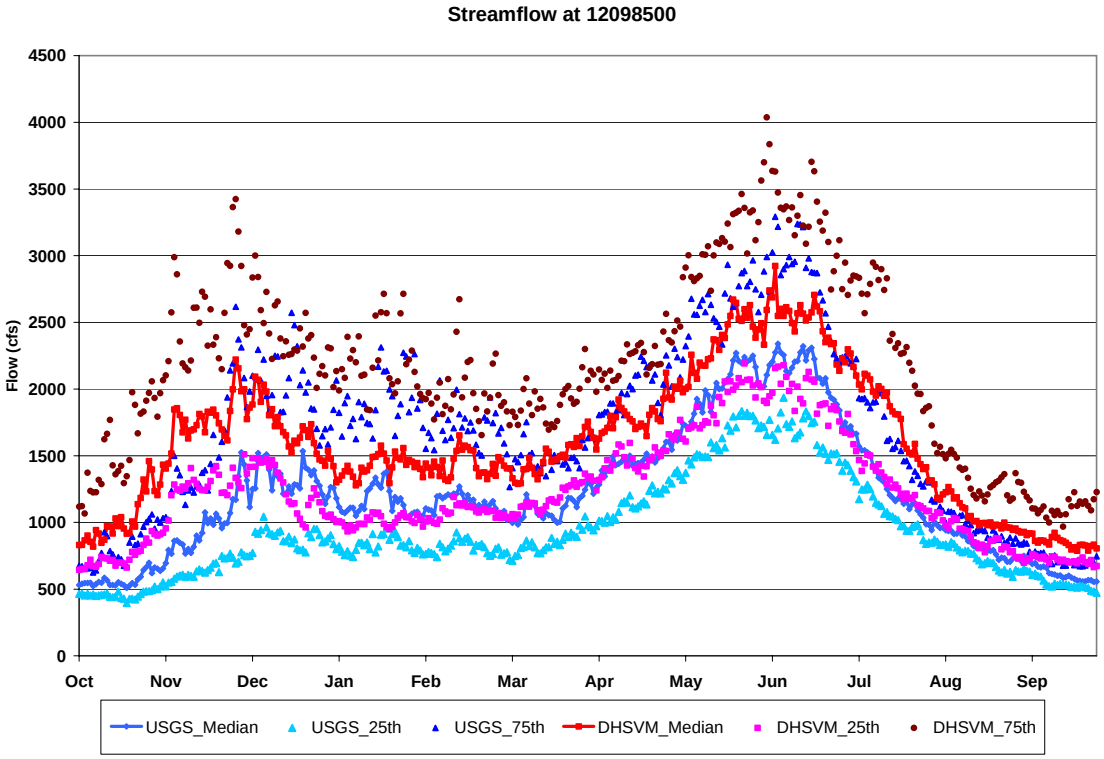

Figure 72: Modeled and Observed Flows at 12098500 before Correction

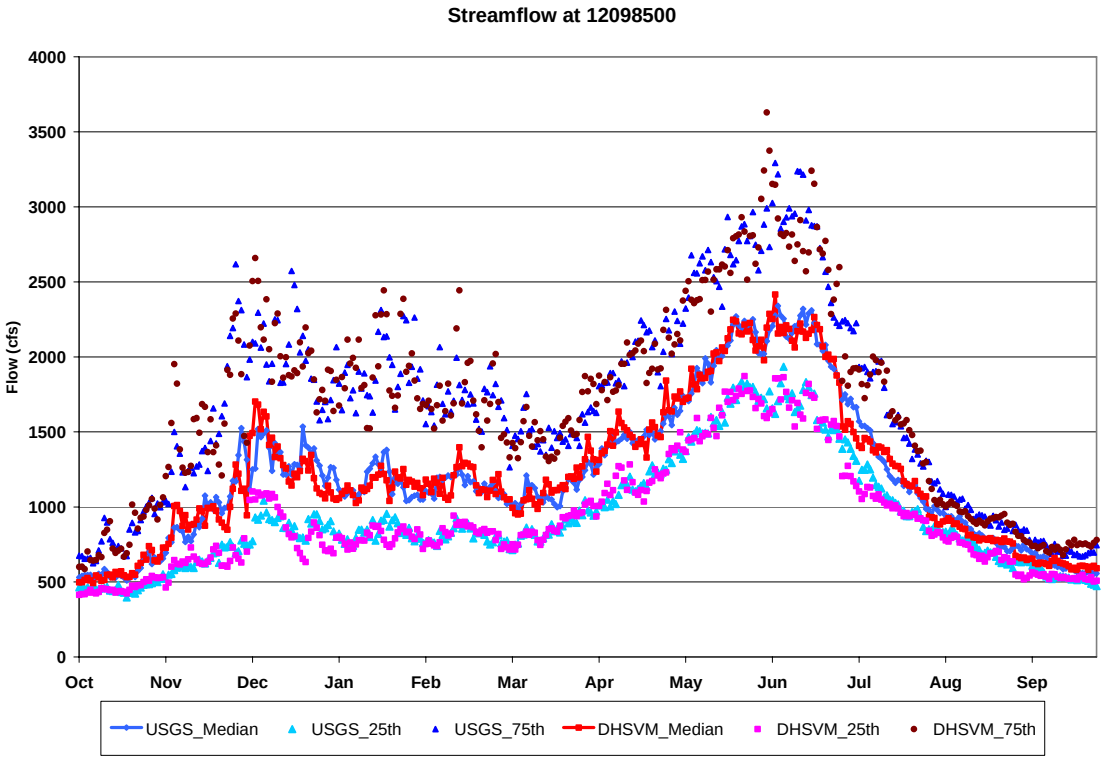

Figure 73: Modeled and Observed Flows at 12098500 after Correction